International Ocean Discovery Program Expedition 349 Scientific Prospectus

South China Sea Tectonics

Opening of the South China Sea and its implications for southeast Asian tectonics, climates, and deep mantle processes since the late Mesozoic

Chun-Feng Li
Co-Chief Scientist
State Key Laboratory of Marine Geology
School of Ocean and Earth Sciences
Tongji University
1239 Siping Road
Shanghai 200092
People's Republic of China

Jian Lin
Co-Chief Scientist
Department of Geology and Geophysics
Woods Hole Oceanographic Institution
360 Woods Hole Road
Woods Hole MA 02543
USA

Denise K. Kulhanek
Expedition Project Manager/Staff Scientist
Integrated Ocean Drilling Program
Texas A&M University
1000 Discovery Drive
College Station TX 77845
USA

Published by
Integrated Ocean Drilling Program Management International, Inc.,
for the Integrated Ocean Drilling Program

Publisher's notes

Citation:
Li, C.-F., Lin, J., and Kulhanek, D.K., 2013. South China Sea tectonics: opening of the South China Sea and its implications for southeast Asian tectonics, climates, and deep mantle processes since the late Mesozoic. *IODP Sci. Prosp.,* 349. doi:10.2204/iodp.sp.349.2013

Distribution:
Electronic copies of this series may be obtained from the Integrated Ocean Drilling Program (IODP) Scientific Publications homepage on the World Wide Web at **www.iodp.org/scientific-publications/.**

This publication was prepared by the Integrated Ocean Drilling Program U.S. Implementing Organization (IODP-USIO): Consortium for Ocean Leadership, Lamont-Doherty Earth Observatory of Columbia University, and Texas A&M University, as an account of work performed under the international Integrated Ocean Drilling Program, which is managed by IODP Management International (IODP-MI), Inc. Funding for the program is provided by the following agencies:

National Science Foundation (NSF), United States

Ministry of Education, Culture, Sports, Science and Technology (MEXT), Japan

European Consortium for Ocean Research Drilling (ECORD)

Ministry of Science and Technology (MOST), People's Republic of China

Korea Institute of Geoscience and Mineral Resources (KIGAM)

Australian Research Council (ARC) and GNS Science (New Zealand), Australian/New Zealand Consortium

Ministry of Earth Sciences (MoES), India

Coordination for Improvement of Higher Education Personnel, Brazil

Disclaimer

This IODP *Scientific Prospectus* is based on precruise Science Advisory Structure panel discussions and scientific input from the designated Co-Chief Scientists on behalf of the drilling proponents. During the course of the cruise, actual site operations may indicate to the Co-Chief Scientists, the Staff Scientist/Expedition Project Manager, and the Operations Superintendent that it would be scientifically or operationally advantageous to amend the plan detailed in this prospectus. It should be understood that any proposed changes to the science deliverables outlined in the plan presented here are contingent upon the approval of the IODP-USIO Science Services, TAMU, Director in consultation with IODP-MI.

ISSN

World Wide Web: 1932-9415

May 2013

Abstract

The South China Sea (SCS) is situated at the junction of the Eurasian, Pacific, and Indo-Australian plates. It has undergone nearly a complete Wilson cycle despite its relatively small size and short evolutionary history, and it is a critical site linking some of the major western Pacific tectonic units. The opening of the SCS reveals complex patterns of continental margin breakup and basin formation. Despite extensive studies, sampling of basement rocks and overlying sediments in the deep basin is currently lacking. This leaves a large margin of error in estimated opening ages and renders various hypotheses regarding its opening mechanism and history untested. This also hampers our understanding of East Asian tectonic and paleoenvironmental evolution. International Ocean Discovery Program Expedition 349 (28 January–30 March 2014) will drill three sites to ~100 m into basement (Sites SCS-3G, SCS-6A, and SCS-4B) in two different sub-basins of the SCS to address questions regarding the opening and evolution of the SCS and how it affected the paleoceanography of the region. These sites are located to determine the timing of onset and cessation of seafloor spreading in the East and Southwest Sub-basins. Geochemical sampling of basement rocks of different ages within the different magnetic zones of the SCS will provide critical information on how the crust and mantle evolved during various stages of basin evolution. Coring of the sedimentary section above basement will provide direct constraints on the age of the underlying basement through biostratigraphy and will allow examination of changes in sedimentation and paleoceanography through time as the basin opened and then began subducting beneath the Manila Trench. All sites will be single cored using the advanced piston corer and extended core barrel to refusal, followed by rotary core barrel drilling through the remaining sediment section and basement. If permitted by the Environmental Protection and Safety Panel, we will drill through the top 900 m of the highest priority site (SCS-6A), which would recover a similar sequence to that cored at the first site (SCS-3G). This option gives the best opportunity of reaching and coring basement at all three primary sites. If full coring is required, two additional sites that reach basement with shallower penetration will be substituted. Downhole logging is planned for all sites using the triple combination and Formation MicroScanner–sonic tool strings. Additional tool strings may be run if time and hole conditions permit, including a check shot survey, the Ultrasonic Borehole Imager, the magnetometer tool, and the magnetic susceptibility sonde.

Schedule for Expedition 349

Expedition 349 is based on Integrated Ocean Drilling Program Proposal 735-CPP2 (available at **iodp.tamu.edu/scienceops/expeditions/south_china_sea.html**). Following ranking by the Integrated Ocean Drilling Program Science Advisory Structure and a commitment from China to contribute to the cost of the expedition, the expedition was scheduled for the research vessel *JOIDES Resolution*, operating under contract with the U.S. Implementing Organization (USIO). At the time of publication of this *Scientific Prospectus*, the expedition is scheduled to start in Manila, Philippines, on 28 January 2014 and to end in Okinawa, Japan, on 30 March 2014. A total of 58 days will be available for the transit, drilling, coring, and downhole measurements described in this report (for the current detailed schedule, see **iodp.tamu.edu/scienceops/**). As Expedition 349 is a Complimentary Project Proposal (CPP) with China contributing to the expedition costs, there will be substantially increased shipboard participation by Chinese scientists. Further details about the facilities aboard the *JOIDES Resolution* and at the USIO can be found at **www.iodp-usio.org/.**

Introduction

Since the late Mesozoic, the South China Sea (SCS) area (Figs. **F1, F2**) has been at the center stage of many first-order tectonic and paleoclimatic events. Mesozoic subduction of the paleo-Pacific plate, a fragment of which developed roughly along the present-day northern SCS continental margin (Jahn et al., 1976; Hilde et al., 1977; Hamilton, 1979; Holloway, 1982; Taylor and Hayes, 1983; Hayes et al., 1995; Zhou and Li, 2000; Yang et al., 2003; Xiao and Zheng, 2004; Zhou et al., 2008; Li et al., 2008a), gradually displaced the paleo-Tethys and built a massive orogen in Southeast Asia (Zhou and Li, 2000; Shi and Li, 2012). Subduction is thought to have ceased in the mid-Cretaceous, with a transition to regional extension during the Late Cretaceous. Opening of the SCS began in the Cenozoic via continental breakup and subsequent seafloor spreading. The early work of Taylor and Hayes (1980, 1983) and Briais et al. (1993) suggested that the SCS opened from ~32 to ~16 Ma during the Oligocene and early Miocene.

Currently, ages of the oceanic crust in the SCS basin are only loosely constrained from magnetic anomaly correlations and empirical relationships between ages and bathymetry and/or heat flow. The many uncertainties in the timing and episodes of the Cenozoic opening of the SCS hampers understanding of other key geological pro-

cesses in Southeast Asia, including the geodynamic transition from Mesozoic subduction to Cenozoic rifting, the Cenozoic opening mechanism, oceanic crustal accretion and mantle evolution, and paleoceanographic and sedimentary responses. In order to address both regional questions related to East Asian geology and fundamental issues regarding continental breakup and basin formation, it is essential to determine when seafloor spreading initiated, the mechanism through which the SCS basin opened, and when spreading ceased. To do this, we plan to drill into the oceanic basement and retrieve both sedimentary and basaltic rocks from various sub-basins of the SCS basin. Timing of the onset and termination of seafloor spreading of the SCS will be critical to correlating regional tectonic events to the tectonic episodes within the SCS that are inferred almost exclusively from geophysical measurements and inversions. Drilling and coring into basement is the only means of validating various opening mechanisms.

Expedition 349 is based on Integrated Ocean Drilling Program Proposal 735-CPP2, developed in part from results of an international workshop held at Tongji University in Shanghai, China, in early 2012 (Li et al., 2012). The primary objectives of the expedition fall under four major categories and address the Earth Connections and Climate and Ocean Change themes in the science plan for the International Ocean Discovery Program (available at **www.iodp.org/science-plan-for-2013-2023**). These primary objectives are

1. To examine mechanisms, timing, and sequences of Cenozoic seafloor spreading and establish the complex opening history of different sub-basins and styles of oceanic crustal accretion in the SCS and constrain the tectonic controls (such as spreading rate) on distinct magnetic contrasts among the three sub-basins;
2. To examine oceanic crustal accretion and mantle evolution and reveal the crustal nature and affinities of different sub-basins and understand oceanic crustal and deep mantle processes associated with tectonic extrusion, magmatism, and magnetization;
3. To examine paleoceanographic and sedimentary responses to tectonic evolution of the SCS and develop a more complete 3-D sedimentation and subsidence model and link it to regional climatic processes in response to various tectonic events; and
4. To examine late Mesozoic and early Cenozoic prerifting tectonic transitions and driving forces leading to continental margin breakup and seafloor spreading; to test various hypotheses of dynamic processes controlling the transition from a Mesozoic active continental margin to a Cenozoic passive one and from conti-

nental rifting and breakup to seafloor spreading; and to constrain whether the forces driving the opening of the SCS were far-field (triggered by the tectonic extrusion of the Indochina block), near-field (due to backarc spreading or slab pull), or in situ (mantle plume and magmatism driven). This will deepen our general understanding of the geodynamic interplay of mantle and lithosphere processes that led to the development of continental margin basins in the geological past and today.

During Expedition 349, we aim to drill and core into basement at three sites in two sub-basins within the SCS (Figs. **F1, F2**) to collect the geological evidence necessary to address these themes.

Background

Geological setting

The SCS is a western Pacific marginal sea situated at the junction of the Eurasian, Pacific, and Indo-Australian plates. It developed from Cenozoic continental margin rifting, and its central portion is floored with oceanic crust. Despite its relatively small size and short evolutionary history, the SCS has undergone nearly a complete Wilson cycle from continental breakup to seafloor spreading to subduction. The SCS is a critical site connecting some of the major tectonic units in the western Pacific. It is also well suited for studying various plate boundary activities, such as continental margin rifting (e.g., Hayes and Nissen, 2005), seafloor subduction (the Manila Trench; e.g., Li et al., 2007a), strike-slip faulting (the Red River fault; e.g., Clift and Sun, 2006), and active orogenic processes (Taiwan; e.g., Huang et al., 2001) (Fig. **F1**).

Hypotheses for the opening mechanism of the SCS differ markedly (Fig. **F3**) and include (1) India-Eurasia collision and the consequent tectonic extrusion mainly along the Red River fault (Tapponnier et al., 1982; Lallemand and Jolivet, 1986; Schärer et al., 1990; Briais et al., 1993; Leloup et al., 2001; Flower et al., 2001), (2) slab pull and subduction of the proto-SCS under Sabah/Borneo (Taylor and Hayes, 1980, 1983; Holloway, 1982; Hall, 2002), (3) extension related to an upwelling mantle plume (e.g., Fan and Menzies, 1992; Xu et al., 2012), and (4) regional extension related to subduction and retreat of the Pacific plate along the western Pacific margin (Taylor and Hayes, 1980, 1983; Shi and Li, 2012). In addition to these end-member models, hybrid models have been proposed (e.g., Cullen et al., 2010).

The original SCS basin before its subduction along the Manila Trench may have been twice the size of what we see today (Sibuet et al., 2002), so the geodynamic model must be able to explain the formation of a large ocean basin. Motion on the Ailao Shan-Red River fault (RRF) has been dated to 35 to 15 Ma, with displacement of as much as several hundreds of kilometers (e.g., Leloup et al., 2001). Ages obtained from ocean basalts at the proposed drilling sites in the SCS will test the hypothesis that the motion on the RRF is coeval to, and may have driven part of, extension and spreading in the SCS, although only a minor amount of extension associated with the SCS spreading center may have been transferred to the RRF (Rangin et al., 1995; Morley, 2002; Clift et al., 2008). Regional rifting in East Asia occurred long before the India-Eurasia collision (Fig. **F3D**) and is thought to be associated mainly with subduction of the paleo-Pacific plate (Taylor and Hayes, 1980, 1983; Shi and Li, 2012).

Some hypotheses suggest the existence of a proto-SCS oceanic basin (Haile, 1973; Madon et al., 2000) that was once connected to the Pacific plate and began to close from ~44 Ma (e.g., Hall, 1996, 2002) in order to accommodate the opening of the SCS (Fig. **F3B**). Supported by the wide occurrence of Mesozoic and/or early Cenozoic marine sediments, a large part of this proto-SCS may have been subducted into, or uplifted as part of, island arcs formed to the south in Borneo/Sabah and Palawan (Hall, 2002; Hutchinson, 1996, 2004), where remnants of the proto-SCS oceanic crust may be present (Hutchison, 2005) and are one possible origin of the ophiolites of South Palawan (Rangin et al., 1990; Tu et al., 1992; Schlüter et al., 1996; Pubellier et al., 2004; Cullen, 2010). Slab-pull force from this subducting proto-SCS plate, along with an in situ mantle plume and massive synrifting volcanism, may also have triggered or contributed to the opening of the SCS, but definitive evidence for these arguments is absent.

The opening of the SCS reveals complex patterns of continental breakup and seafloor spreading. Magnetic and seismic data suggest that the SCS basin can be divided into five magnetically distinct zones (Li et al., 2008b) (Fig. **F4**). In particular, magnetic amplitudes and orientations in the Southwest Sub-basin (Zone E) differ markedly from those in the East Sub-basin (Zone D). These two sub-basins are divided by a complex boundary called the Zhongnan fault (Figs. **F2, F4**) according to some authors (Yao, 1995; Jin et al., 2002; Li et al., 2007b, 2008b). This magnetic contrast may support an episodic seafloor-spreading model (Ru and Pigott, 1986) or may be attributed to different crustal types within which the two sub-basins evolved independently. Pautot et al. (1986) suggested that the youngest part of the East Sub-basin developed within an older, preexisting oceanic crust, whereas the Southwest Sub-basin resulted from

continental rifting that led to seafloor spreading. Within the East Sub-basin, two distinct negative magnetic anomalies (M1 and M2 in Fig. **F4**), thought to be the same age, further divide the sub-basin into a central part with high magnetic amplitudes and two separated parts with slightly weaker magnetization (C1 and C1′) near the two conjugate continental margins. The magnetic pattern of the Northwest Sub-basin also differs from its adjacent segment in the East Sub-basin.

Table **T1** shows additional contrasts between the East and Southwest Sub-basins, some of which are rather perplexing. For example, the greater water depths of the Southwest Sub-basin may imply relatively older crustal ages (Ru and Pigott, 1986; Yao et al., 1994; Li et al., 2008b), which conflict with younger ages inferred from the higher heat flow and shallower Curie-point depths there (Ru and Pigott, 1986; Li et al., 2010). Recent heating from magmatic activities could have contributed to the high heat flow in the Southwest Sub-basin (Ru and Pigott, 1986; Li and Song, 2012), but this hypothesis needs to be confirmed through drilling.

A number of Cenozoic tectonic models have been proposed, but it remains uncertain whether the SCS basin experienced primarily a single episode or multiple episodes of extension and seafloor spreading and, if multiple episodes, in what sequence the sub-basins evolved (e.g., Taylor and Hayes, 1980; Pautot et al., 1986; Ru and Pigott, 1986; Briais et al., 1993; Yao et al., 1994; Hayes and Nissen, 2005; Li et al., 2007b, 2008b). For example, the opening of the East and Northwest Sub-basins may have predated, or been synchronous with, that of the Southwest Sub-basin (Taylor and Hayes, 1983; Briais et al., 1993; Lee and Lawver, 1995; Tongkul, 1994; Honza, 1995; Zhou et al., 1995; Schlüter et al., 1996; Hall, 2002; Hall and Morley, 2004; Hayes and Nissen, 2005; Braitenberg et al., 2006; Sun et al., 2009). This model contrasts with others in which earlier opening of the Southwest Sub-basin is preferred (Fig. **F5**) (e.g., Ru and Pigott, 1986; Yao et al., 1994; Li et al., 2007b). This latter group of models considers the sharp contrasts between the East and the Southwest Sub-basins and the important roles of the Zhongnan fault (Figs. **F2, F4**), which the first group often ignore. There are also two models of propagation of SCS spreading, one propagating northeast toward the Taiwan Strait (Chung et al., 1994) and the other toward the Southwest Sub-basin (Zhou et al., 1995). Furthermore, Barckhausen and Roeser (2004) concluded that seafloor spreading at the southwest rift tip ceased at 20.5 Ma (Anomaly 6a1), ~4 m.y. earlier than interpreted in previous studies.

Previous drilling

Five sites were drilled in the peripheral continental slope of the central SCS basin during Ocean Drilling Program (ODP) Leg 184 (Feb–April 1999) (Wang, Prell, Blum, et al., 2000). That expedition cored hemipelagic sediments in the SCS to determine the evolution and variability of the East Asian monsoon during the late Cenozoic. All Leg 184 sites are located on the continental slope, and none penetrated into basement rocks. The deepest hole cored during the leg reached 861 meters below seafloor (mbsf) at Site 1148 in 3294 m of water (Figs. **F2, F4**), recovering lower Oligocene sediments. The major objectives of Leg 184 were to improve our knowledge of the variability of monsoonal climates (including millennial- to possibly centennial-scale variability from high-sedimentation rate records), orbital-scale variability from records at all SCS sites, and tectonic-scale variability from late Cenozoic sections. The records from the SCS from both Leg 184 and Expedition 349 will be used to establish links between the East Asian and Indian monsoons and to evaluate mechanisms of internal (climate system feedbacks) and external (orbital and tectonic) climate forcing.

One particularly interesting feature recovered at Site 1148 is a slump zone dated to between 28 and 23 Ma, which spans the Oligocene/Miocene boundary and coincides with a "double seismic reflector" (Wang, Prell, Blum, et al., 2000; Li et al., 2004, 2005; Wang and Li, 2009). The Oligocene/Miocene boundary at Site 1148 also marks sharp uphole decreases in sedimentation rates, organic carbon, and opal contents; changes in Nd; and fluctuations in many logging and elemental records. Subsequent investigations indicated that this slump zone might be related to a major tectonic event synchronizing with a possible ridge jump (Briais et al., 1993; Wang, Prell, Blum, et al., 2000; Li et al., 2005) and/or an episode of regional magmatism associated with the opening of the SCS (Li and Song, 2012). Unfortunately, Leg 184 had very low recovery within this critical zone, and thus the true nature of this major tectonostratigraphic event needs to be further investigated. Expedition 349, targeting the oldest possible oceanic crust and overlying sediments, as well as the oceanic basalts at approximately the Oligocene/Miocene boundary, will help pinpoint the geodynamic cause and paleoceanographic and sedimentary effects of this regional event.

Seismic studies and site survey data

Figure **F2** shows the proposed drill sites and available multichannel seismic (MCS) lines used to locate these sites. All proposed primary sites and most alternate sites are located at the intersections of two MCS lines (Table **T2**). Three of the proposed sites

(SCS-6C, SCS-4E, and SCS-4F) are not located on crossing points but require thin sedimentary penetration. All proposed sites were selected from original Society of Exploration Geophysicists (SEGY) data on a SUN workstation. A dense 2-D MCS grid exists in the northern SCS continental margin and the northern part of the central SCS basin. The Chinese National Offshore Oil Corporation (CNOOC) acquired most of these high-quality data recently. The number of MCS lines in the central basin is increasing rapidly, contributed mostly by the South China Sea Institute of Oceanology (SCSIO) of the Chinese Academy of Sciences, Guangzhou Marine Geological Survey (GMGS) of the Land and Resources, the 2nd Institute of Oceanography (SIO) of the State Oceanic Administration, and the Federal Institute for Geosciences and Natural Resources (BGR).

GMGS has undertaken extensive geophysical and geological mapping of a large portion of the central SCS basin in recent years. As a result, multichannel reflection seismic data and shallow sediment cores are regularly added to our existing site survey database. This mapping activity has already started producing 2-D seismic grids around our proposed sites. Although most of these new data are either being processed or in a proprietary state, partial access has been made possible through close collaboration with three co-proponents of Proposal 735-CPP2 from GMGS.

Other MCS and magnetic data were collected near these sites by the R/Vs *Vema*, *Conrad*, and *Haiyang IV* (Taylor and Hayes, 1980, 1983; Yao et al., 1994; Hayes et al., 1995) (Fig. **F2**). Two stages of Sino-US cooperation in the early 1980s added more dense geophysical data coverage, which includes sonobuoy measurements, two ship expanding spread profiles, and piston cores (Taylor and Hayes, 1983; Yao et al., 1994; Hayes et al., 1995). The German R/V *Sonne* carried out five cruises in 1987 (SO-49, SO-50B), 1990 (SO-72A), 1994 (SO-95), and 2008 (SO-197) (Franke et al., 2011) and collected >10,000 km of MCS data and high-resolution echograms (Lüdmann and Wong, 1999; Lüdmann et al., 2001).

The area surrounding alternate Site SCS-1C is also well studied and imaged with numerous geophysical surveys during Cruises SCSIO87, 973GMGS, ACT, TAICRUST, ORI645, and ORI689. More recent geophysical studies include the TAiwan Integrated GEodynamics Research (TAIGER) project (McIntosh et al., 2012) and surveys for gas hydrate. There are also various earthquake hypocenter relocations and tomographic studies (Wu et al., 1997; Cheng et al., 1998; Kao et al., 2000).

Swath bathymetry data (Fig. F6) are available for the entire SCS basin (Li et al., 2011), and Generic Mapping Tools (GMT) grids of multibeam bathymetry data around eight of the proposed drill sites have been submitted to the Integrated Ocean Drilling Program Site Survey Data Bank. Digital grid data of swath bathymetry will be available upon request from GMGS and the SIO of the State Oceanic Administration.

Magnetic anomalies covering all proposed drill sites were compiled by the Geological Survey of Japan and Coordinating Committee for Coastal and Offshore Geoscience Programmes in East and Southeast Asia (CCOP) in 1996 (Fig. F4). This compilation offers remarkable coverage and accuracy and yields many new insights into the dynamic opening process of the SCS (Li et al., 2008b, 2010, 2012). 3-D deep crustal and mantle structures in the area have also been imaged with surface wave tomography (Wu et al., 2004).

Previous ocean bottom seismometer (OBS) studies reveal the crustal thickness and velocity structures of the central basin. Yan et al. (2001) conducted an OBS experiment near these sites. In 2006, three OBS profiles were shot by the SIO of the State Oceanic Administration, one on the northern continental margin and the other two crossing the Northwest Sub-basin. In early 2011, the South China Sea Deep (SCSD), a comprehensive 8 y research program, was approved by the National Science Foundation of China (NSFC) (Wang, 2012). With a total budget of ~$23 million US, this program has funded coincident refraction/reflection surveys and deep-tow magnetic surveys near these sites. The two most recent OBS surveys in the SCS in 2012 included an active source 3-D survey around the relict spreading center and a larger scale passive source OBS survey in the central basin. Several of the proposed drill sites (notably Sites SCS-3G and SCS-3H) are located within these survey areas. Preliminary results from these surveys have just been published (Zhang et al., 2013).

Two deep-tow magnetic cruises in the SCS were done in 2012 and 2013. Both deep-towed and conventional surface-towed magnetometers were deployed along four survey lines, which were designed to traverse the four primary sites. High-resolution magnetic anomalies from this survey allow more accurate calibration between magnetic susceptibilities and radiometric ages of core samples and the observed seafloor magnetic anomalies in the vicinity of the drill sites. These site surveys add crucial new data for establishing the best possible model of magnetic anomalies for the whole basin and the age of the ocean crust at the drill sites.

Finally, numerous piston cores were taken in the SCS by the R/V *Vema* and R/V *Conrad* (Damuth, 1980). Shallow sediment coring using the French R/V *Marion Dufresne* near Sites SCS-6A, SCS-6B, SCS-2C, and SCS-2D was also completed in 2012.

The supporting site survey data for Expedition 349 are archived at the **Integrated Ocean Drilling Program Site Survey Data Bank.**

Scientific objectives

Expedition 349 focuses on coring basement at multiple sites around the SCS basin to better understand seafloor spreading, ocean crust accretion, and mantle evolution. In addition, coring the sedimentary sections above basement will allow examination of the sedimentary and paleoceanographic responses to basin opening and eventual subduction beneath the Manila Trench. Drilling in the SCS will allow us to address key problems in tectonics, mantle evolution, and paleoceanography.

1. *Date the timing of the opening of different sub-basins of the SCS and correlate the ages from magnetic anomalies to fossil, magnetostratigraphic, and radiometric ages.*

Accurate age estimates for the opening history of the sub-basins of the SCS can be correlated with the uplift history of the Tibetan Plateau to further advance our understanding of the possible links between extrusion tectonics (Tapponnier et al., 1982; Briais et al., 1993; Clift et al., 2008) and the proposed continental breakup leading to the formation of the SCS.

Magnetostratigraphy, biostratigraphy, and radiometric dating are the three principal techniques that will be used for chronostratigraphic analysis of the recovered sequences. Age control in the sedimentary section will be made from routine microfossil analyses, paleomagnetism, and isotope analysis. The age sequences can also be constrained by correlating seismic reflections to different drill sites. Because drilling at all proposed sites intends to recover the oldest sediments deposited directly on the top of oceanic basement, paleontological analyses provide a minimum age constraint for the basement. Except for the upper ~900 m at proposed Site SCS-6A in the primary operations plan, we plan to core all intervals within the three primary sites, with micropaleontological analyses conducted on all core catcher material and additional samples from split-core sections to refine the biostratigraphy as time permits. At Site SCS-6A, we expect to recover a shallow to deep marine carbonate succession of Oligocene to middle Miocene age, with a shallow-marine depositional environment ex-

pected to have been deposited soon after the rifting–drifting transition. Calcareous microfossils, including nannofossils and foraminifers, should be abundant in the carbonate successions at all sites. Within some intervals, particularly in the Neogene, we expect to find well-preserved and abundant siliceous microfossils (biogenic silica dominated by diatoms and radiolarians) that can provide additional biostratigraphic control.

Basement volcanic rocks will be dated with $^{40}Ar/^{39}Ar$ and other high-resolution zircon dating techniques with uranium-series isotopes (Goldstein et al., 1991, 1994; Goldstein, 1995; Schwartz et al., 2005). As we plan to drill ~100 m into basaltic basement at all three of our primary sites, we hope to retrieve sufficiently unaltered basaltic rocks for these analyses. Oceanic crust rocks are typically very low in K concentrations and therefore more vulnerable to disturbances by submarine alteration. To ensure high-quality $^{40}Ar/^{39}Ar$ dating on submarine samples collected in the SCS, we plan to (1) carefully select and prepare fresh highly crystalline groundmass and plagioclase phenocrysts, which are the most suitable for $^{40}Ar/^{39}Ar$ dating, and (2) apply acid leaching to remove altered portions of the groundmass or mineral separates (Koppers et al., 2011).

The half-spreading rates of the SCS were between 20 and 40 mm/y, as part of a slow-spreading basin (Briais et al., 1993; Song and Li, 2012). Some new geophysical evidence suggests that near the continent/ocean boundary (COB), where proposed Sites SCS-6A and SCS-6B are located, hyperextended crust exhuming possible lower crust and upper mantle could exist (Franke et al., 2011). If so, gabbros with late-stage minerals or felsic lithologies could be available for uranium-lead zircon dating using sensitive high-resolution ion microprobe reverse geometry (SHRIMP-RG), as well as for $^{40}Ar/^{39}Ar$ dating of plagioclase, biotite, and/or hornblende mineral separates. Uranium-bearing minerals, such as zircon, are much more common in oceanic crust than conventionally thought, and a newly developed method that detects tiny amounts of zircon in rock could reliably date the age of ocean crust (Schwartz et al., 2005; Grimes et al., 2007).

2. *Measure the magnetization, mineralization, and geochemical compositions of basement rocks to understand the causes of the sharp magnetic contrast between different sub-basins.*

Magnetic susceptibilities of extrusive basalts normally decrease with increasing degree of alteration, which reduces their titanomagnetite content (e.g., Bleil and Petersen, 1983). Serpentinization of peridotite at deeper depths is also known to smear surface magnetic anomalies (e.g., Dyment et al., 1997). Detailed mineralogical studies

are essential to understand these processes that may be causing the magnetic contrast between the East and the Southwest Sub-basins.

Because of the intriguing patterns of magnetic anomalies in the SCS, careful measurements of magnetic susceptibility are needed to constrain models of, for example, tectonic settings or spreading rates (Dyment and Arkani-Hamed, 1995) that can explain the distinct differences in magnetic patterns between different sub-basins, as well as their crustal affinities. Magnetization measurements from cores are also vital for creation of an initial model for magnetic modeling and inversion in order to better understand the observed magnetic anomalies.

3. *Evaluate the origin and source evolution of SCS basement rocks to better understand the formation of SCS oceanic crust and the deep mantle processes driving this formation.*

Chemical and isotope compositions of Sr, Pb, and Nd isotopes and other isotopic systems will provide insights into the material influx and deep crustal and mantle processes (Castillo et al., 1991; Tejada et al., 2004). The opening mechanism of the SCS can be constrained by investigating the variation in the Pb-Nd-Sr isotopic composition of cored basement rocks. Variations in εNd values and Pb and Sr isotopic compositions measured at different sites will help us to understand how the SCS mantle evolved through time.

The basement rocks to be cored during this expedition have three potential mantle sources: (1) Indian Ocean/Eurasian lithospheric mantle, (2) Pacific mantle, or (3) a putative mantle plume. Each of these sources has a distinct composition and therefore distinctive geochemical characteristics. For this purpose, we plan to use incompatible trace element and long-lived radiogenic isotope ratios, as these geochemical tracers are not generally affected by variations in degree of partial melting of the mantle and fractional crystallization of the resultant melt. Using our analytical strategy and proposed drilling transect, we should be able to test several geochemical evolution scenarios corresponding to the rifting and spreading models of the SCS, including (1) normal continental rifting leading to seafloor (backarc) spreading, (2) magma-poor rifting due to Indochina extrusion tectonism, and (3) plume-initiated rifting.

These models, as well as others that may be proposed after initial observations are made during the expedition, can be successfully tested with our planned analytical approach. Through this and geochronologic analyses, we seek to understand the relationship between compositional evolution of the lavas and tectonic changes, as

such a combination will provide the best tectono-magmatic model for the formation of the SCS.

4. *Evaluate the paleoceanographic and climatic responses to the opening of the SCS and develop a 3-D sedimentation and subsidence model.*

With three drilling sites within the SCS, we can build a detailed 3-D postspreading model of seismic stratigraphy that will offer invaluable insights into deepwater sedimentary processes and how they evolved through time. This sedimentary model will be coupled with paleoenvironmental and paleoceanographic data from analyses of sediment cores to detect major geological events.

Information on sedimentation rates, provenance, water depths, tectonic subsidence, and facies changes will be determined from coring and will be correlated to known tectonic and climatic events onshore. By correlating drilling and coring information with regional seismic sections, we can build detailed 3-D sedimentation models. Major unconformities revealed in the central basin will be correlated with those in the continental slopes and rifting basins to trace the dynamic transitional process from rifting to drifting. Oligocene shallow-marine sediments deposited at the very early opening stages will also constrain critical paleoceanographic and tectonic changes at the onset of opening of the SCS.

Structural analyses of core samples will focus on brittle deformation features such as fractures, faults, veins, deformation bands, and so on. Statistical analyses on these structures will help reveal the regional stress field and its changes through time. These structures could record major events in the drifting stage and later events, such as magmatism, initiation of subduction along the Manila Trench, and tectonic events in the surrounding blocks.

Mineralogical and geochemical analyses will help identify sediment provenance in the SCS and how it has evolved through time. This is critical for studying sediments deposited before 25 Ma in the SCS, which are potentially shallow-marine sediments that contain information on the rifting–drifting transition. Therefore, mineralogical and geochemical analyses coupled with paleontological and paleoenvironmental studies can reveal early processes associated with continental breakup of the SCS. Analyses of detrital zircon in the sediments, for example, can (1) determine the maximum age of stratigraphic successions and help understand source-to-sink processes, (2) determine provenance characteristics such as age and composition, (3) test regional paleogeographic reconstruction models via provenance analysis, and (4) un-

ravel facets of geological history locked in the mineral chemistry of detrital zircon (Fedo et al., 2003).

5. *Obtain downhole geophysical logs to reveal physical properties of the sediments and the top oceanic basement and to provide a record of nonrecovered intervals.*

Our proposed deployment of a minimum of two wireline logging tool strings (the standard triple combination [triple combo] and the Formation MicroScanner [FMS]-sonic) will measure a wide spectrum of geophysical properties to provide structural, mineralogical, and geochemical information of the penetrated sequences. These data will be particularly important for nonrecovered intervals that occur when using the extended core barrel (XCB) and rotary core barrel (RCB).

The triple combo tool string records geophysical signals of the penetrated sediments and basement rocks by measuring the total and spectral natural gamma radiation (NGR), density, porosity, and resistivity of the formation. Gamma ray data will be used to infer lithology and provenance. Porosity, sonic, and density logs together will be critical for decompaction and backstripping analyses and for constraining the tectonic subsidence and opening history of the SCS sub-basins. The subsidence and rifting parameters so obtained can offer new insights on the proposed episodic opening history and reveal mantle properties.

Wireline logs will provide a continuous record to aid in the detection of lava flow boundaries, interlayered sediments, and alteration zones in the basement and will enable the dip of lava flows to be evaluated. The number of lava flow units penetrated has implications for how well geomagnetic secular variation has been sampled and hence the extent to which paleolatitudes can be most precisely constrained.

With FMS-sonic logging, we will gain high-resolution quasi-2-D images (electrofacies) of the borehole wall and the structure and orientation of the rocks. These data together will put much needed constraints on volcanostratigraphy and crustal accretion processes (Tominaga et al., 2009). The high-resolution FMS images will help to detect small-scale fractures and lithologic variations, evaluate the dips of lava flows, and reorient core pieces. The General Purpose Inclinometry Tool (GPIT), which includes both a three-axis inclinometer and a three-axis magnetometer, will be used to measure changes in magnetic properties of lithologies and in paleomagnetic direction.

Drilling and coring strategy

Our operations plan for this expedition consists of drilling three sites to ~100 m into basement (Sites SCS-3G, SCS-6A, and SCS-4B). In order to complete these three sites within the amount of time available for the expedition, we need to drill (without coring) through the uppermost 900 m of Site SCS-6A, which is the highest priority site. If the Environmental Protection and Safety Panel (EPSP) does not permit this and full coring is necessary, our backup operations plan will be substituted. This plan includes coring at two sites where basement can be reached at shallower depths of penetration and consists of Sites SCS-3F, SCS-6A, and SCS-4C. In addition, we have proposed a number of other alternate sites that reach basement at a range of penetration depths to allow flexibility during the expedition should we be unable to achieve our objectives at any of the primary sites.

Proposed drill sites

All proposed sites are located within areas floored by oceanic crust, except for alternate Site SCS-1C, which has the potential to core the continent–ocean transition zone (COT) or attenuated continental crust. This makes the proposed sites different from those drilled previously during Leg 184 (Wang, Prell, Blum, et al., 2000), which are all located on the continental shelf and slope and targeted scientific problems primarily related to sedimentation, paleoceanography, and paleoclimate.

Sites SCS-6A (primary), SCS-6B, and SCS-6C (alternates)

Sites SCS-6A and SCS-6B are located near the northern COB and are chosen to recover the oldest oceanic crust and the oldest sedimentary rocks in the East Sub-basin to test the hypothesis that the opening of the SCS occurred here first around 32 Ma (Figs. **F2, F4, F7**). This part of the basin shows the deepest basement and is likely the oldest among the sub-basins based on magnetic anomalies (Taylor and Hayes, 1980, 1983; Pautot et al., 1986; Briais et al., 1993). Both sites are also located near magnetic Anomaly 11, the oldest anomaly identified by Taylor and Hayes (1980) and Briais et al. (1993) and hence will provide key calibrations between ages estimated from magnetic anomalies and those from biostratigraphy, radiometric dating, and magnetostratigraphy.

These two sites are located ~60–65 km south of Site 1148, which is located within the COT and recovered an important stratigraphic sequence spanning the Oligocene to present (Wang, Prell, Blum, et al., 2000; Li et al., 2004; Wang and Li, 2009). These sites

together will help address key problems in the early tectonic transition and associated paleoenvironmental changes from rifting to drifting.

Site SCS-6C is located on a basement high between the extended continental crust and the oceanic basin (Fig. F7). Similar conspicuous basement high features can be found on the COB in many other seismic profiles and therefore represent an important tectonic structure. The true lithology and formation mechanism of this basement high is still speculative; it could be a volcanic extrusion associated with early continental breakup and the onset of seafloor spreading, extruded lower crust materials from preferential lower crust extension, exhumed mantle materials, or a basement high composed of Mesozoic rocks. Coring at this location will help pinpoint the exact nature of this structure and improve our understanding of early seafloor spreading processes.

Sites SCS-3G (primary), SCS-3F (backup primary), SCS-3E, SCS-3H, and SCS-3I (alternates)

These five sites are located in the East Sub-basin. Primary Site SCS-3G is located near the relict spreading ridge and the youngest magnetic anomaly (Figs. F2, F4, F7), and coring here will help determine the termination age of seafloor spreading in the East Sub-basin. The thick overlying sediments at this site will also provide important constraints on the evolution of the ridge and associated late-stage magmatism. The alternate sites will achieve similar goals to those for primary Site SCS-3G. Alternate Site SCS-3H, south of the spreading center, is located near identified magnetic Anomalies C5e and C6. These sites will allow correlation of ages from magnetic anomalies to biostratigraphic, magnetostratigraphic, and radiometric ages. Composition and magnetic susceptibility measurements from basement rocks will help to explain the sharp differences in magnetic amplitudes and strikes between the East and Southwest Sub-basins. Furthermore, this site will allow testing of the hypothesis that the East Sub-basin formed in an area already floored by oceanic crust (Pautot et al., 1986).

Sites SCS-4B (primary), SCS-4C (backup primary), SCS-4D, SCS-4E, and SCS-4F (alternates)

Owing to the marked contrast between the Southwest and East Sub-basins (Fig. F4; Table T1) (Yao, 1995; Jin et al., 2002; Li et al., 2007b), it is justifiable to question whether rifting and drifting within these two sub-basins was synchronous or diachronous and how they evolved in comparison to the Northwest Sub-basin. Sites SCS-4B and SCS-4C are located in the Southwest Sub-basin near the relict spreading center and magnetic Anomaly C5e identified by Briais et al. (1993) (Figs. F2, F4, F8). To-

gether with Sites SCS-3G and SCS-3H in the East Sub-basin, coring at one of these sites will help to explain the sharp differences in magnetic amplitude and strike between the East and Southwest Sub-basins and test the hypothesis that the Southwest Sub-basin was initiated by continental rifting, a formation mechanism that might be in sharp contrast to that of the East Sub-basin (Pautot et al., 1986). Coring will help determine the age of this sub-basin and correlate ages from magnetic anomalies with biostratigraphic, magnetostratigraphic, and radiometric ages. The apparent weak magnetizations in basement rocks will be examined via studies of chemical compositions and measurements of magnetic susceptibility.

Alternate Sites SCS-4D, SCS-4E, and SCS-4F are located northwest of Sites SCS-4B and SCS-4C. Together they form a sampling transect in the Southwest Sub-basin (Fig. **F9**) and would achieve similar objectives to those of the primary and backup primary sites in this sub-basin. These alternate sites are all located on basement highs, with sedimentary cover no thicker than ~300 m. Based on our interpretation of seismic and regional magnetic data, we conclude that these basement highs are not younger volcanic extrusions; they show clear magnetic anomalies typical of other oceanic crust (e.g., Fig. **F4**). In particular, Sites SCS-4E and SCS-4F are located on the uplifted shoulders of the relict spreading center, and rock samples cored here will place immediate constraints on cessation of seafloor spreading of the Southwest Sub-basin and on the terminal processes of oceanic crustal accretion and postspreading volcanism.

Sites SCS-2C and SCS-2D (alternates)

As mentioned above, two striking magnetic anomalies (M1 and M2) in the East Sub-basin further divide the sub-basin into a central part with strong magnetic strengths bounded by M1 and M2 and two weakly magnetized parts (C1 and C1′, respectively) near the two conjugate continental margins (Fig. **F4**). Based on traditional interpretations (Taylor and Hayes, 1980, 1983; Briais et al., 1993), these two anomalies correspond to magnetic Anomaly C8 (~26 Ma), which is most likely linked to a large-scale magmatic and compressional event all along the Chinese continental margin (Wang, Prell, Blum, et al., 2000; Li et al., 2004; Su et al., 2010; Li and Song, 2012). Ridge jump is another favored explanation, although Briais et al. (1993) suggested that a minor ridge jump occurred after magnetic Anomaly C7 rather than during C8.

Alternate Sites SCS-2C and SCS-2D are located near magnetic Anomalies C7 and C8 (Figs. **F2, F4**). At these sites, we will test various hypotheses regarding the age and mechanism of the presumed ridge jump through an integrated age calibration with magnetic anomalies, biostratigraphy, radiometric dating, and magnetostratigraphy

and test alternative hypotheses on regional transformations in magmatism and stress field (and consequently in spreading rate). Magnetization measurements will help us to investigate the causes of the sharp increase in the magnetic amplitude of magnetic Anomaly C8.

Site SCS-1C (alternate)

This site is located in magnetic Zone A of the northeasternmost SCS near the Manila Trench (Figs. **F2, F4**). This northeastern area is characterized by 11–15 km thick crust that is either thinned and magmatically modified continental crust (Nissen et al., 1995; Wang et al., 2006) or thick oceanic crust (Hsu et al., 2004; Yeh et al., 2010). Furthermore, part of the area interpreted as thick oceanic crust may be as old as 37 Ma, some 5+ m.y. older than other oceanic crust of the SCS (Hsu et al., 2004), whereas an adjacent area is possibly a remnant of the proto-SCS (Yeh et al., 2010). The impact of coring here could be very substantial if initial spreading is confirmed to have begun around 37 Ma, which could eliminate some of the existing models proposed for the SCS opening. Conversely, if thin continental crust is cored, it would document a globally significant 150–200 km wide zone of extended crust. This result would also offer better understanding of the rifting history of this margin, including the transition from Mesozoic subduction to Paleogene rifting and subsequent spreading.

In addition to answering questions about the fundamental nature of the northeastern SCS, coring in this area would also test contrasting regional tectonic models that suggest different sizes for the initial SCS. Most tectonic reconstructions argue that the northern SCS passive margin extended northeast of present-day Taiwan, substantially larger than at present (Teng, 1990; Hall, 2002; Clift et al., 2003); however, Sibuet and Hsu (1997) and Sibuet et al. (2002) argued that prior to 15 Ma the Ryukyu subduction zone extended south to the northeasternmost SCS. In this interpretation an abandoned portion of the Philippine Sea plate, formerly subducting beneath the southwest extension of the Ryukyu arc, may exist in this area southwest of Taiwan. Drilling at Site SCS-1C would directly test this hypothesis.

Drilling and coring operations

The overall primary operations plan and time estimates for Expedition 349 are summarized in Table **T3.** We have also developed a backup operations plan, which is summarized in Table **T4.** Multiple alternate sites have been selected for each of the primary sites to allow for the best chance to achieve the expedition objectives within the amount of time available. Proposed operations plans for all sites available for the

expedition are summarized in Table **T5.** Time estimates are based on formation lithologies and depths inferred from seismic and regional geological interpretation, including prior drilling in the area during Leg 184 (Wang, Prell, Blum, et al., 2000). After departing from Manila, Philippines, we will transit for ~1 day to the first site and prepare for drilling operations.

Primary operations plan

In order to address the expedition objectives to date the onset and cessation of seafloor spreading in the SCS and to examine the differences between the East and Southwest Sub-basins, the primary operations plan includes coring 100 m into basement at three sites: SCS-3G, SCS-6A, and SCS-4B (Table **T3**). We propose a basement penetration of 100 m at each site to guarantee obtaining the amount of fresh material necessary for studying lithology, geochemistry, physical properties, and affiliations of basement rocks. Additionally, drilling ~100 m into basement should recover enough lava flows (20–45) to average out secular variations in the paleomagnetic measurements and to establish the paleolatitude of each site.

Site 1148 (ODP Leg 184) and Sites SCS-6A and SCS-3G (Expedition 349) together form a sampling transect from the COT to the relict spreading ridge (Fig. **F7**). Reaching basement at Sites SCS-3G and SCS-6A would allow dating of the oldest and youngest oceanic crust in the East Sub-basin. This drilling strategy is strongly endorsed by the participants of the 2012 SCS international workshop held at Tongji University (People's Republic of China; Li et al., 2012). Coring to basement at a site in the Southwest Sub-basin (Site SCS-4B) will address questions regarding the evolution of different sub-basins of the SCS, which show distinct differences in magnetic character (Fig. **F4**). Together, coring basement rocks at these three primary sites would sample a range of distinct mantle and crustal compositions in different sub-basins, offering a means to investigate such important issues as the geochemical evolution of the mantle from the onset to the cessation of seafloor spreading, temporal and spatial scales of mantle convection, and lithosphere-mantle interactions.

There is unanimous support from the 2012 SCS international workshop for a deep hole to obtain the oldest ocean crust near the northern COB (Li et al., 2012). Sites SCS-6A and SCS-6B (alternate) are designed to achieve this goal. These sites require a thick penetration of up to ~1930 mbsf. In order to recover the oldest oceanic basement basalts and the oldest sediments deposited at the onset of seafloor spreading, but at the same time retain reasonable core recovery and on-site time, the primary operations plan adopts the following strategy:

1. Complete coring at Site SCS-3G first. This site requires a total penetration of 1061 m (961 m of sediments and 100 m of basement), with the oldest sediments estimated to be ~15 Ma. At this site we plan a single hole, with advanced piston corer (APC) coring to refusal (~200 mbsf), followed by XCB coring to refusal. A free-fall funnel (FFF) will be dropped to allow for reentry before changing to the RCB, which should reach the target depth of 100 m into basement.
2. At Site SCS-6A, drilling without coring to ~900 mbsf and then coring the remaining ~1030 m with the RCB. A reentry system including three strings of casing will be required at this site for deep coring and logging. Drilling through the top 900 m requires approval by the EPSP; if this strategy is not approved, then complete coring of the section will be required (see **"Backup operations plan"**). Drilling without coring is proposed because Site SCS-3G will record essentially the same shallow sedimentary section that will be drilled through at Site SCS-6A. Furthermore, Site 1148 is only ~65 km north of Site SCS-6A, and the sedimentary section recovered at Site 1148 can provide some guidance to the shallow lithologies of Site SCS-6A (Figs. **F2, F4, F7**).
3. Complete coring of Site SCS-4B, which requires a total penetration of 965 m (865 m of sediment and 100 m of basement). A single hole is planned for this site, with APC coring to refusal (~200 mbsf), followed by XCB coring to refusal. After dropping a FFF, the hole will be reentered with the RCB to reach the target depth of 100 m of basement.

Nonmagnetic core barrels, drill collars, and shoes/core catcher subs (if available for the RCB) will be used for APC and RCB coring operations at all sites. In addition, the FlexIT tool will be deployed above the core barrel during APC operations so that the cores can be oriented.

Backup operations plan

Drilling through the top ~900 m of sediment at Site SCS-6A, as proposed in the primary operations plan (Table **T3**), requires approval from EPSP and the Texas A&M Safety Panel, which has not yet been granted. In case either of these panels denies this request, we have developed a backup operations plan (Table **T4**), as complete coring at Site SCS-6A will take a substantial amount of the operations time available for the expedition. Because reaching basement at Site SCS-6A (or alternate Site SCS-6B) is one of the highest priorities of the expedition, full coring will significantly reduce the amount of time available to reach basement at two other sites. Thus, the backup operations plan includes sites where basement can be penetrated at shallower depths

than the sites included in the primary operations plan. The backup operations plan includes coring at Sites SCS-3F, SCS-6A, and SCS-4C. The backup operations plan adopts the following strategy:

1. Complete coring at Site SCS-3F, which requires penetration of 197 m of sediment and 100 m of basement. This may be completed in one hole, with APC coring to refusal, which should recover the entire sedimentary section, although XCB coring will be used if APC coring does not reach basement. A FFF may be dropped to allow for reentry with the RCB to core 100 m of basement.
2. Complete coring at Site SCS-6A in three holes. The first hole will be cored to refusal with the APC (~200 mbsf), followed by XCB coring to refusal. The hole will then be conditioned and logged with the triple combo and FMS-sonic tool strings (see **"Downhole measurements strategy"**). The second hole will be to detect the depth of the seafloor and to perform a jet-in test for the 20 inch casing string that will be deployed as part of the reentry system in the third hole. A reentry system with three strings of casing will be deployed in the third hole to the depth reached in the first (APC/XCB) hole. The RCB will then be used to reach the target depth of ~1930 mbsf, with one bit change planned at ~1830 mbsf before coring basement.
3. Complete coring at Site SCS-4C, which requires penetration of 689 m of sediment and 100 m of basement. This will be completed in one hole, with APC coring to refusal (~200 mbsf), followed by XCB coring, which should recover the remainder of the sediment section. A FFF will be dropped and the hole reentered with the RCB to recover ~100 m of basement.

Nonmagnetic core barrels, drill collars, and shoes/core catcher subs (if available for the RCB) will be used for APC and RCB coring operations at all sites. In addition, the FlexIT tool will be deployed above the core barrel during APC operations so that the cores can be oriented.

Table **T5** summarizes the proposed operations for all 16 sites (primary and alternate) approved for Expedition 349. This table also summarizes the different operational options for Sites SCS-6A and SCS-6B (drilling through the top ~900 m or full coring). Multiple alternate sites were identified near each of the proposed primary sites because reaching and coring 100 m of basement at the primary sites is operationally challenging (see **"Risks and contingency"**). Many of these alternate sites would reach basement at shallower penetration depths, offering options during the expedition should reaching basement at any of the primary sites not be possible.

Risks and contingency

A number of undersea telecommunications cables cross the SCS. Although none are located in the vicinity of the proposed sites, a camera survey will be performed at each site prior to spudding. The highest cable density occurs in the Luzon Straight and the northeasternmost SCS, where alternate Site SCS-1C is located.

The time available to complete coring operations at the three preferred primary sites during the expedition is very limited, and this may well be the biggest risk to achieving all of the expedition objectives. Several steps have been taken to mitigate this problem, but if any of the primary sites consume more time than has been allocated, it may become necessary to substitute less desirable alternate sites that require less operations time into the schedule. If too much time has been used at any of the primary sites, it may become impossible to achieve all of the objectives at the remaining primary sites.

If Site SCS-6A is drilled to the planned depth, it will be the third deepest hole in Deep Sea Drilling Project/ODP/Integrated Ocean Drilling Program history. The depth of this hole and the basement objective at the bottom of the hole present several challenges for successful drilling. Hole stability is always a risk during coring operations, and the longer the open-hole sections, the higher the risk. Casing has been planned to 900 mbsf to mitigate the risk of hole collapse and to provide a smaller annulus for improved annular velocity for hole cleaning. Hole cleaning also becomes a problem in the deeper sections of the hole, particularly when dense basement material is cored. Additional mud sweeps with larger volumes of mud will be planned for this section. The same problems apply to the other primary sites, but no casing has been planned to achieve the depth objectives. Lower annular velocities will make hole cleaning more difficult in the deeper sections of these holes. Increasing flow rates to ensure hole cleaning will likely result in washed-out sections of sediment in the upper part of the hole. This can also cause hole stability problems toward the end of the drilling process.

FFFs have been planned for primary Sites SCS-3G and SCS-4B (as well as many of the alternate sites) to decrease the amount of time allocated to reaching the planned objective. There are several risks associated with FFF deployment. The FFF can be dislodged while pulling out of the hole. The FFF can become buried or impossible to use for reentry. The use of the FFF leaves the open-hole section open longer, which can contribute to hole instability. The contingency plan is to redrill the APC/XCB section

with an RCB bit with a center bit installed. This will require additional time and will put more strain on achieving expedition objectives in the time allocated.

A stuck drill string is always a risk during coring operations and can consume expedition time while attempting to free the stuck drill string or in the worst case, severing the stuck drill string. This can result in the complete loss of the hole, lost equipment, and lost time while starting a new hole. The *JOIDES Resolution* carries sufficient spare drilling equipment to enable the continuation of coring, but the time lost to the expedition can be significant.

Downhole measurements strategy

Wireline logging

The downhole measurement plan aims to provide continuous stratigraphic coverage of in situ formation properties at all three Expedition 349 sites. Both sedimentary and basement intervals will be logged, but the main focus is characterizing the basement section. Downhole logging data will provide the only stratigraphic data where core recovery is incomplete, which is likely when sites are single-cored with XCB and RCB coring.

The two standard Integrated Ocean Drilling Program tool strings will be deployed at each logged site, and additional tool strings may be deployed at Site SCS-6A (or alternate Site SCS-6B) if conditions and time permit. The first run will be the triple combo tool string, which logs formation resistivity, density, porosity, NGR, and borehole diameter. The GPIT will be added to the triple combo because it includes a fluxgate magnetometer that can provide information on the magnetization of the basement rocks. The borehole diameter log provided by the caliper on the density tool will allow assessment of hole conditions (e.g., washouts of sandy beds), log quality, and the potential for success of the following runs. The second run will be the FMS-sonic tool string, which provides an oriented resistivity image of the borehole wall and logs of formation acoustic velocity, NGR, GPIT magnetometry, and borehole diameter. To provide a link between borehole stratigraphy and the seismic section, sonic velocity and density data will be combined to generate synthetic seismograms for detailed well-seismic correlations. Details of the logging tools are available at **iodp.ldeo.columbia.edu/TOOLS_LABS/tools.html.**

In the primary operations plan, the upper ~900 m of Site SCS-6A/6B would not be cored or logged, apart from NGR logs, which obtain a good but attenuated signal through casing and pipe. However, in the backup operations plan, the upper 900 m of this site would be logged with the triple combo and FMS-sonic tool strings. Additional tool strings may be run in the lower half of Site SCS-6A/6B, depending on the condition of the borehole and the time available. A check shot survey may be run using the Versatile Seismic Imager (VSI), with a station spacing of ~25 m where the borehole diameter is narrow enough to give good coupling of the tool's geophone with the borehole wall. The objective would be to directly establish the link between lithostratigraphic depths in the borehole and reflectors in the seismic profiles. The seismic source for the check shots will be a generator-injector (GI) air gun, and its deployment is subject to the Integrated Ocean Drilling Program marine mammal policy; the check shot survey would have to be postponed or cancelled if policy conditions are not met. Another possible additional tool string is the Ultrasonic Borehole Imager (UBI), which logs 360° ultrasonic amplitude and radius images of the borehole wall. This would be useful to map the features, fractures, and dip and strike directions, particularly in the basement section. Finally, the Lamont-Doherty magnetic logging tools, the magnetometer tool (MMM) and the magnetic susceptibility tool (MSS), would provide accurate magnetic field and susceptibility information for both the basement and sediment sections. Both tools should be available during the expedition, although temperatures at the base of the Site SCS-6A/6B borehole will probably exceed their temperature ratings (~70°C). These additional tool strings will also be available to run at the other expedition sites, if time and hole conditions permit.

Formation temperature measurements

Temperature measurements are planned for all sites with APC coring to reconstruct the thermal gradient at each location; the results will be compared with temperature measurements of nearby ODP Leg 184 sites (Clift et al., 2001). Typically, ~3–5 measurements are made at one hole per site using the advanced piston corer temperature tool (APCT-3), potentially supplemented by the Sediment Temperature Tool (SET) if necessary where sediments are more consolidated.

Risks and contingency

There are several risks involved in logging the very deep holes that are planned for Expedition 349. First, the upper parts of the holes will have been open for >7 days before logging, and high levels of fluid circulation will have been used to raise the cut-

tings and clear the hole. Therefore, the hole will likely be washed out (wide) where there is unlithified sediment, and log quality will be reduced for those tools that need good contact with the borehole wall (density, porosity, FMS resistivity images, VSI check shots).

Secondly, there will be a risk of bridging where the hole closes up. This would mean either not reaching the total depth of the hole, or, in the worst case scenario, getting a tool string stuck in the hole. A good guide to this will be the conditions during drilling and a wiper trip. If the risk is considered to be significant, the radioactive source will be left out of the density tool.

Thirdly, there is a high geothermal gradient in the SCS (e.g., 84°C/km at nearby Site 1148; Wang, Prell, Blum, et al., 2000; Clift et al., 2001). If the same gradient exists at Site SCS-6A/6B, the temperature at the bottom of the hole would reach ~160°C. Most of the Schlumberger logging tools are rated to 175°C, and because the borehole fluid temperature would take time to warm up to the formation temperature, most tools should be able to be deployed. However, temperatures will very likely be too hot for magnetic logging tools. The APCT-3 temperature measurements will provide a valuable guide to the temperature gradients for at least the shallow depths at the Expedition 349 sites prior to logging.

Sampling and data sharing strategy

Shipboard and shore-based researchers should refer to the current Integrated Ocean Drilling Program Sample, Data, and Obligations policy (**www.iodp.org/program-policies/**). Any policy changes that may occur with the beginning of the International Ocean Discovery Program will be distributed to the Shipboard Scientific Party and interested shore-based scientists as soon as possible. This policy describes the review and approval procedure for receiving samples and data, as well as the publication obligations incurred by sample and data recipients. All requests for samples and data must be approved by the Sample Allocation Committee (SAC), which is composed of the Co-Chief Scientists, Expedition Project Manager, and USIO curator onshore and curatorial representative onboard the ship.

Scientists must submit research plans using the Sample and Data Request Database (**web.iodp.tamu.edu/sdrm/**) ~3 months before the beginning of the expedition. The preexpedition planning process is necessary to coordinate the research to be conducted and to ensure that the expedition scientific objectives are achieved. Based on

sample requests (shore based and shipboard) submitted by this deadline, the SAC will prepare a tentative sampling and data-sharing plan for shipboard and postexpedition activities, which will be revised on the ship as dictated by recovery and expedition objectives. The sampling plan will be subject to modification depending upon the actual material recovered and collaborations that may evolve between scientists during the expedition. The SAC must approve modifications to the sampling plan during the expedition.

All sample frequencies and sizes must be justified scientifically and will depend on core recovery, the full spectrum of other requests, and the expedition objectives. Some redundancy of measurement is unavoidable, but minimizing the duplication of measurements among the shipboard party and identified shore-based collaborators will be a factor in evaluating sample requests. All shipboard scientists are expected to collaborate and cooperate within the framework of this plan.

The planned operations for this expedition minimize duplicate coring in order to maximize time to reach the highest priority deep drilling objectives, so each site is likely to have only one copy of the lithologic section for core description and sampling. The minimum permanent archive will be the standard archive half of each core. If some critical intervals are recovered (e.g., prominent unconformities, sediment/basement contacts), there may be considerable demand for samples from a limited amount of cored material. These intervals may require modifications to the sampling plan (e.g., special handling, reduced sample size, or deferring sampling until after the expedition is completed). Although shipboard sampling for materials with ephemeral properties (e.g., whole rounds for pore water and microbiological samples) is a priority, these may be limited or shifted away from critical boundaries.

Sampling for individual scientist's postexpedition research may be conducted during the expedition or may be deferred until postexpedition based on core recovery, available time, and the scope of samples requested. Following Expedition 349, cores will be delivered to the Integrated Ocean Drilling Program Kochi Core Center (KCC) in Kochi, Japan. All collected expedition cores and data will be protected by a 1 y postexpedition moratorium, during which time data and samples will be available only to the Expedition 349 science party and approved shore-based participants. This moratorium will extend either 1 y from the end of the expedition or 1 y from the completion of a postexpedition sampling party at KCC if most samples are taken at that time.

References

Barckhausen, U., and Roeser, H.A., 2004. Seafloor spreading anomalies in the South China Sea revisited. *In* Clift, P., Wang, P., Kuhnt, W., and Hayes, D. (Eds.), *Continent-Ocean Interactions within East Asian Marginal Seas*. Geophys. Monogr., 149:121–125. **doi:10.1029/149GM07**

Bleil, U., and Petersen, N., 1983. Variations in magnetization intensity and low-temperature titanomagnetite oxidation of ocean floor basalts. *Nature (London, U. K.),* 301(5899):384–388. **doi:10.1038/301384a0**

Braitenberg, C., Wienecke, S., and Wang, Y., 2006. Basement structures from satellite-derived gravity field: South China Sea ridge. *J. Geophys. Res.: Solid Earth,* 111(B5):B05407. **doi:10.1029/2005JB003938**

Briais, A., Patriat, P., and Tapponnier, P., 1993. Updated interpretation of magnetic anomalies and seafloor spreading stages in the South China Sea: implications for the Tertiary tectonics of Southeast Asia. *J. Geophys. Res.: Solid Earth,* 98(B4):6299–6328. **doi:10.1029/92JB02280**

Castillo, P.R., Carlson, R.W., and Batiza, R., 1991. Origin of Nauru Basin igneous complex: Sr, Nd, and Pb isotope and REE constraints. *Earth Planet. Sci. Lett.,* 103(1–4):200–213. **doi:10.1016/0012-821X(91)90161-A**

Cheng, W.-B., Wang, C., Shyu, C.-T., and Shin, T.-C., 1998. A three-dimensional V_p model of the southeastern Taiwan area and its tectonic implications. *Terr. Atmos. Ocean Sci.,* 9(3):425–452. **http://tao.cgu.org.tw/pdf/v93p425.pdf**

Chung, S.-L., Sun, S., Tu, K., Chen, C.-H., and Lee, C., 1994. Late Cenozoic basaltic volcanism around the Taiwan Strait, SE China: product of lithosphere-asthenosphere interaction during continental extension. *Chem. Geol.,* 112(1–2):1–20. **doi:10.1016/0009-2541(94)90101-5**

Clift, P., Lee, G.H., Duc, N.A., Barckhausen, U., Long, H.V., and Zhen, S., 2008. Seismic reflection evidence for a Dangerous Grounds miniplate: no extrusion origin for the South China Sea. *Tectonics,* 27(3):TC3008. **doi:10.1029/2007TC002216**

Clift, P.D., Lin, J., and ODP Leg 184 Scientific Party, 2001. Patterns of extension and magmatism along the continent-ocean boundary, South China margin. *In* Wilson, R.C.L., Beslier, M.-O., Whitmarsh, R.B., Froitzheim, N., and Taylor, B. (Eds.), *Non-Volcanic Rifting of Continental Margins: A Comparison of Evidence from Land and Sea*. Geol. Soc. Spec. Publ., 187:489–510. **doi:10.1144/GSL.SP.2001.187.01.24**

Clift, P.D., Schouten, H., and Draut, A.E., 2003. A general model of arc-continent collision and subduction polarity reversal from Taiwan and the Irish Caledonides. *In* Larter, R.D., and Leat, P.T. (Eds.), *Intra-Oceanic Subduction Systems: Tectonic and Magmatic Processes*. Geol. Soc. Spec. Publ., 219(1):81–98. **doi:10.1144/GSL.SP.2003.219.01.04**

Clift, P.D., and Sun, Z., 2006. The sedimentary and tectonic evolution of the Yinggehai-Song Hong Basin and the southern Hainan margin, South China Sea: implications for Tibetan uplift and monsoon intensification. *J. Geophys. Res.: Solid Earth,* 111(B6):B06405. **doi:10.1029/2005JB004048**

Cullen, A., Reemst, P., Henstra, G., Gozzard, S., and Ray A., 2010. Rifting of the South China Sea: new perspectives. *Pet. Geosci.,* 16(3):273–282. **doi:10.1144/1354-079309-908**

Cullen, A.B., 2010. Transverse segmentation of the Baram-Balabac Basin, NW Borneo: refining the model of Borneo's tectonic evolution. *Pet. Geosci.,* 16(1):3–29. **doi:10.1144/1354-079309-828**

Damuth, J.E., 1980. Quaternary sedimentation processes in the South China basin as revealed by echo-character mapping and piston-core studies. *In* Hayes, D.E. (Ed.), *The Tectonic and Geologic Evolution of Southeast Asian Seas and Islands*. Geophys. Monogr., 23:105–125. **doi:10.1029/GM023p0105**

Dyment, J., and Arkani-Hamed, J., 1995. Spreading-rate-dependent magnetization of the oceanic lithosphere inferred from the anomalous skewness of marine magnetic anomalies. *Geophys. J. Int.,* 121(3):789–804. **doi:10.1111/j.1365-246X.1995.tb06439.x**

Dyment, J., Arkani-Hamed, J., and Ghods, A., 1997. Contribution of serpentinized ultramafics to marine magnetic anomalies at slow and intermediate spreading centres: insights from the shape of the anomalies. *Geophys. J. Int.,* 129(3):691–701. **doi:10.1111/j.1365-246X.1997.tb04504.x**

Fan, W., and Menzies, M., 1992. Destruction of aged lower lithosphere and accretion of asthenosphere mantle beneath eastern China. *Geotecton. Metallog.,* 16:171–180.

Fedo, C.M., Sircombe, K.N., and Rainbird, R.H., 2003. Detrital zircon analysis of the sedimentary record. *In* Hanchar, J.M., and Hoskin, P.W.O. (Eds.), *Zircon*. Rev. Mineral. Geochem., 53(1):277–303. **doi:10.2113/0530277**

Flower, M.F.J., Russo, R.M., Tamaki, K., and Hoang, N., 2001. Mantle contamination and the Izu-Bonin-Mariana (IBM) "high-tide mark": evidence for mantle extrusion caused by Tethyan closure. *Tectonophysics,* 333(1–2):9–34. **doi:10.1016/S0040-1951(00)00264-X**

Franke, D., Barckhausen, U., Baristeas, N., Engels, M., Ladage, S., Lutz, R., Montano, J., Pellejera, N., Ramos, E.G., and Schnabel, M., 2011. The continent–ocean transition at the southeastern margin of the South China Sea. *Mar. Pet. Geol.,* 28(6):1187–1204. **doi:10.1016/j.marpetgeo.2011.01.004**

Goldstein, S.J., 1995. Uranium-series chronology of subsurface basalts, 9°31′N East Pacific Rise. *In* Batiza, R., Storms, M.A., and Allan, J.F. (Eds.), 1995. *Proc. ODP, Sci. Results,* 142: College Station, TX (Ocean Drilling Program), 37–39. **doi:10.2973/odp.proc.sr.142.115.1995**

Goldstein, S.J., Murrell, M.T., Janecky, D.R., Delaney, J.R., and Clague, D.A., 1991. Geochronology and petrogenesis of MORB from the Juan de Fuca and Gorda Ridges by ^{238}U-^{230}Th disequilibrium. *Earth Planet. Sci. Lett.,* 107(1):25–41. **doi:10.1016/0012-821X(91)90041-F**

Goldstein, S.J., Perfit, M.R., Batiza, R., Fornari, D.J., and Murrell, M.T., 1994. Off-axis volcanism at the East Pacific Rise detected by uranium-series dating of basalts. *Nature (London, U. K.),* 367(6459):157–159. **doi:10.1038/367157a0**

Grimes, C.B., John, B.E., Kelemen, P.B., Mazdab, F.K., Wooden, J.L., Cheadle, M.J., Hanghøj, K., and Schwartz, J.J., 2007. Trace element chemistry of zircons from oceanic crust: a method for distinguishing detrital zircon provenance. *Geology,* 35(7):643–646. **doi:10.1130/G23603A.1**

Haile, N.S., 1973. The recognition of former subduction zones in Southeast Asia. *In* Tarling, D.H., and Runcorn, S.K., (Eds.), *Implications of Continental Drift to the Earth Sciences*, Vol. 2: London (Academic Press), 885–892.

Hall, R., 1996. Reconstructing Cenozoic SE Asia. *In* Hall, R., and Blundell, D.J. (Eds.), *Tectonic Evolution of Southeast Asia*. Geol. Soc. Spec. Publ., 106(1):153–184. **doi:10.1144/GSL.SP.1996.106.01.11**

Hall, R., 2002. Cenozoic geological and plate tectonic evolution of SE Asia and the SW Pacific: computer-based reconstructions, model and animations. *J. Asian Earth Sci.,* 20(4):353–431. **doi:10.1016/S1367-9120(01)00069-4**

Hall, R., and Morley, C.K., 2004. Sundaland basins. *In* Clift, P.D., Kuhnt, W., Wang, P., and Hayes, D. (Eds.), *Continent-Ocean Interactions with East Asian Marginal Seas*. Geophys. Monogr., 149:55–85. **doi:10.1029/149GM04**

Hamilton, W.B., 1979. Tectonics of the Indonesian Region. *U.S. Geol. Surv. Prof. Pap.,* 1078.

Hayes, D.E., and Nissen, S.S., 2005. The South China Sea margins: implications for rifting contrasts. *Earth Planet. Sci. Lett.,* 237(3–4):601–616. **doi:10.1016/j.epsl.2005.06.017**

Hayes, D.E., Nissen, S.S., Buhl, P., Diebold, J., Yao, B., Zeng, W., and Chen, Y., 1995. Throughgoing crustal faults along the northern margin of the South China Sea and their role in crustal extension. *J. Geophys. Res.: Solid Earth,* 100(B11):22435–22446. **doi:10.1029/95JB01867**

Hilde, T., Uyeda, S., and Kroenke, L., 1977. Evolution of the western Pacific and its margin. *Tectonophysics,* 38(1–2):145–165. **doi:10.1016/0040-1951(77)90205-0**

Holloway, N.H., 1982. North Palawan Block, Philippines: its relation to the Asian mainland and role in evolution of South China Sea. *AAPG Bull.,* 66(9):1355–1383. **http://aapgbull.geoscienceworld.org/content/66/9/1355.abstract**

Honza, E., 1995. Spreading mode of backarc basins in the western Pacific. *Tectonophysics,* 251(1–4):139–152. **doi:10.1016/0040-1951(95)00054-2**

Hsu, S.-K., Yeh, Y., Doo, W.-B., and Tsai, C.-H., 2004. New bathymetry and magnetic lineations identifications in the northernmost South China Sea and their tectonic implications. *Mar. Geophys. Res.,* 25(1–2):29–44. **doi:10.1007/s11001-005-0731-7**

Huang, C.-Y., Xia, K., Yuan, P.B., and Chen, P.-G., 2001. Structural evolution from Paleogene extension to latest Miocene–recent arc-continent collision offshore Taiwan: comparison with on land geology. *J. Asian Earth Sci.,* 19(5):619–639. **doi:10.1016/S1367-9120(00)00065-1**

Hutchison, C.S., 1996. The "Rajang accretionary prism" and "Lupar Line" problem of Borneo. *In* Hall, R., and Blundell, D.J. (Eds.), *Tectonic Evolution of Southeast Asia*. Geol. Soc. Spec. Publ., 106(1):247–261. **doi:10.1144/GSL.SP.1996.106.01.16**

Hutchison, C.S., 2004. Marginal basin evolution: the southern South China Sea. *Mar. Pet. Geol.,* 21(9):1129–1148. **doi:10.1016/j.marpetgeo.2004.07.002**

Hutchison, C.S., 2005. *Geology of North-West Borneo:* Amsterdam (Elsevier B.V.). **http://www.sciencedirect.com/science/book/9780444519986**

Jahn, B.-M., Chen, P.Y., and Yen, T.P., 1976. Rb-Sr ages of granitic rocks in southeastern China and their tectonic significance. *Geol. Soc. Am. Bull.,* 87(5):763–776. **doi:10.1130/0016-7606(1976)87<763:RAOGRI>2.0.CO;2**

Jin, Z., Xu, S., and Li, Z., 2002. Inversion of heterogeneous magnetism for seamounts in the South China Sea. *J. Ocean Univ. Qingdao,* 32:926–934. (in Chinese)

Kao, H., Huang, G.-C., and Liu, C.-S., 2000. Transition from oblique subduction to collision in the northern Luzon arc-Taiwan region: constraints from bathymetry and seismic observations. *J. Geophys. Res.: Solid Earth,* 105(B2):3059–3079. **doi:10.1029/1999JB900357**

Koppers, A.A.P., Russell, J.A., Roberts, J., Jackson, M.G., Konter, J.G., Wright, D.J., Staudigel, H., and Hart, S.R., 2011. Age systematics of two young en echelon Samoan volcanic trails. *Geochem., Geophys., Geosyst.,* 12(7):Q07025. **doi:10.1029/2010GC003438**

Lallemand, S., and Jolivet, L., 1986. Japan Sea: a pull apart basin? *Earth Planet. Sci. Lett.,* 76(3–4):375–389. **doi:10.1016/0012-821X(86)90088-9**

Lee, T.-Y., and Lawver, L.A., 1995. Cenozoic plate reconstruction of Southeast Asia. *Tectonophysics,* 251(1–4): 85–138. **doi:10.1016/0040-1951(95)00023-2**

Leloup, P.H., Arnaud, N., Lacassin, R., Kienast, J.R., Harrison, T.M., Trong, T.T.P., Replumaz, A., and Tapponnier, P., 2001. New constraints on the structure, thermochronology, and timing of the Ailao Shan-Red River shear zone, SE Asia. *J. Geophys. Res.: Solid Earth,* 106(B4):6683–6732. **doi:10.1029/2000JB900322**

Li, C.-F., Shi, X., Zhou, Z., Li, J., Geng, J., and Chen, B., 2010. Depths to the magnetic layer bottom in the South China Sea area and their tectonic implications. *Geophys. J. Int.,* 182(3):1229–1247. **doi:10.1111/j.1365-246X.2010.04702.x**

Li, C.-F., and Song, T., 2012. Magnetic recording of the Cenozoic oceanic crustal accretion and evolution of the South China Sea Basin. *Chin. Sci. Bull.,* 57(24):3165–3181. **doi:10.1007/s11434-012-5063-9**

Li, C.-F., Wang, P., Franke, D., Lin, J., and Tian, J., 2012. Unlocking the opening processes of the South China Sea. *Sci. Drill.,* 14:55–59. **doi:10.2204/iodp.sd.14.07.2012**

Li, C.-F., Zhou, Z., Hao, H., Chen, H., Wang, J., Chen, B., and Wu, J., 2008a. Late Mesozoic tectonic structure and evolution along the present-day northeastern South China Sea continental margin. *J. Asian Earth Sci.,* 31(4–6):546–561. **doi:10.1016/j.jseaes.2007.09.004**

Li, C.-F., Zhou, Z., Li, J., Chen, B., and Geng, J., 2008b. Magnetic zoning and seismic structure of the South China Sea ocean basin. *Mar. Geophys. Res.,* 29(4):223–238. **doi:10.1007/s11001-008-9059-4**

Li, C.-F., Zhou, Z., Li, J., Chen, H., Geng, J., and Li, H., 2007a. Precollisional tectonics and terrain amalgamation offshore southern Taiwan: characterizations from reflection seismic and potential field data. *Sci. China, Ser. D: Earth Sci.,* 50(6):897–908. **doi:10.1007/s11430-007-0025-9**

Li, C.-F., Zhou, Z., Li, J., Hao, H., and Geng, J., 2007b. Structures of the northeasternmost South China Sea continental margin and ocean basin: geophysical constraints and tectonic implications. *Mar. Geophys. Res.,* 28(1):59–79. **doi:10.1007/s11001-007-9014-9**

Li, J.-B., Ding, W.-W., Gao, J.-Y., Wu, Z.-Y.,and Zhang, J., 2011. Cenozoic evolution model of the sea-floor spreading in South China Sea: new constraints from high resolution geophysical data. *Chin. J. Geophys.,* 54(6):894–906. **http://www.agu.org/wps/ChineseJGeo/54/06/ljb2.pdf**

Li, Q., Jian, Z., and Li, B., 2004. Oligocene–Miocene planktonic foraminifer biostratigraphy, Site 1148, northern South China Sea. *In* Prell, W.L., Wang, P., Blum, P., Rea, D.K., and Clemens, S.C. (Eds.), *Proc. ODP, Sci. Results,* 184: College Station, TX (Ocean Drilling Program), 1–26. **doi:10.2973/odp.proc.sr.184.220.2004**

Li, Q., Jian, Z., and Su, X, 2005. Late Oligocene rapid transformations in the South China Sea. *In* Wang, P., and Lipps, J. (Eds.), *Marine Micropaleontology of the South China Sea.* Mar. Micropaleontol., 54(1–2):5–25. **doi:10.1016/j.marmicro.2004.09.008**

Lüdmann, T., and Wong, H.K., 1999. Neotectonic regime on the passive continental margin of the northern South China Sea. *Tectonophysics,* 311(1–4):113–138 **doi:10.1016/S0040-1951(99)00155-9**

Lüdmann, T., Wong, H.K., and Wang, P., 2001. Plio-Quaternary sedimentation processes and neotectonics of the northern continental margin of the South China Sea. *Mar. Geol.,* 172(3–4):331–358. **doi:10.1016/S0025-3227(00)00129-8**

Madon, M.B.H., Meng, L.K., and Anuar, A., 2000. Sabah Basin. *In* Leong, K.M. (Ed.), *The Petroleum Geology and Resources of Malaysia.* Kuala Lumpur, Malaysia (Petroliam Nasional Berhad), 499–542.

McIntosh, K.D., Liu, C.-S., and Lee, C.-S., 2012. Introduction to the TAIGER special issue of Marine Geophysical Research. *Mar. Geophys. Res.,* 33(4):285–287. **doi:10.1007/s11001-013-9170-z**

Morley, C.K., 2002. A tectonic model for the Tertiary evolution of strike-slip faults and rift basins in SE Asia. *Tectonophysics,* 347(4):189–215. **doi:10.1016/S0040-1951(02)00061-6**

Nissen, S.S., Hayes, D.E., Yao, B., Zeng, W., Chen, Y., and Nu, X., 1995. Gravity, heat flow, and seismic constraints on the processes of crustal extension: northern margin of the South China Sea. *J. Geophys. Res.: Solid Earth,* 100(B11):22447–22483. **doi:10.1029/95JB01868**

Pautot, G., Rangin, C., Briais, A., Tapponnier, P., Beuzart, P., Lericolais, G., Mathieu, X., Wu, J., Han, S., Li, H., Lu, Y., and Zhao, J., 1986. Spreading direction in the central South China Sea. *Nature (London, U. K.),* 321(6066):150–154. **doi:10.1038/321150a0**

Pubellier, M., Monnier, C., Maury, R., and Tamayo, R., 2004. Plate kinematics, origin and tectonic emplacement of supra-subduction ophiolites in SE Asia. *Tectonophysics,* 392(1–4):9–36. **doi:10.1016/j.tecto.2004.04.028**

Rangin, C., Jolivet, L., and Pubellier, M., 1990. A simple model for the tectonic evolution of Southeast Asia and Indonesia regions for the past 43 m.y. *Bull. Soc. Geol. Fr.,* 6(6):889–905.

Rangin, C., Klein, M., Roques, D., Le Pichon, X., and Trong, L.V., 1995. The Red River fault system in the Tonkin Gulf, Vietnam. *Tectonophysics,* 243(3–4)209–222. **doi:10.1016/0040-1951(94)00207-P**

Ru, K., and Pigott, J.D., 1986. Episodic rifting and subsidence in the South China Sea. *AAPG Bull.,* 70(9):1136–1155. **http://aapgbull.geoscienceworld.org/content/70/9/1136.short**

Schärer, U., Tapponnier, P., Lacassin, R., Leloup, P.H., Dalai, Z., and Ji, S., 1990. Intraplate tectonics in Asia: a precise age for large-scale Miocene movement along the Ailao Shan-Red River shear zone, China. *Earth Planet. Sci. Lett.,* 97(1–2):65–77. **doi:10.1016/0012-821X(90)90099-J**

Schlüter, H.U., Hinz, K., and Block, M., 1996. Tectono-stratigraphic terranes and detachment faulting of the South China Sea and Sulu Sea. *Mar. Geol.,* 130(1–2):39–78. **doi:10.1016/0025-3227(95)00137-9**

Schwartz, J.J., John, B.E., Cheadle, M.J., Miranda, E.A., Grimes, C.B., Wooden, J.L., and Dick, H.J.B., 2005. Dating the growth of oceanic crust at a slow-spreading ridge. *Science,* 310(5748):654–657. **doi:10.1126/science.1116349**

Shi, H., and Li, C.-F., 2012. Mesozoic and early Cenozoic tectonic convergence-to-rifting transition prior to opening of the South China Sea. *Int. Geol. Rev.,* 54(15):1801–1828. **doi:10.1080/00206814.2012.677136**

Sibuet, J.-C., and Hsu, S.-K., 1997. Geodynamics of the Taiwan arc-arc collision. *Tectonophysics,* 274(1–3):221–251. **doi:10.1016/S0040-1951(96)00305-8**

Sibuet, J.-C., Hsu, S.-K., Le Pichon, X., Le Formal, J.-P., Reed, D., Moore, G., and Liu, C.-S., 2002. East Asia plate tectonics since 15 Ma: constraints from the Taiwan region. *Tectonophysics,* 344(1–2):103–134. **doi:10.1016/S0040-1951(01)00202-5**

Smith, W.H.F., and Sandwell, D.T., 1997. Global seafloor topography from satellite altimetry and ship depth soundings. *Science,* 277(5334):1956–1962. **doi:10.1126/science.277.5334.1956**

Song, T., and Li, C.-F., 2012. The opening ages and mode of the South China Sea estimated from high-density magnetic tracks. *Prog. Geophys.,* 27(4):1432–1442.

Su, C., Li, C.-F., and Ge, H.-P., 2010. Characteristics and causes of anomalous reflections on the Oligocene–Miocene transition in the Xihu Depression, East China Sea basin. *J. Mar. Sci.,* 28(4):14–21. (in Chinese)

Sun, Z., Zhong, Z., Keep, M., Zhou, D., Cai, D., Li, X., Wu, S., and Jiang, J., 2009. 3D analogue modeling of the South China Sea: a discussion on breakup pattern. *J. Asian Earth Sci.,* 34(4):544–556. **doi:10.1016/j.jseaes.2008.09.002**

Tapponnier, P., Lacassin, R., Leloup, P.H., Shärer, U., Zhong, D., Wu, H., Liu, X., Ji, S., Zang, L., and Zhong, J., 1990. The Ailao Shan/Red River metamorphic belt: Tertiary left-lateral shear between Indochina and South China. *Nature (London, U. K.),* 343(6257):431–437. **doi:10.1038/343431a0**

Tapponnier, P., Peltzer, G., Le Dain, A.Y., Armijo, R., and Cobbold, P., 1982. Propagating extrusion tectonics in Asia: new insights from simple experiments with plasticene. *Geology,* 10(12):611–616. **doi:10.1130/0091-7613(1982)10<611:PETIAN>2.0.CO;2**

Taylor, B., and Hayes, D.E., 1980. The tectonic evolution of the South China Basin. *In* Hayes, D.E. (Ed.), *The Tectonic and Geologic Evolution of Southeast Asian Seas and Islands*. Geophys. Monogr., 23:89–104. **doi:10.1029/GM023p0089**

Taylor, B., and Hayes, D.E., 1983. Origin and history of the South China Sea Basin. *In* Hayes, D.E. (Ed.), *The Tectonic and Geologic Evolution of Southeast Asian Seas and Islands* (Pt. 2). Geophys. Monogr., 27:23–56. **doi:10.1029/GM027p0023**

Tejada, M.L.G., Mahoney, J.J., Castillo, P.R., Ingle, S.P., Sheth, H.C., and Weis, D., 2004. Pin-pricking the elephant: evidence on the origin of the Ontong Java Plateau from Pb-Sr-Hf-Nd isotopic characteristics of ODP Leg 192 basalts. *In* Fitton, J.G., Mahoney, J.J., Wallace, P.J., and Saunders, A.D. (Eds.), *Origin and Evolution of the Ontong Java Plateau.* Geol. Soc. Spec. Publ., 229(1):133–150. **doi:10.1144/GSL.SP.2004.229.01.09**

Teng, L.S., 1990. Geotectonic evolution of late Cenozoic arc-continent collision in Taiwan. *Tectonophysics,* 183(1–4):57–76. **doi:10.1016/0040-1951(90)90188-E**

Tominaga, M., Teagle, D.A.H., Alt, J.C., and Umino, S., 2009. Determination of the volcanostratigraphy of the oceanic crust formed at superfast spreading ridge: electrofacies analyses of ODP/IODP Hole 1256D. *Geochem., Geophys., Geosyst.,* 10(1):Q01003. **doi:10.1029/2008GC002143**

Tongkul, F., 1994. The geology of northern Sabah, Malaysia: its relationship to the opening of the South China Sea basin. *Tectonophysics,* 235(1–2):131–147. **doi:10.1016/0040-1951(94)90021-3**

Tu, K., Flower, M.F.J., Carlson, R.W., Xie, G., Chen, C-Y., and Zhang, M., 1992. Magmatism in the South China Basin: 1. Isotopic and trace-element evidence for an endogenous Dupal mantle component. *Chem. Geol.,* 97(1–2):47–63. **doi:10.1016/0009-2541(92)90135-R**

Wang, P., 2012. Tracing the life history of a marginal sea—on "The South China Sea Deep" research program. *Chin. Sci. Bull.,* 57(24):3093–3114. **doi:10.1007/s11434-012-5087-1**

Wang, P., Prell, W.L., Blum, P., et al., 2000. *Proc. ODP, Init. Repts.,* 184: College Station, TX (Ocean Drilling Program). **doi:10.2973/odp.proc.ir.184.2000**

Wang, P., and Li, Q. (Eds.), 2009. The South China Sea: paleoceanography and sedimentology. *Dev. Paleoenviron. Res.,* 13.

Wang, T.K., Chen, M.-K., Lee, C.-S., and Xia, K., 2006. Seismic imaging of the transitional crust across the northeastern margin of the South China Sea. *Tectonophysics,* 412(3–4):237–245. **doi:10.1016/j.tecto.2005.10.039**

Wu, F.T., Rau, R.-J., and Salzberg, D., 1997. Taiwan orogeny: thin-skinned or lithospheric collision? *Tectonophysics,* 274(1–3):191–220. **doi:10.1016/S0040-1951(96)00304-6**

Wu, H.-H., Tsai, Y.-B., Lee, T.-Y., Lo, C.-H., Hsieh, C.-H., and Toan, D.V., 2004. 3-D shear wave velocity structure of the crust and upper mantle in South China Sea and its surrounding regions by surface wave dispersion analysis. *Mar. Geophys. Res.,* 25(1–2):5–27. **doi:10.1007/s11001-005-0730-8**

Xiao, G., and Zheng, J., 2004. New opinions about "residual Tethys" in northern South China Sea slope and southern East China Sea. *Geoscience,* 18(1):103–108. (in Chinese)

Xu, Y., Wei, J., Qiu, H., Zhang, H., and Huang, X., 2012. Opening and evolution of the South China Sea constrained by studies on volcanic rocks: preliminary results and a research design. *Chin. Sci. Bull.,* 57(24):3150–3164. **doi:10.1007/s11434-011-4921-1**

Yan, P., Zhou, D., and Liu, Z., 2001. A crustal structure profile across the northern continental margin of the South China Sea. *Tectonophysics,* 338(1):1–21. **doi:10.1016/S0040-1951(01)00062-2**

Yang, J., Feng, X., Fan, Y., and Zhu, S., 2003. An analysis of middle–late Mesozoic tectonics, paleogeography, and petroleum potential in the northeastern South China Sea. *China Offshore Oil and Gas (Geol.),* 17:89–103. **http://en.cnki.com.cn/Article_en/CJFDTOTAL-ZHSD200302002.htm**

Yao, B., 1995. Characteristics and tectonic significance of the Zhongnan-Lile fault. *Geol. Res. South China Sea, Mem.,* 7:1–14. (in Chinese)

Yao, B., Zeng, W., Hayes, D.E., and Spangler, S., 1994. *The Geological Memoir of South China Sea Surveyed Jointly by China and USA:* Wuhan (China Univ. Geosci. Press). (in Chinese)

Yeh, Y.-C., Sibuet, J.-C., Hsu, S.-K., and Liu, C.-S., 2010. Tectonic evolution of the northeastern South China Sea from seismic interpretation. *J. Geophys. Res.: Solid Earth,* 115(B6):B06103. **doi:10.1029/2009JB006354**

Zhang, L., Zhao, M.H., Wang, J., He, E.Y., Ao, W., Qiu, X.L., Xu, H.L., Wei, X.D., and Zhang, J.Z., 2013. The correction of OBS position and recent advances of 3D seismic exploration in the central sub-basin of South China Sea. *Earth Sci.,* 38:33–42. (in Chinese)

Zhou, D., Ru, K., and Chen, H., 1995. Kinematics of Cenozoic extension on the South China Sea continental margin and its implications for the tectonic evolution of the region. *Tectonophysics,* 251(1–4):161–177. **doi:10.1016/0040-1951(95)00018-6**

Zhou, D., Sun, Z., Chen, H., Xu, H., Wang, W., Pang, X., Cai, D., and Hu, D., 2008. Mesozoic paleogeography and tectonic evolution of South China Sea and adjacent areas in the context of Tethyan and Paleo-Pacific interconnections. *Isl. Arc,* 17(2):186–207. **doi:10.1111/j.1440-1738.2008.00611.x**

Zhou, X.M., and Li, W.X., 2000. Origin of late Mesozoic igneous rocks in southeastern China: implications for lithosphere subduction and underplating of mafic magmas. *Tectonophysics,* 326(3–4):269–287. **doi:10.1016/S0040-1951(00)00120-7**

Table T1. Differences between the East and Southwest Sub-basins in the South China Sea.

Attributes	East Sub-basin	Southwest Sub-basin
Water depth	Shallower on average	Deeper on average
Depth to basement	Close (deepens toward margins)	Close (deepens to west)
Heat flow	Lower	Higher
Magnetic strikes	East–west	Northeast–southwest
Magnetic amplitudes	Stronger	Weaker
Magnetic spectra	Preferentially low in high–wave number components	Preferentially high in high–wave number components
Free-air gravity anomalies	Higher	Lower
Curie depths	Mostly deeper	Mostly shallower
Seismicity	Stronger	Weaker

Table T2. Summary of multichannel seismic lines used to locate proposed drill sites, Expedition 349.

Sites	MCS	Acquisition date	Channels	Processing	Stacking/Interval velocity
SCS-2C*	973SCSIO_1c	2001	48	Time migration	
	ZSHL295	2008	480	Time migration	
SCS-2D*	ZSH275	2008	480	Time migration	
	ZSHL295	2008	480	Time migration	
SCS-6A	08ec1573	2008	480	Time migration	Yes
	08ec2678	2008	480	Time migration	Yes
SCS-6B*	08ec1602	2008	480	Time migration	Yes
	08ec2696	2008	480	Time migration	Yes
SCS-6C*	973SCSIO01e	2001	48	Time migration	
SCS-3E*	BGR08-124	2008	312	Time migration	
	SO49-017a	1987	48	Time migration	
SCS-3F†	BGR08-124	2008	312	Time migration	
	BGR08-123	2008	312	Time migration	
SCS-3G	973SCSIO01e	2001	48	Time migration	
	SO49-017a	1987	48	Time migration	
SCS-3H*	BGR08-123	2008	312	Time migration	
	SO49-018_1	1987	48	Time migration	
SCS-3I*	BGR08-123	2008	312	Time migration	
	973SCSIO01e	2001	48	Time migration	
SCS-4B	973SCSIO_2b	2001	48	Time migration	
	SIOSOA_NDS3			Time migration	
SCS-4C†	973SCSIO_2b	2001	48	Time migration	
	A3B6	2008	240	Time migration	
SCS-4D*	SIOSOA_NDS3			Time migration	
	A3B6	2008	240	Time migration	
SCS-4E*	SIOSOA_NDS3			Time migration	
SCS-4F*	SIOSOA_NDS3			Time migration	
SCS-1C*	973GMGS_2	2001	240	Time migration	
	ACT105	1996	6	Time migration	

* = Alternate site. † = Primary site for backup operations plan. Site SCS-6A is a primary site for both the operations plan and the backup operations plan.

Table T3. Expedition 349 operations plan, primary sites.

Expedition 349 (P735-CPP2) - South China Sea

Operations Plan Summary

Site No.	Location (Latitude Longitude)	Seafloor Depth (mbrf)	Operations Description	Transit (days)	Drilling Coring (days)	Log (days)
Manila			Begin Expedition 3.0 port call days			
			Transit ~245 nmi to SCS-3G @ 10.5	1.0		
SCS-3G	15°22.5480'N	4224	Hole A - APC/XCB coring to 961 mbsf, drop FFF and RCB core from 961 to 1061 mbsf		11.1	1.6
EPSP	117°0.0000'E		1. APC core to refusal ~ 200 mbsf. Change coring system and XCB core to refusal			
to 1061 mbsf			2. Drop FFF, POOH, change bit, RIH and RCB core from ~961 to ~1061 mbsf			
			3. Condition hole and log with triple combo and FMS-sonic			
			Subtotal Days On-Site: 12.7			
			Transit ~181 nmi to SCS-6A @ 10.5	0.7		
SCS-6A	18°21.1170'N	3854	Hole A - Depth check and jet-in test		1.1	
EPSP	116°23.4500'E		Hole B - Install re-entry system to ~900 mbsf		8.6	
pending			1. Deploy reentry cone and jet-in ~40 m 20" 95 lb/ft casing (to ~40 mbsf)			
approval			2. Drill 22" dia. hole w/ underreamer ~ into sediment (~250 mbsf)			
			3. Deploy 16" csg/land hanger in re-entry cone, place shoe at ~245 mbsf			
			4. Cement casing shoe /release casing hanger/flush pipe/POOH			
			5. Drill out cement with 14 3/4" bit and drill to ~900 mbsf			
			6. Deploy 10 3/4" casing to ~900 mbsf with underreamer and mud motor			
			Hole B - RCB coring from 900 to 1930 mbsf - 100 m into basement		14.8	1.7
			1. RCB core sediments from 900 mbsf to ~1830 mbsf			
			2. Change bit and RCB core from ~1830 to ~1930 mbsf			
			3. Condition hole and log with triple combo and FMS-sonic			
			Subtotal Days On-Site: 26.2			
			Transit ~335 nmi to SCS-4B @ 10.5	1.3		
SCS-4B	12°55.1370'N	4391	Hole A - APC/XCB coring to 865 mbsf, drop FFF and RCB core from 865 to 965 mbsf		10.4	1.5
EPSP	115°2.8326'E		1. APC core to refusal ~ 200 mbsf. Change coring system and XCB core to refusal			
to 965 mbsf			2. Drop FFF, POOH, change bit, RIH and RCB core from ~865 to ~965 mbsf			
			3. Condition hole and log with triple combo and FMS-sonic			
			Subtotal Days On-Site: 11.9			
			Transit ~1065 nmi to Okinawa @ 10.5	4.2		
Okinawa			End Expedition	7.2	46.0	4.8

Port Call:	3.0	Total Operating Days:	58.0
Subtotal On-Site:	50.8	Total Expedition:	61.0

All sites approved to basement plus 100 m. Environmental Protection and Safety Panel (EPSP) number given is estimated sediment coverage plus 100 m of basement. APCT-3 measurements to be taken on advanced piston corer (APC) sections on Cores 4H, 7H, 10H, and 13H. Nonmagnetic coring equipment to be used wherever possible (both APC and rotary core barrel [RCB] hole sections). FlexIT orientation tool to be deployed on all APC hole sections starting at Core 1H. Mechanical bit release to be run with all RCB bottom-hole assemblies. XCB = extended core barrel, FFF = free-fall funnel, POOH = pull out of hole, RIH = run in hole, FMS = Formation MicroScanner.

Table T4. Expedition 349 backup operations plan, primary sites.

Expedition 349 (P735-CPP2) - South China Sea

Backup Operations Plan Summary

Site No.	Location (Latitude Longitude)	Seafloor Depth (mbrf)	Operations Description	Transit (days)	Drilling Coring (days)	Log (days)
Manila			Begin Expedition 3.0 port call days			
			Transit ~228 nmi to SCS-3F @ 10.5	0.9		
SCS-3F	14°50.1960'N	4291	Hole A - APC/XCB coring to 197 mbsf, drop FFF and RCB core from 197 to 297 mbsf		5.4	1.1
EPSP	117°10.0800'E		1. APC core to refusal ~ 197 mbsf. Change coring system and XCB core if necessary			
to 297 mbsf			2. Drop FFF, POOH, change bit, RIH and RCB core from ~197 to ~297 mbsf			
			3. Condition hole and log with triple combo and FMS-sonic			
			Subtotal Days On-Site: 6.5			
			Transit ~216 nmi to SCS-6A @ 10.5	0.9		
SCS-6A	18°21.1170'N	3854	Hole A - APC/XCB coring to ~900 mbsf.		6.4	1.3
EPSP	116°23.4500'E		1. APC core to refusal ~ 200 mbsf. Change coring system and XCB core to refusal			
to 1930 mbsf			2. Condition hole and log with triple combo and FMS-sonic			
			Hole B - Depth check and jet-in test		0.8	
			Hole C - Install re-entry system to ~900 mbsf.		8.6	
			1. Deploy re-entry cone and jet-in ~40 m 20" 95 lb/ft casing (to ~40 mbsf)			
			2. Drill 22" dia. hole w/ underreamer ~ into sediment (~250 mbsf)			
			3. Deploy 16" casing/land hanger in re-entry cone, place shoe at ~245 mbsf			
			4. Cement casing shoe /release casing hanger/flush pipe/POOH			
			5. Drill out cement with 14 3/4" bit and drill to ~900 mbsf			
			6. Deploy 10 3/4" casing to ~ 900 mbsf with underreamer and mud motor			
			Hole C - RCB coring from 900 to 1930 mbsf - 100 m into basement		15.0	1.6
			1. RCB core sediments from 900 mbsf to ~1830 mbsf			
			2. Change bit and RCB core from ~1830 to ~1930 mbsf			
			3. Condition hole and log with triple combo and FMS-sonic			
			Subtotal Days On-Site: 33.7			
			Transit ~330 nmi to SCS-4C @ 10.5	1.3		
SCS-4C	12°59.0330'N	4391	Hole A - APC/XCB coring to 689 mbsf, drop FFF and RCB core from 689 to 789 mbsf		9.1	1.4
EPSP	115°9.4000'E		1. APC core to refusal ~ 200 mbsf. Change coring system and XCB core to refusal			
to 789 mbsf			2. Drop FFF, POOH, change bit, RIH and RCB core from ~689 to ~789 mbsf			
			3. Condition hole and log with triple combo and FMS-sonic			
			Subtotal Days On-Site: 10.5			
			Transit ~1057 nmi to Okinawa @ 10.5	4.2		
Okinawa			End Expedition	7.3	45.3	5.4

Port Call:	3.0	Total Operating Days:	58.0
Subtotal On-Site:	50.7	Total Expedition:	61.0

All sites approved to basement plus 100 m. Environmental Protection and Safety Panel (EPSP) number given is estimated sediment coverage plus 100 m of basement. APCT-3 measurements to be taken on advanced piston corer (APC) sections on Cores 4H, 7H, 10H, and 13H. Nonmagnetic coring equipment to be used wherever possible (both APC and rotary core barrel [RCB] hole sections). FlexIT orientation tool to be deployed on all APC hole sections starting at Core 1H. Mechanical bit release to be run with all RCB bottom-hole assemblies. XCB = extended core barrel, FFF = free-fall funnel, POOH = pull out of hole, RIH = run in hole, FMS = Formation MicroScanner.

Table T5. Expedition 349 operations plans for all sites. (Continued on next page.)

All Expedition 349 Sites

Site No.	Location (Latitude Longitude)	Seafloor Depth (mbrf)	Operations Description	Drilling Coring (days)	LWD/ MWD Log (days)
SCS-1C	21°0.1500'N	3317	Hole A - APC/XCB coring to 1110 mbsf drop FFF and RCB core from 1110 to 1210 mbsf	11.7	1.7
EPSP	119°47.1000'E				
to 1210 mbsf					
			Subtotal Days On-Site: 13.4		
SCS-2C	17°20.4720'N	4016	Hole A - APC/XCB coring to 1115 mbsf, drop FFF, and RCB core from 1115 to 1215 mbsf	12.8	1.8
EPSP	116°47.8020'E				
to 1215 mbsf					
			Subtotal Days On-Site: 14.6		
SCS-2D	17°20.6520'N	3953	Hole A - APC/XCB coring to 1040 mbsf, drop FFF, and RCB core from 1040 to 1140 mbsf	12.0	1.7
EPSP	116°38.7180'E				
to 1140 mbsf					
			Subtotal Days On-Site: 13.8		
SCS-3E	14°50.2020'N	4302	Hole A - APC/XCB coring to 505 mbsf, drop FFF, and RCB core from 505 to 605 mbsf	8.0	1.4
EPSP	117°19.9560'E				
to 605 mbsf					
			Subtotal Days On-Site: 9.3		
SCS-3F	14°50.1960'N	4291	Hole A - APC/XCB coring to 197 mbsf, drop FFF, and RCB core from 197 to 297 mbsf	5.6	1.1
EPSP	117°10.0800'E				
to 297 mbsf					
			Subtotal Days On-Site: 6.7		
SCS-3G	15°22.5480'N	4224	Hole A - APC/XCB coring to 961 mbsf, drop FFF, and RCB core from 961 to 1061 mbsf	11.7	1.7
EPSP	117°0.0000'E				
to 1061 mbsf					
			Subtotal Days On-Site: 13.4		
SCS-3H	14°28.3680'N	4315	Hole A - APC/XCB coring to 766 mbsf, drop FFF, and RCB core from 766 to 866 mbsf	10.1	1.5
EPSP	116°50.0820'E				
to 866 mbsf					
			Subtotal Days On-Site: 11.6		
SCS-3I	14°39.0120'N	4276	Hole A - APC/XCB coring to 574 mbsf, drop FFF, and RCB core from 574 to 674 mbsf	8.4	1.4
EPSP	116°59.9940'E				
to 674 mbsf					
			Subtotal Days On-Site: 9.9		
SCS-4B	12°55.1370'N	4391	Hole A - APC/XCB coring to 865 mbsf, drop FFF, and RCB core from 865 to 965 mbsf	10.9	1.6
EPSP	115°2.8326'E				
to 965 mbsf					
			Subtotal Days On-Site: 12.5		
SCS-4C	12°59.0330'N	4391	Hole A - APC/XCB coring to 689 mbsf, drop FFF, and RCB core from 689 to 789 mbsf	9.5	1.5
EPSP	115°9.4000'E				
to 789 mbsf					
			Subtotal Days On-Site: 11.0		

Table T5 (continued).

SCS-4D	12°59.9940'N	4286	Hole A - APC/XCB coring to 204 mbsf, drop FFF, and RCB core from 204 to 304 mbsf	5.6	1.1
EPSP	115°0.7440'E				
to 304 mbsf					
			Subtotal Days On-Site: 6.8		
SCS-4E	13°11.5080'N	4036	Hole A - APC/XCB coring to 304 mbsf, drop FFF, and RCB core from 304 to 404 mbsf	6.3	1.2
EPSP	114°55.3980'E				
to 404 mbsf					
			Subtotal Days On-Site: 7.5		
SCS-4F	13°33.6060'N	4229	Hole A - APC/XCB coring to 190 mbsf, drop FFF, and RCB core from 190 to 290 mbsf	5.5	1.1
EPSP	114°36.4140'E				
to 290 mbsf					
			Subtotal Days On-Site: 6.6		
SCS-6A	18°21.1170'N	3854	Hole A - APC/XCB to 900 mbsf.	6.7	1.4
EPSP	116°23.4500'E		Hole B - Jet-in test	0.8	
to 1930 mbsf			Hole C - Install re-entry system to 900 mbsf.	9.0	
			Hole C - RCB coring from 900 to 1930 mbsf - 100 m into basement	15.6	2.0
			Subtotal Days On-Site: 35.5		
SCS-6A	18°21.1170'N	3854	Hole A - Jet-in test	1.1	
EPSP	116°23.4500'E		Hole B - Install re-entry system to 900 mbsf.	9.1	
pending			Hole B - RCB coring from 900 to 1930 mbsf - 100 m into basement	15.6	2.1
approval					
			Subtotal Days On-Site: 27.9		
SCS-6B	18°20.1670'N	3917	Hole A - APC/XCB to 900 mbsf.	6.8	1.4
EPSP	116°42.2800'E		Hole B - Jet-in test	0.8	
to 1879 mbsf			Hole C - Install re-entry system to 900 mbsf.	9.0	
			Hole C - RCB coring from 900 to 1879 mbsf - 100 m into basement	14.9	2.0
			Subtotal Days On-Site: 34.9		
SCS-6B	18°20.1670'N	3917	Hole A - Jet-in test	1.1	
EPSP	116°42.2800'E		Hole B - Install re-entry system to 900 mbsf.	9.1	
pending			Hole B - RCB coring from 900 to 1879 mbsf - 100 m into basement	14.9	2.0
approval					
			Subtotal Days On-Site: 27.2		
SCS-6C	18°33.3840'N	3305	Hole A - RCB coring to 110 mbsf - 100 m into basement	2.8	
EPSP	116°36.5760'E				
to 110 mbsf					
			Subtotal Days On-Site: 2.8		

All sites except SCS-6C are approved to basement plus 100 m. Environmental Protection and Safety Panel (EPSP) number given is estimated sediment coverage plus 100 m of basement. Two sites are pending EPSP approval. APC = advanced piston corer, XCB = extended core barrel, FFF = free-fall funnel, RCB = rotary core barrel.

Figure F1. Regional topography and geodynamic framework of Southeast Asia. Data based on Smith and Sandwell (1997). Red lines = regional faults. Red arrows show directions of plate movements. Red dots in the South China Sea = primary drill sites for this expedition.

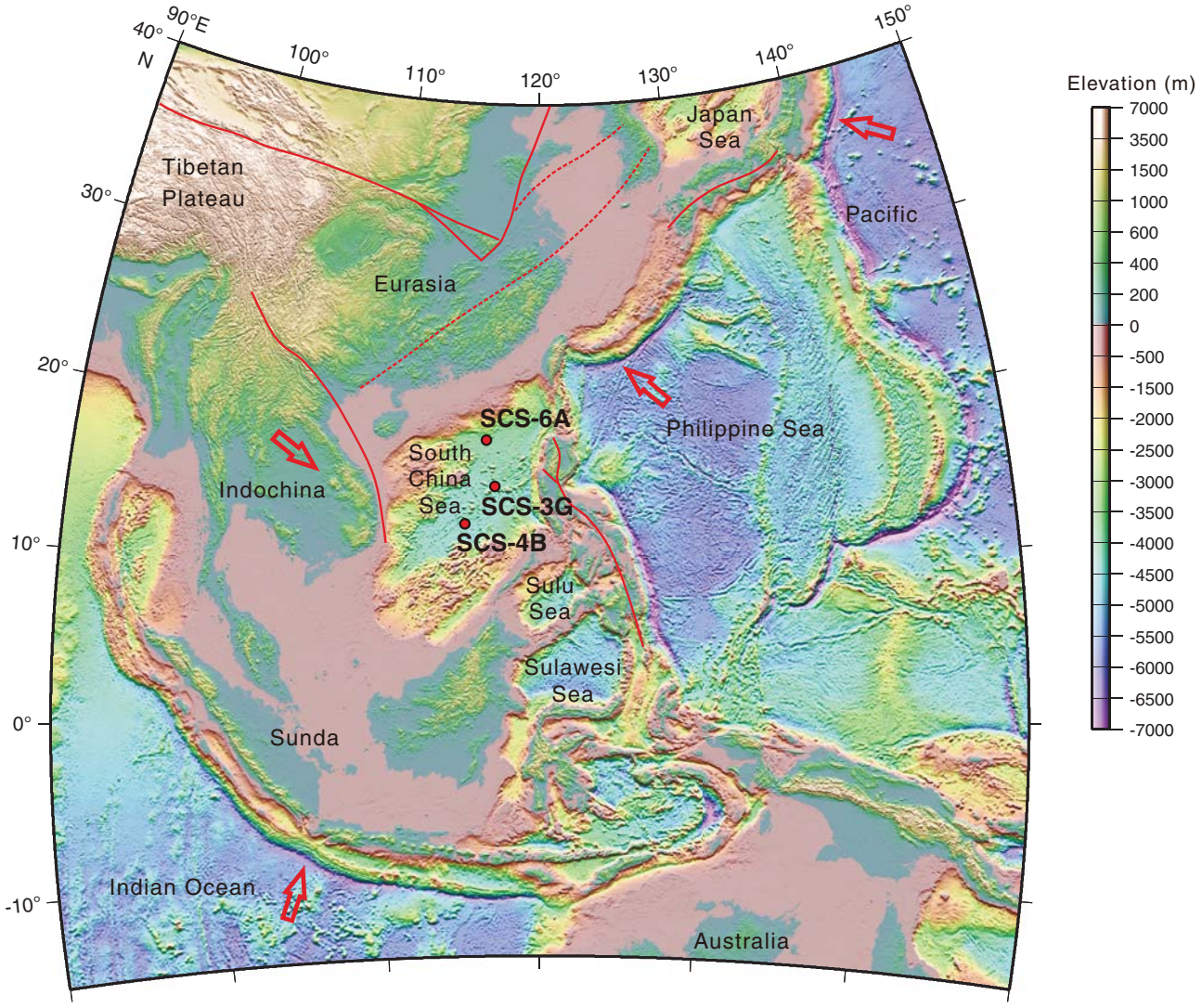

Figure F2. Topographic and bathymetric map of the South China Sea and surrounding region. Dashed red line = inferred Zhongnan fault. Red dots = primary sites for the operations plan. Green dots = primary sites for the backup operations plan (Site SCS-6A is a primary site for both operations plans). Yellow dots = alternate sites. White dot = location of ODP Site 1148. Pink lines = seismic surveys collected by the BGR using the R/V *Sonne* in 1987 (SO49) and 2008 (SO197). Blue, red, and black solid lines = seismic data collected by Chinese research institutes and oil companies. Turquoise lines = reflection seismic data acquired in the 1980s from Cruises V3607, V3608, V3613, V3614, and RC2006.

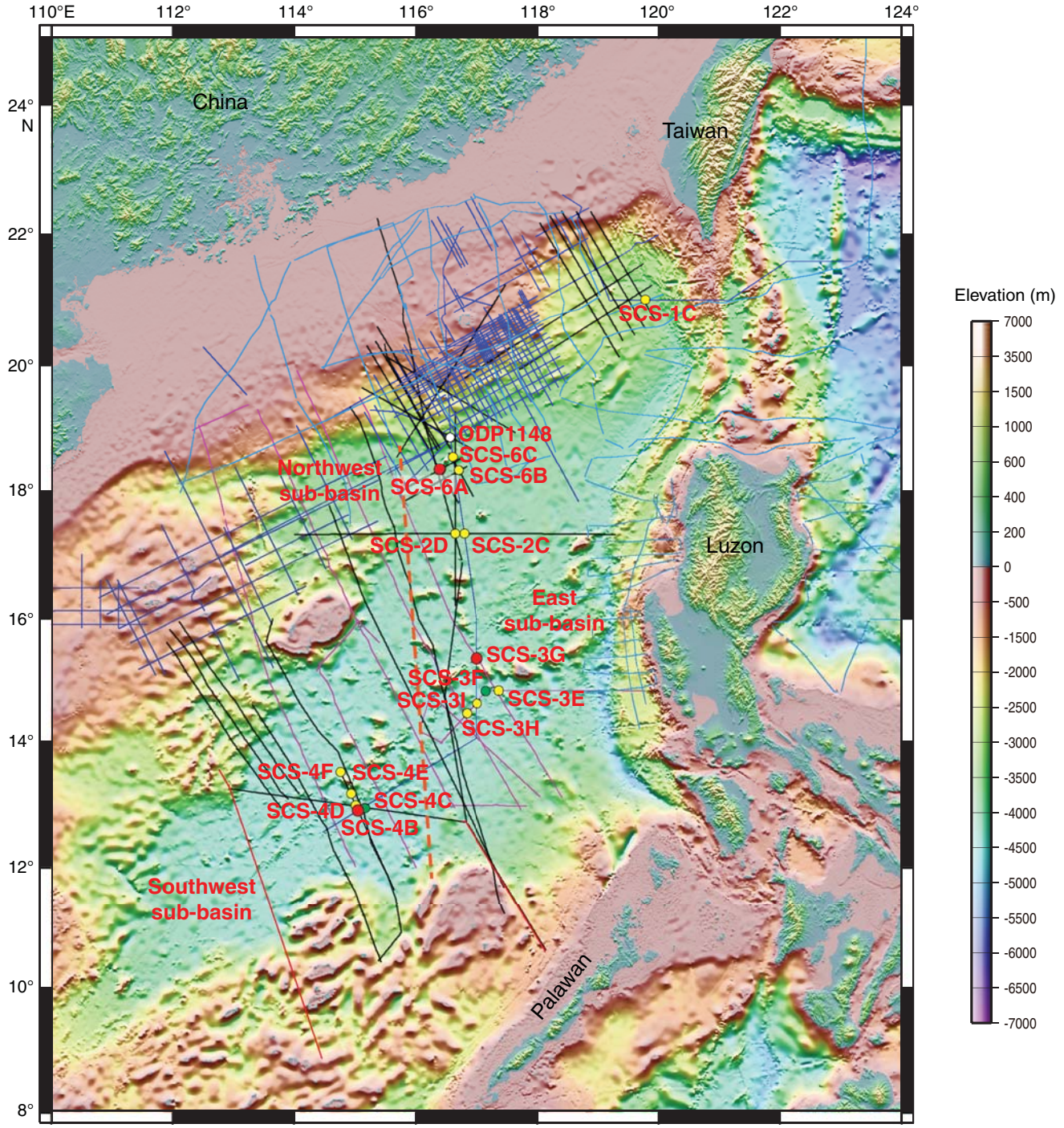

Figure F3. Different hypothetical models for the driving mechanisms of the opening of the South China Sea (SCS). **A.** Opening induced by India-Eurasia continental collision and consequent tectonic extrusion (Tapponnier et al., 1982, 1990; Briais et al., 1993; Leloup et al., 2001; Flower et al., 2001). (Continued on next two pages.)

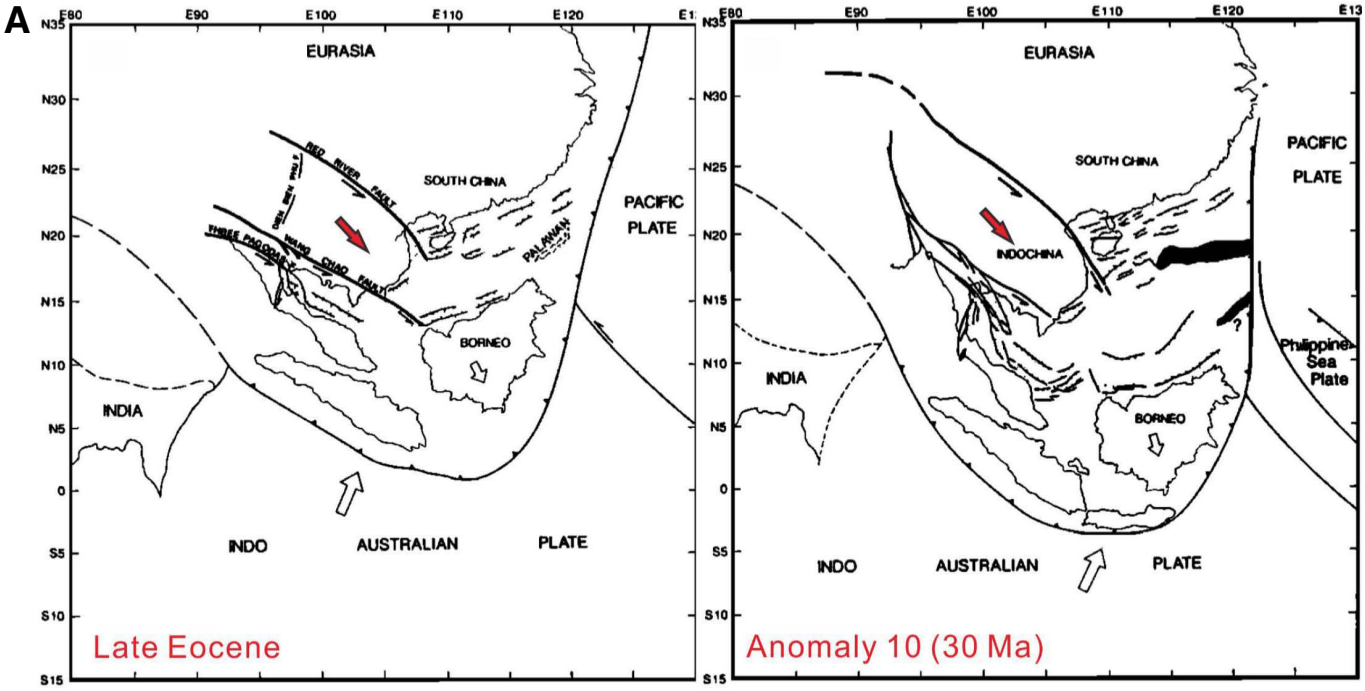

Figure F3 (continued). B. Opening induced by slab pull and subduction of the proto-SCS (Taylor and Hayes, 1980, 1983; Holloway, 1982; Hall, 2002). **C.** Opening induced by an upwelling mantle plume (e.g., Fan and Menzies, 1992; Xu et al., 2012). (Continued on next page.)

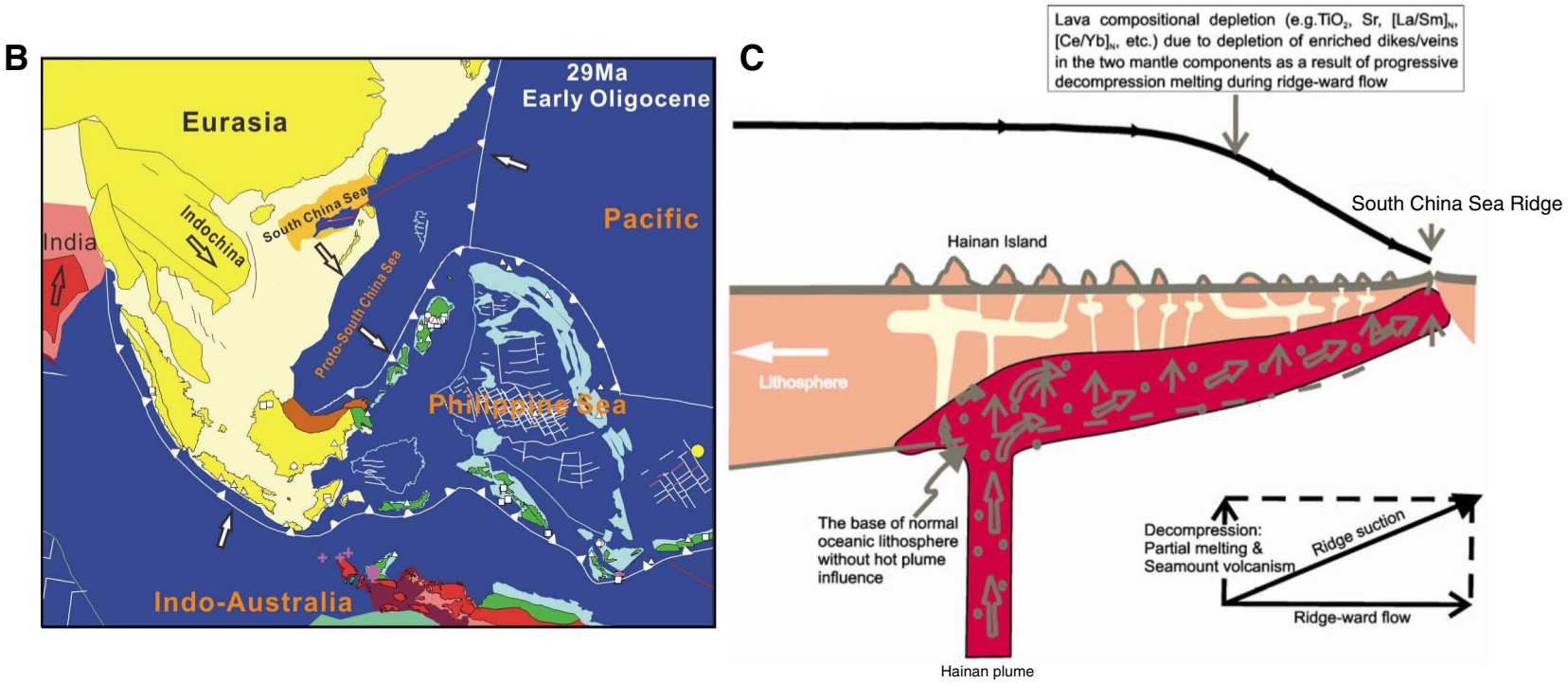

Figure F3 (continued). D. Opening induced by regional extension related to subduction and retreat of the Pacific plate (Taylor and Hayes, 1980, 1983; Shi and Li, 2012).

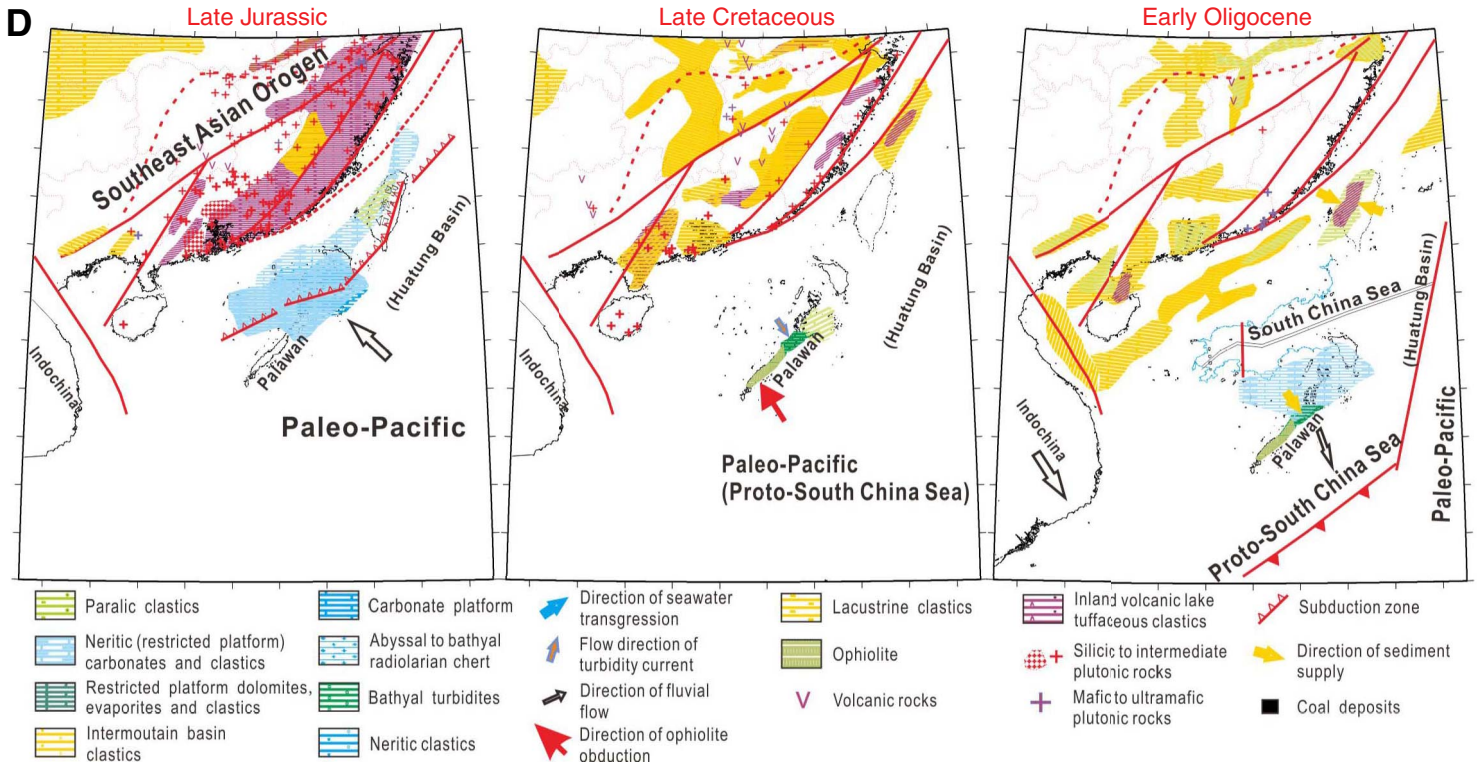

Figure F4. Total field magnetic map (based on globalchange.nasa.gov/r/d/[GCMD]GSJ_EASTASIA_CDROM) showing major magnetic zones (A, B, C1, C1′, C2, D, and E). M1 and M2 are two major magnetic anomalies in the East Sub-basin. ZNF = Zhongnan fault; LRTPB = Luzon-Ryukyu transform plate boundary; DS = Dongsha Rise; SCMA = offshore south China magnetic anomaly; XS = Xisha; ZB = Zhongsha (Macclesfield) Bank; LB = Reed Bank; NM = Dangerous Grounds. Red lines = transform faults. Red dots = primary sites for the operations plan. Green dots = primary sites for the backup operations plan (Site SCS-6A is a primary site for both operations plans). Yellow dots = alternate sites. White dot = location of ODP Site 1148. (After Li et al., 2008b.)

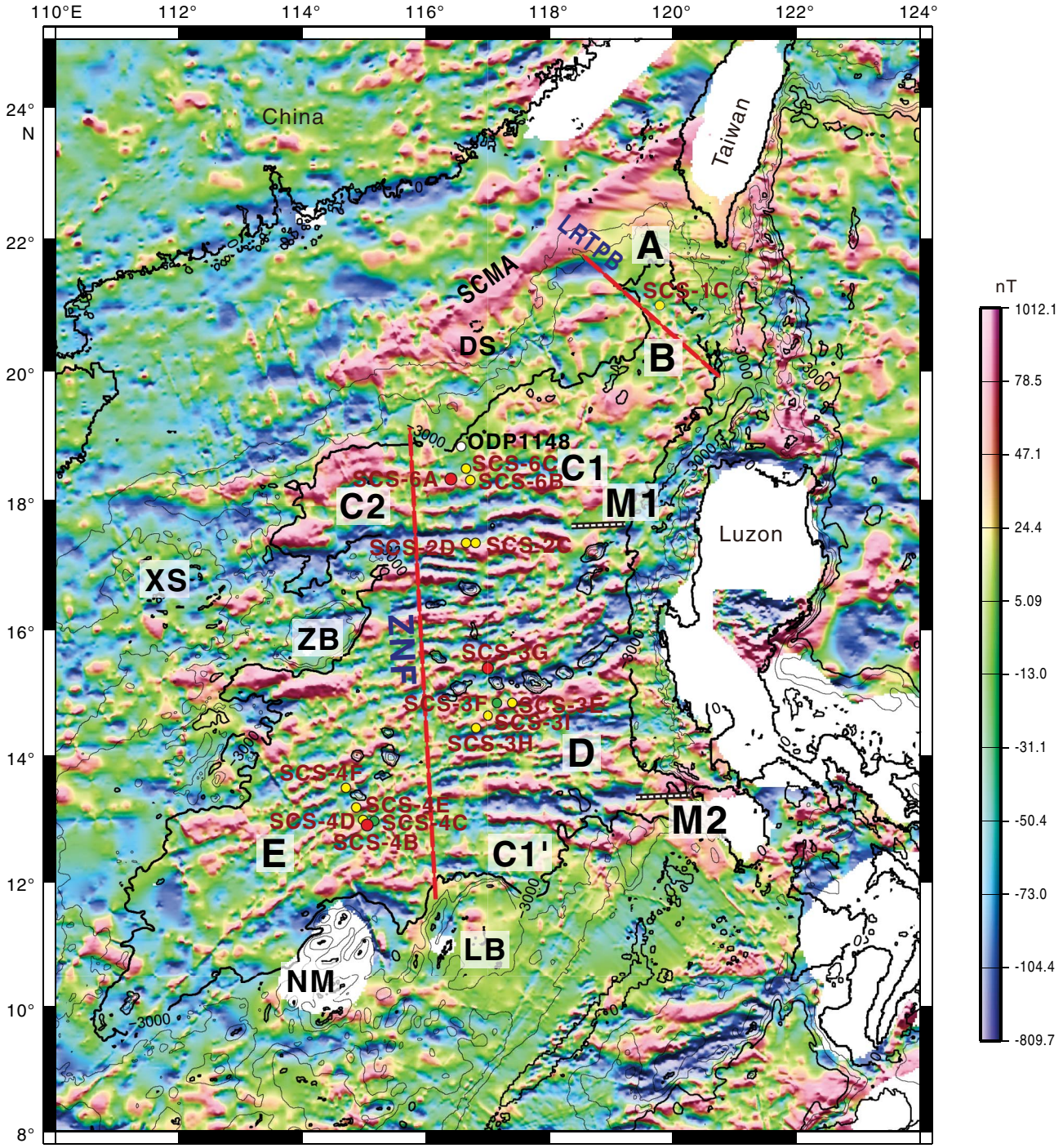

Figure F5. Examples of two groups of contrasting tectonic models for the opening phases of the South China Sea. **A.** Multiphase episodic rifting model in which the Southwest Sub-basin is the first to open from continental rifting (after Ru and Pigott, 1986). N.P. = Northwest Palawan, S.P. = South Palawan, M.B. = Macclesfield Bank, R.B. = Reed Bank. (Continued on next page.)

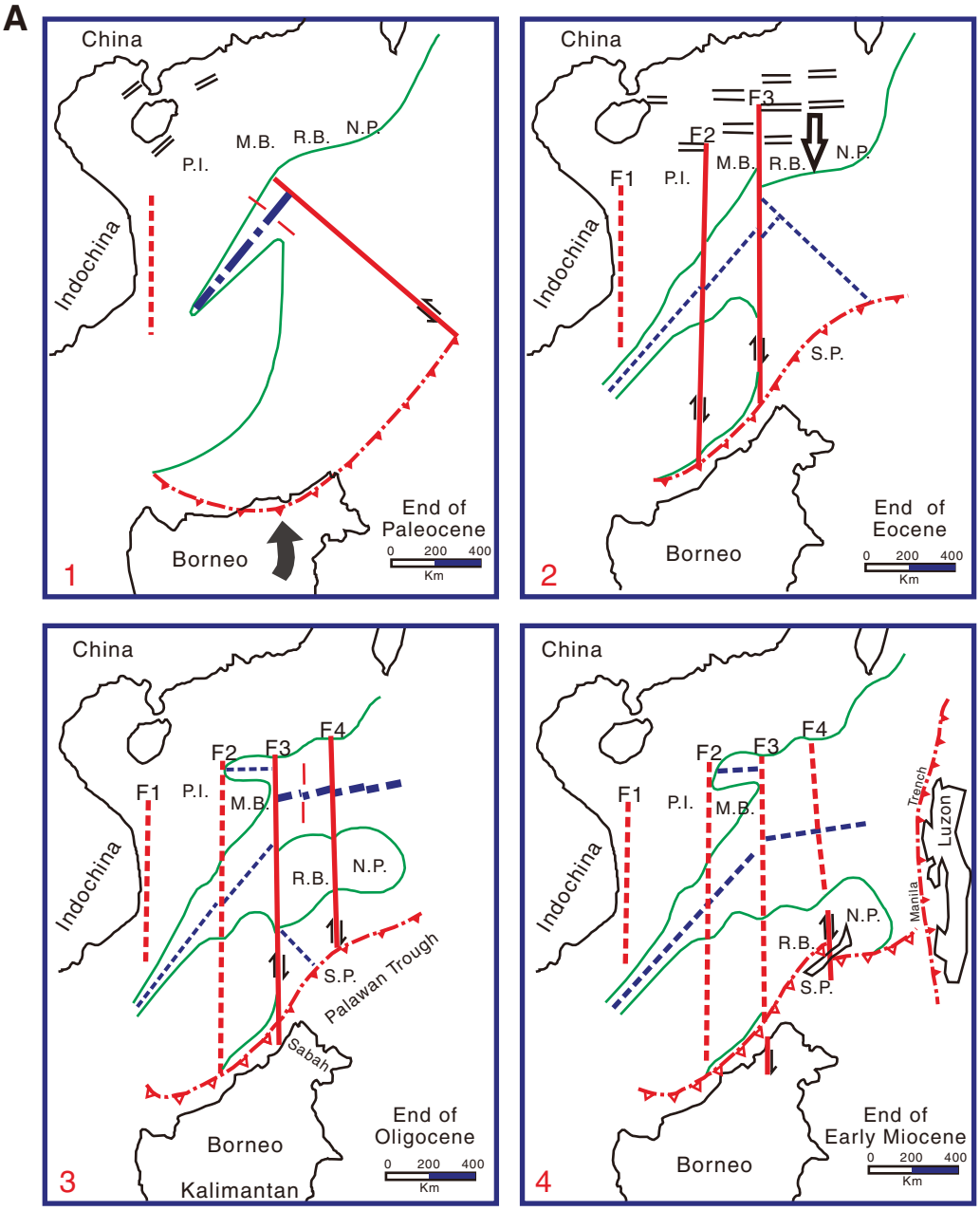

Figure F5 (continued). B. Southwestward continuous propagating model in which the Southwest Sub-basin is coeval with the central East Sub-basin (after Briais et al., 1993).

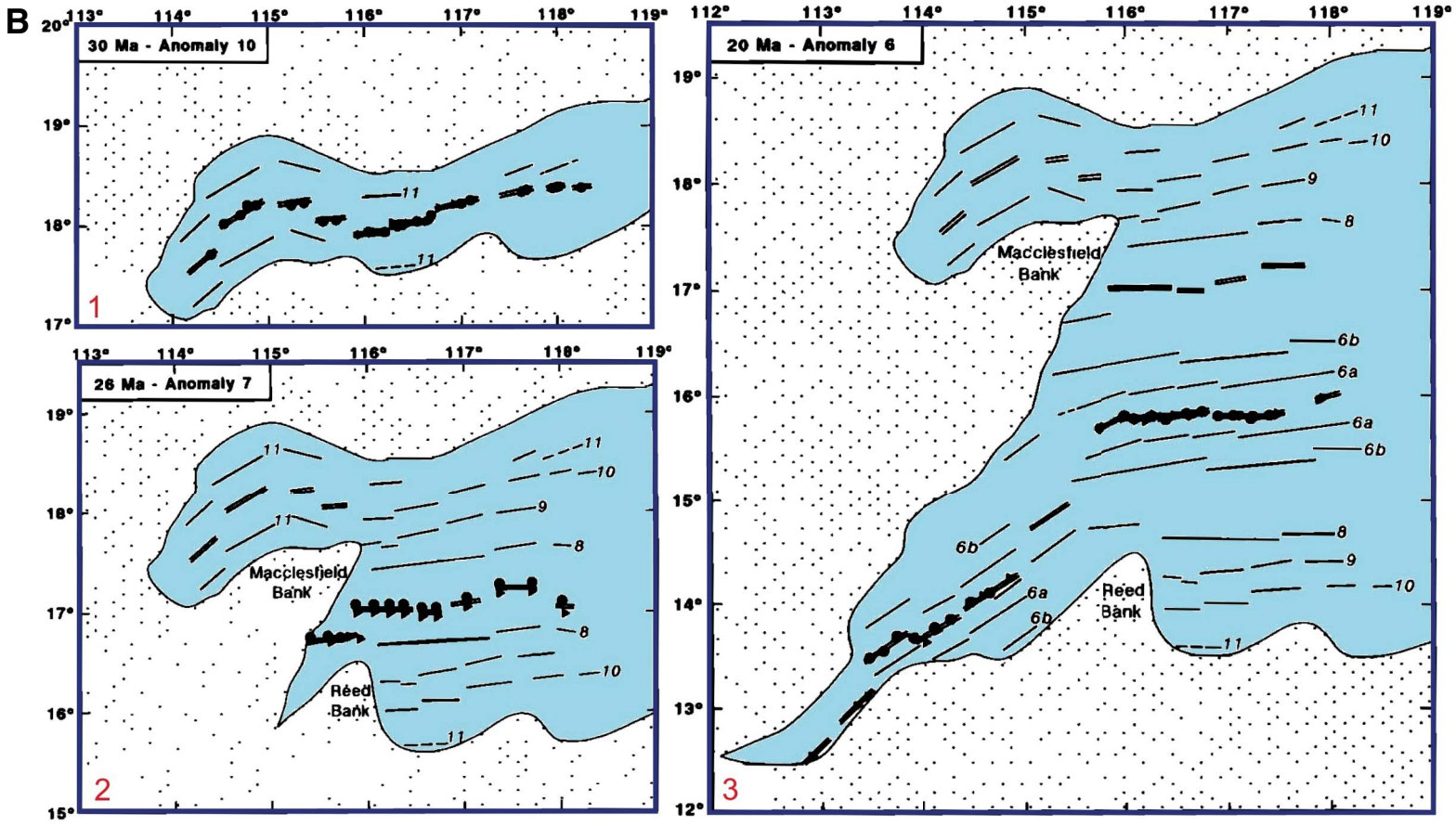

Figure F6. Swath bathymetry map of the South China Sea basin showing 12 of the proposed sites. Red dots = primary sites for the operations plan. Green dots = primary sites for the backup operations plan. Yellow dots = alternate sites. (After Li et al., 2011.)

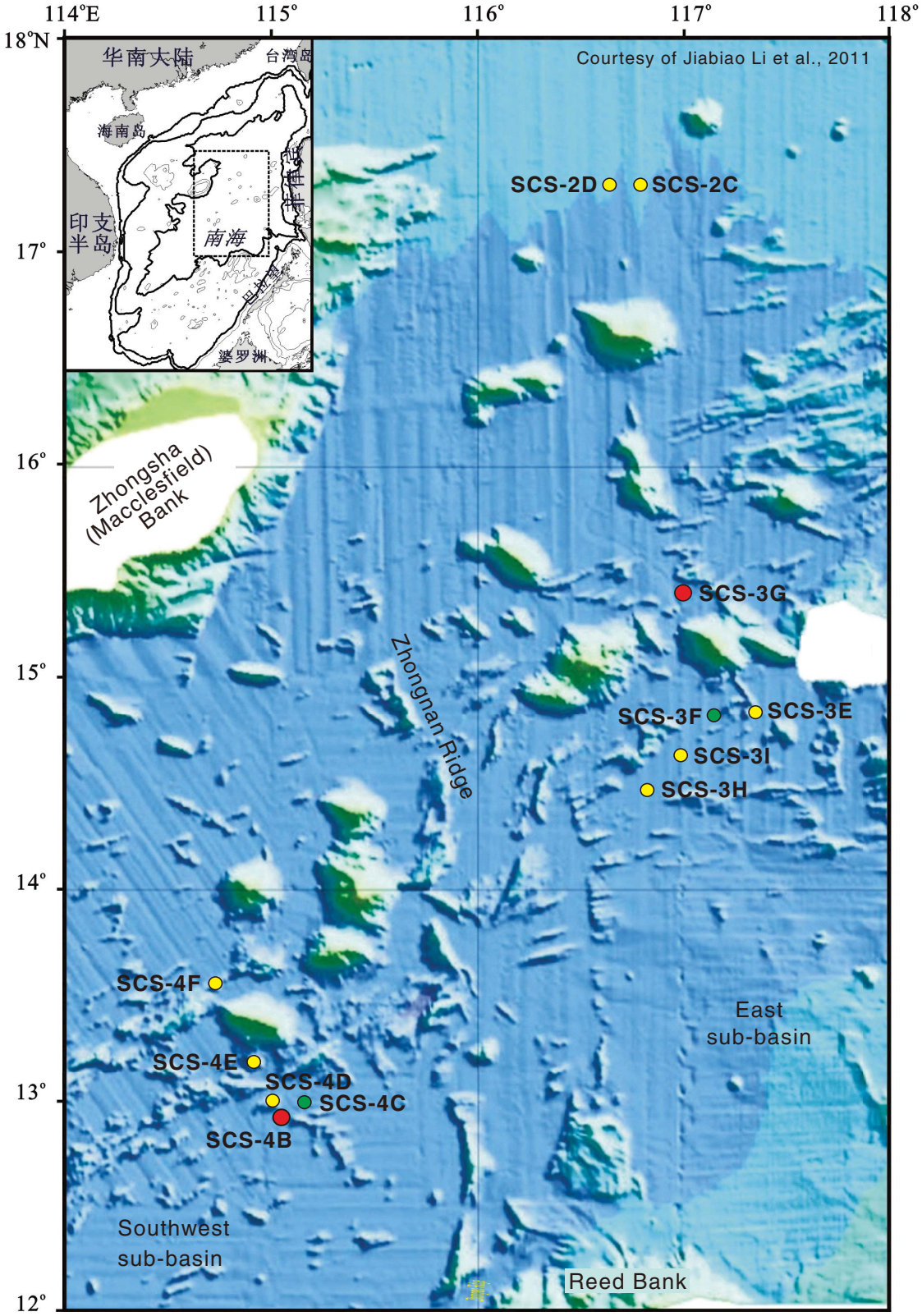

Figure F7. Proposed sampling transect in the East Sub-basin (after Li et al., 2010). **A.** Total field magnetic anomaly (blue) and Bouguer anomaly (green) along the seismic line shown in B. **B.** Proposed drill sites in the East Sub-basin and ODP Site 1148 shown on a composite seismic line. Solid lines = sites that fall on the seismic profile. Dashed lines = site locations projected onto the line. **C.** Depths to the Moho and Curie point estimated from gravity and magnetic anomalies, respectively. TWTT = two-way traveltime; COT = continent–ocean transition zone; PRMB = Pearl River Mouth Basin; w = width of moving windows.

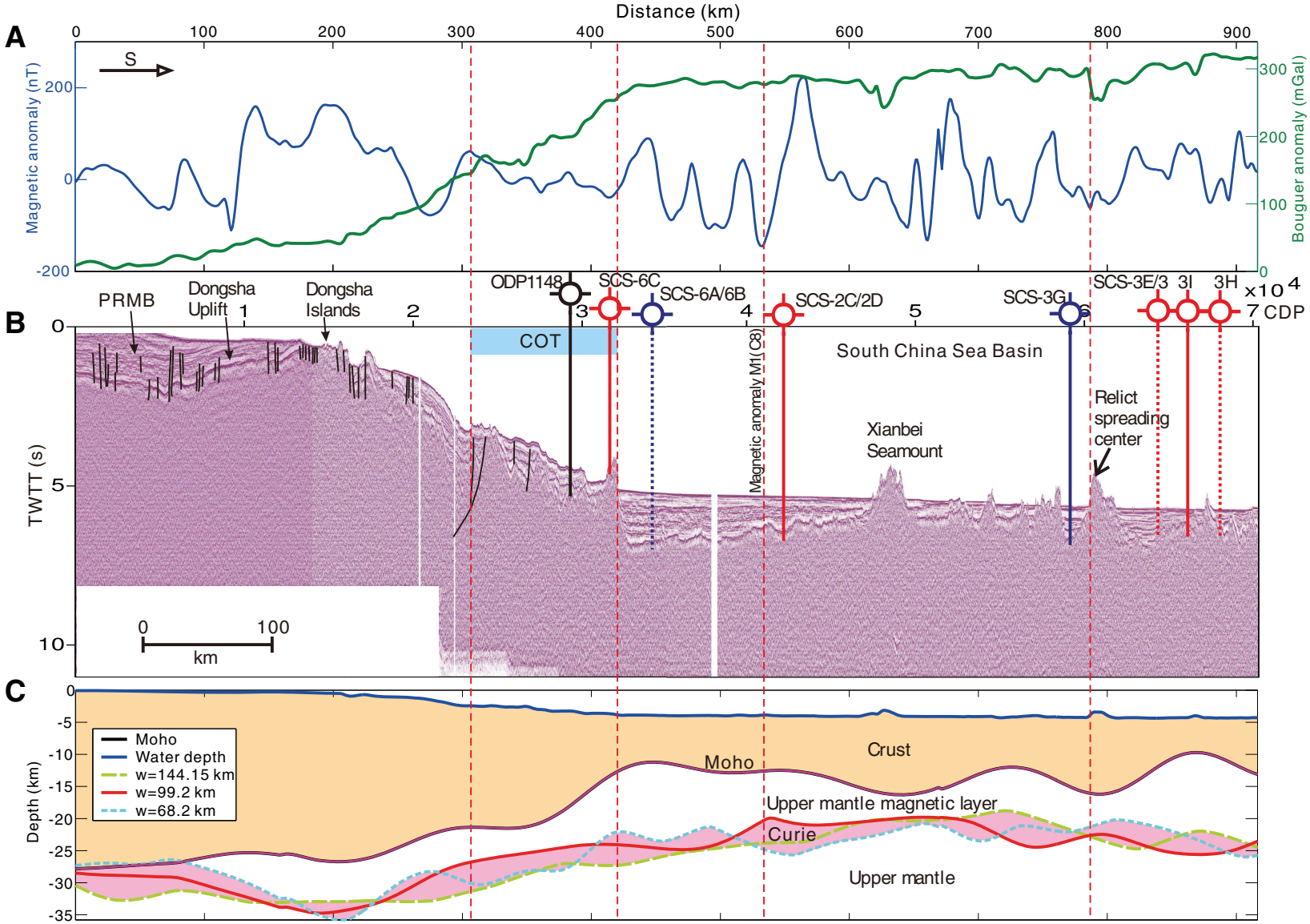

Figure F8. Seismic profile showing the structures of the Southwest and the East Sub-basins and the transition zone in between. Tg = Cenozoic basement. (After Li et al., 2008b.)

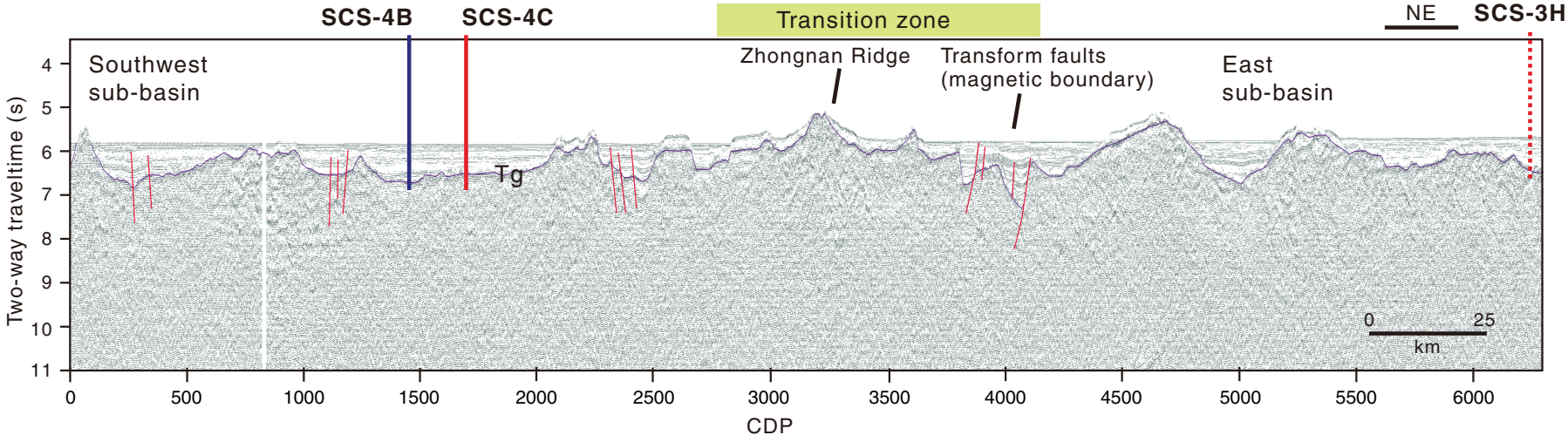

Figure F9. Seismic profile Line NDS3 showing the sampling transect in the Southwest Sub-basin and location of four proposed drill sites.

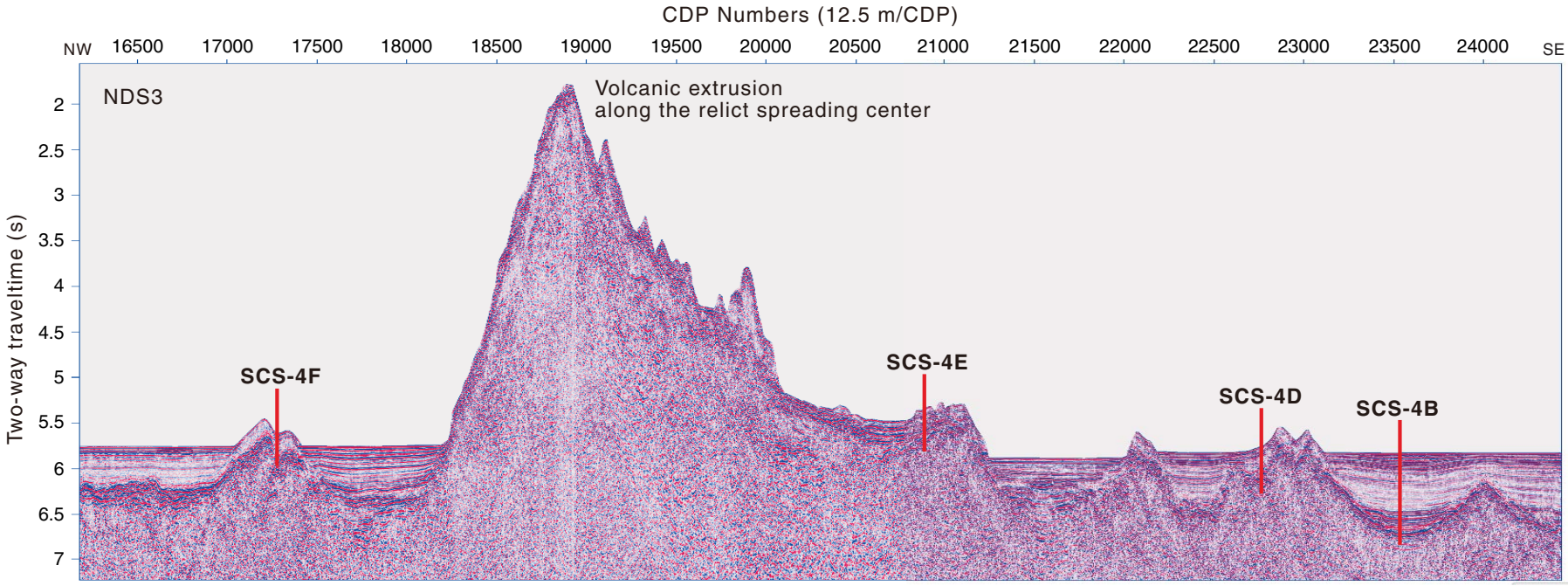

Site summaries

Site SCS-6A

Priority:	Primary (high)
Position:	18°21.117′N, 116°23.45′E
Water depth (m):	3843
Target drilling depth (mbsf):	1930
Approved maximum penetration:	Approved to basement + 100 m with full coring. Drilling through the top 900 m without coring is pending EPSP approval. (Estimated total depth = 1930 mbsf)
Survey coverage (track map; seismic profile):	Bathymetric sketch and site track map (Figs. **AF1, AF2**) Deep-penetration seismic reflection: • Primary line: 08ec1573 (SP400) (Fig. **AF3**) • Crossing line: 08ec2678 (SP6149) (Fig. **AF4**)
Objectives:	• Date the oldest oceanic crust near the continent/ocean boundary of the South China Sea • Measure magnetization, mineralization, and geochemical compositions of basement rocks • Obtain basement rocks to ascertain the causes of sharp magnetic contrasts between different sub-basins • Study the paleoceanographic response to the opening of the South China Sea
Drilling program:	Hole A (APC/XCB coring will only be completed if full coring is required by EPSP): • APC to refusal with nonmagnetic core barrels, core orientation (FlexIT tool), and APCT-3 • XCB to refusal Hole B: • Jet-in test for reentry system Hole C: • Reentry system (20, 16, and 10¾ inch casing to ~900 mbsf) • RCB with nonmagnetic core barrels to 1930 mbsf (one bit change at ~1830 mbsf)
Downhole logging program:	Hole A: • Triple combo • FMS-sonic Hole C: • Triple combo • FMS-sonic • VSI if time and hole conditions allow • UBI/MMM if time and hole conditions allow
Nature of rock anticipated:	(Calcareous) mudstone, siltstone, sandstone, basalt

Site summaries (continued)

Site SCS-6B

Priority:	Alternate
Position:	18°20.167′N, 116°42.28′E
Water depth (m):	3906
Target drilling depth (mbsf):	1879
Approved maximum penetration:	Approved to basement + 100 m with full coring. Drilling through the top 900 m without coring is pending EPSP approval. (Estimated total depth = 1879 mbsf)
Survey coverage (track map; seismic profile):	Bathymetric sketch and site track map (Figs. **AF1, AF5**) Deep-penetration seismic reflection: • Primary line: 08ec1602 (SP3300) (Fig. **AF6**) • Crossing line: 08ec2696 (SP6098) (Fig. **AF7**)
Objectives:	Alternate for SCS-6A • Date the oldest oceanic crust near the continent/ocean boundary of the South China Sea • Measure magnetization, mineralization, and geochemical compositions of basement rocks • Obtain basement rocks to ascertain the causes of sharp magnetic contrasts between different sub-basins • Study the paleoceanographic response to the opening of the South China Sea
Drilling program:	Hole A (APC/XCB coring will only be completed if full coring is required by EPSP): • APC to refusal with nonmagnetic core barrels, core orientation (FlexIT tool), and APCT-3 • XCB to refusal Hole B: • Jet-in test for reentry system Hole C: • Reentry system (20, 16, and 10¾ inch casing to ~900 mbsf) • RCB with nonmagnetic core barrels to 1879 mbsf (one bit change at ~1779 mbsf)
Downhole logging program:	Hole A: • Triple combo • FMS-sonic Hole C: • Triple combo • FMS-sonic • VSI if time and hole conditions allow • UBI/MMM if time and hole conditions allow
Nature of rock anticipated:	(Calcareous) mudstone, siltstone, sandstone, basalt

Site summaries (continued)

Site SCS-6C

Priority:	Alternate
Position:	18°33.384′N, 116°36.576′E
Water depth (m):	3294
Target drilling depth (mbsf):	110
Approved maximum penetration (mbsf):	110
Survey coverage (track map; seismic profile):	Bathymetric sketch and site track map (Fig. **AF1**) Deep-penetration seismic reflection: • Primary line: 08ec1602 (CDP6312) (Fig. **AF8**) • Crossing line: 973SCSIO_01A (projected at SP7920) (Fig. **AF9**)
Objectives:	• Examine the lithological nature of the boundary uplift between extended continental crust and oceanic crust • Measure magnetization, mineralization, and geochemical compositions of basement rocks • Model early-phase opening to better understand the rift-to-drift transition
Drilling program:	Hole A: • RCB with nonmagnetic core barrels to 110 mbsf
Downhole logging program:	None
Nature of rock anticipated:	(Calcareous) mudstone, siltstone, sandstone, basalt, gabbro, serpentinite

Site summaries (continued)

Site SCS-3G

Priority:	Primary
Position:	15°22.548′N, 117°0.0′E
Water depth (m):	4213
Target drilling depth (mbsf):	1061
Approved maximum penetration:	Approved to basement + 100 m (Estimated total depth = 1061 mbsf)
Survey coverage (track map; seismic profile):	Bathymetric sketch and site track map (Fig. **AF10, AF11**) Deep-penetration seismic reflection: • Primary line: 973SCSIO01e (CDP59300) (Fig. **AF12**) • Crossing line: SO49-017a (projected at CDP10867) (Fig. **AF13**)
Objectives:	• Determine the age of the East Sub-basin • Date the timing of seafloor spreading cessation in the South China Sea • Test if the East Sub-basin formed in an area floored by older oceanic crust • Measure magnetization, mineralization, and geochemical compositions of basement rocks • Obtain basement rocks to ascertain the causes of sharp magnetic contrasts between different sub-basins • Study the paleoceanographic response to the opening of the South China Sea
Drilling program:	Hole A: • APC to refusal with nonmagnetic core barrels, core orientation (FlexIT tool), and APCT-3 • XCB to refusal • Drop FFF • RCB with nonmagnetic core barrels to 1061 mbsf
Downhole logging program:	• Triple combo • FMS-sonic
Nature of rock anticipated:	(Calcareous) mudstone, siltstone, sandstone, basalt

Site summaries (continued)

Site SCS-3F

Priority:	Primary for backup operations plan
Position:	14°50.196′N, 117°10.08′E
Water depth (m):	4280
Target drilling depth (mbsf):	297
Approved maximum penetration:	Approved to basement + 100 m (Estimated total depth = 297 mbsf)
Survey coverage (track map; seismic profile):	Bathymetric sketch and site track map (Fig. **AF10**) Deep-penetration seismic reflection: • Primary line: BGR08-124 (CDP10110) (Fig. **AF14**) • Crossing line: BGR08-123 (CDP19938) (Fig. **AF15**)
Objectives:	Alternate for SCS-3G • Determine the age of the East Sub-basin • Date the timing of seafloor spreading cessation in the South China Sea • Test if the East Sub-basin formed in an area floored by older oceanic crust • Measure magnetization, mineralization, and geochemical compositions of basement rocks • Obtain basement rocks to ascertain the causes of sharp magnetic contrasts between different sub-basins • Study the paleoceanographic response to the opening of the South China Sea
Drilling program:	Hole A: • APC to refusal with nonmagnetic core barrels, core orientation (FlexIT tool), and APCT-3 • XCB to refusal • Drop FFF • RCB with nonmagnetic core barrels to 297 mbsf
Downhole logging program:	• Triple combo • FMS-sonic
Nature of rock anticipated:	(Calcareous) mudstone, siltstone, sandstone, basalt

Site summaries (continued)

Site SCS-3E

Priority:	Alternate
Position:	14°50.202′N, 117°19.956′E
Water depth (m):	4291
Target drilling depth (mbsf):	605
Approved maximum penetration (mbsf):	Basement + 100 m (Estimated total depth = 605 mbsf)
Survey coverage (track map; seismic profile):	Bathymetric sketch and site track map (Fig. **AF10**) Deep-penetration seismic reflection: • Primary line: BGR08-124 (CDP11527) (Fig. **AF16**) • Crossing line: SO49-017a (CDP8298) (Fig. **AF17**)
Objectives:	Alternate for SCS-3G • Determine the age of the East Sub-basin • Date the timing of seafloor spreading cessation in the South China Sea • Test if the East Sub-basin formed in an area floored by older oceanic crust • Measure magnetization, mineralization, and geochemical compositions of basement rocks • Obtain basement rocks to ascertain the causes of sharp magnetic contrasts between different sub-basins • Study the paleoceanographic response to the opening of the South China Sea
Drilling program:	Hole A: • APC to refusal with nonmagnetic core barrels, core orientation (FlexIT tool), and APCT-3 • XCB to refusal • Drop FFF • RCB with nonmagnetic core barrels to 605 mbsf
Downhole logging program:	• Triple combo • FMS-sonic
Nature of rock anticipated:	(Calcareous) mudstone, siltstone, sandstone, basalt

Site summaries (continued)

Site SCS-3H

Priority:	Alternate
Position:	14°28.368′N, 116°50.082′E
Water depth (m):	4304
Target drilling depth (mbsf):	866
Approved maximum penetration:	Approved to basement + 100 m (Estimated total depth = 866 mbsf)
Survey coverage (track map; seismic profile):	Bathymetric sketch and site track map (Fig. **AF10, AF18**) Deep-penetration seismic reflection: • Primary line: BGR08-123 (CDP15625) (Fig. **AF19**) • Crossing line: SO49-018_1 (projected at CDP10680) (Fig. **AF20**)
Objectives:	Alternate for SCS-3G • Determine the age of the East Sub-basin • Date the timing of seafloor spreading cessation in the South China Sea • Test if the East Sub-basin formed in an area floored by older oceanic crust • Measure magnetization, mineralization, and geochemical compositions of basement rocks • Obtain basement rocks to ascertain the causes of sharp magnetic contrasts between different sub-basins • Study the paleoceanographic response to the opening of the South China Sea
Drilling program:	Hole A: • APC to refusal with nonmagnetic core barrels, core orientation (FlexIT tool), and APCT-3 • XCB to refusal • Drop FFF • RCB with nonmagnetic core barrels to 866 mbsf
Downhole logging program:	• Triple combo • FMS-sonic
Nature of rock anticipated:	(Calcareous) mudstone, siltstone, sandstone, basalt

Site summaries (continued)

Site SCS-3I

Priority:	Alternate
Position:	14°39.012′N, 116°59.994′E
Water depth (m):	4265
Target drilling depth (mbsf):	674
Approved maximum penetration:	Approved to basement + 100 m (Estimated total depth = 674 mbsf)
Survey coverage (track map; seismic profile):	Bathymetric sketch and site track map (Fig. **AF10**) Deep-penetration seismic reflection: • Primary line: 973SCSIO01e (CDP65500) (Fig. **AF21**) • Crossing line: BGR08-123 (projected at CDP17700) (Fig. **AF22**)
Objectives:	Alternate for SCS-3G • Determine the age of the East Sub-basin • Date the timing of seafloor spreading cessation in the South China Sea • Test if the East Sub-basin formed in an area floored by older oceanic crust • Measure magnetization, mineralization, and geochemical compositions of basement rocks • Obtain basement rocks to ascertain the causes of sharp magnetic contrasts between different sub-basins • Study the paleoceanographic response to the opening of the South China Sea
Drilling program:	Hole A: • APC to refusal with nonmagnetic core barrels, core orientation (FlexIT tool), and APCT-3 • XCB to refusal • Drop FFF • RCB with nonmagnetic core barrels to 674 mbsf
Downhole logging program:	• Triple combo • FMS-sonic
Nature of rock anticipated:	(Calcareous) mudstone, siltstone, sandstone, basalt

Site summaries (continued)

Site SCS-4B

Priority:	Primary
Position:	12°55.137′N, 115°2.8326′E
Water depth (m):	4380
Target drilling depth (mbsf):	965
Approved maximum penetration:	Approved to basement + 100 m (Estimated total depth = 965 mbsf)
Survey coverage (track map; seismic profile):	Bathymetric sketch and site track map (Fig. **AF23, AF24**) Deep-penetration seismic reflection: • Primary line: 973SCSIO_2b (SP4847) (Fig. **AF25**) • Crossing line: SIOSOA_NDS3 (CMP23521) (Fig. **AF26**)
Objectives:	• Determine the age of the Southwest Sub-basin • Test the hypothesis that the Southwest Sub-basin evolved within continental crust by rifting • Measure magnetization, mineralization, and geochemical compositions of basement rocks • Examine the paleoceanographic response to the opening of the South China Sea
Drilling program:	Hole A: • APC to refusal with nonmagnetic core barrels, core orientation (FlexIT tool), and APCT-3 • XCB to refusal • Drop FFF • RCB with nonmagnetic core barrels to 965 mbsf
Downhole logging program:	• Triple combo • FMS-sonic
Nature of rock anticipated:	(Calcareous) mudstone, siltstone, sandstone, basalt

Site summaries (continued)

Site SCS-4C

Priority:	Primary for backup operations plan
Position:	12°59.033′N, 115°9.40′E
Water depth (m):	4380
Target drilling depth (mbsf):	789
Approved maximum penetration:	Approved to basement + 100 m (Estimated total depth = 789 mbsf)
Survey coverage (track map; seismic profile):	Bathymetric sketch and site track map (Fig. **AF23, AF27**) Deep-penetration seismic reflection: • Primary line: 973SCSIO_2b (SP4575) (Fig. **AF28**) • Crossing line: A3B6 (SP7489) (Fig. **AF29**)
Objectives:	Alternate for SCS-4B • Determine the age of the Southwest Sub-basin • Test the hypothesis that the Southwest Sub-basin evolved within continental crust by rifting • Measure magnetization, mineralization, and geochemical compositions of basement rocks • Examine the paleoceanographic response to the opening of the South China Sea
Drilling program:	Hole A: • APC to refusal with nonmagnetic core barrels, core orientation (FlexIT tool), and APCT-3 • XCB to refusal • Drop FFF • RCB with nonmagnetic core barrels to 789 mbsf
Downhole logging program:	• Triple combo • FMS-sonic
Nature of rock anticipated:	(Calcareous) mudstone, siltstone, sandstone, basalt

Site summaries (continued)

Site SCS-4D

Priority:	Alternate
Position:	12°59.994′N, 115°0.744′E
Water depth (m):	4275
Target drilling depth (mbsf):	304
Approved maximum penetration:	Approved to basement + 100 m (Estimated total depth = 304 mbsf)
Survey coverage (track map; seismic profile):	Bathymetric sketch and site track map (Fig. **AF23**) Deep-penetration seismic reflection: • Primary line: NDS3-2 (CDP22750) (Fig. **AF30)** • Crossing line: A3B6 (CDP740) (Fig. **AF31**)
Objectives:	Alternate for SCS-4B • Determine the age of the Southwest Sub-basin • Test the hypothesis that the Southwest Sub-basin evolved within continental crust by rifting • Measure magnetization, mineralization, and geochemical compositions of basement rocks • Examine the paleoceanographic response to the opening of the South China Sea
Drilling program:	Hole A: • APC to refusal with nonmagnetic core barrels, core orientation (FlexIT tool), and APCT-3 • XCB to refusal • Drop FFF • RCB with nonmagnetic core barrels to 304 mbsf
Downhole logging program:	• Triple combo • FMS-sonic
Nature of rock anticipated:	(Calcareous) mudstone, siltstone, sandstone, basalt

Site summaries (continued)

Site SCS-4E

Priority:	Alternate
Position:	13°11.508′N, 114°55.398′E
Water depth (m):	4025
Target drilling depth (mbsf):	404
Approved maximum penetration:	Approved to basement + 100 m (Estimated total depth = 404 mbsf)
Survey coverage (track map; seismic profile):	Bathymetric sketch and site track map (Fig. **AF23**) Deep-penetration seismic reflection: • Primary line: NDS3-2 (CDP20884) (Fig. **AF32**)
Objectives:	Alternate for SCS-4B • Determine the age of the Southwest Sub-basin • Test the hypothesis that the Southwest Sub-basin evolved within continental crust by rifting • Measure magnetization, mineralization, and geochemical compositions of basement rocks • Examine the paleoceanographic response to the opening of the South China Sea
Drilling program:	Hole A: • APC to refusal with nonmagnetic core barrels, core orientation (FlexIT tool), and APCT-3 • XCB to refusal • Drop FFF • RCB with nonmagnetic core barrels to 404 mbsf
Downhole logging program:	• Triple combo • FMS-sonic
Nature of rock anticipated:	(Calcareous) mudstone, siltstone, sandstone, basalt

Site summaries (continued)

Site SCS-4F

Priority:	Alternate
Position:	13°33.606′N, 114°36.414′E
Water depth (m):	4218
Target drilling depth (mbsf):	290
Approved maximum penetration:	Approved to basement + 100 m (Estimated total depth = 290 mbsf)
Survey coverage (track map; seismic profile):	Bathymetric sketch and site track map (Fig. **AF23**) Deep-penetration seismic reflection: • Primary line: NDS3-1 (CDP17292) (Fig. **AF33**)
Objectives:	Alternate for SCS-4B • Determine the age of the Southwest Sub-basin • Test the hypothesis that the Southwest Sub-basin evolved within continental crust by rifting • Measure magnetization, mineralization, and geochemical compositions of basement rocks • Examine the paleoceanographic response to the opening of the South China Sea
Drilling program:	Hole A: • APC to refusal with nonmagnetic core barrels, core orientation (FlexIT tool), and APCT-3 • XCB to refusal • Drop FFF • RCB with nonmagnetic core barrels to 290 mbsf
Downhole logging program:	• Triple combo • FMS-sonic
Nature of rock anticipated:	(Calcareous) mudstone, siltstone, sandstone, basalt

Site summaries (continued)

Site SCS-2C

Priority:	Alternate
Position:	17°20.472′N, 116°47.802′E
Water depth (m):	4005
Target drilling depth (mbsf):	1215
Approved maximum penetration:	Approved to basement + 100 m (Estimated total depth = 1215 mbsf)
Survey coverage (track map; seismic profile):	Bathymetric sketch and site track map (Fig. **AF34**) Deep-penetration seismic reflection: • Primary line: 973SCSIO_1c (SP10576) (Fig. **AF35**) • Crossing line: ZSHL295 (SP8714) (Fig. **AF36**)
Objectives:	• Test the hypothesis that a ridge jump occurred around 26 Ma • Measure magnetization, mineralization, and geochemical compositions of basement rocks • Obtain basement rocks to ascertain the causes of sharp magnetic contrasts between different sub-basins and around magnetic Anomaly C8 • Study the paleoceanographic response to the opening of the South China Sea
Drilling program:	Hole A: • APC to refusal with nonmagnetic core barrels, core orientation (FlexIT tool), and APCT-3 • XCB to refusal • Drop FFF • RCB with nonmagnetic core barrels to 1215 mbsf
Downhole logging program:	• Triple combo • FMS-sonic
Nature of rock anticipated:	(Calcareous) mudstone, siltstone, sandstone, basalt

Site summaries (continued)

Site SCS-2D

Priority:	Alternate
Position:	17°20.652′N, 116°38.718′E
Water depth (m):	3942
Target drilling depth (mbsf):	1140
Approved maximum penetration:	Approved to basement + 100 m (Estimated total depth = 1140 mbsf)
Survey coverage (track map; seismic profile):	Bathymetric sketch and site track map (Fig. **AF37**) Deep-penetration seismic reflection: • Primary line: ZSH275 (SP4976) (Fig. **AF38**) • Crossing line: ZSHL295 (SP8495) (Fig. **AF39**)
Objectives:	• Test the hypothesis that a ridge jump occurred around 26 Ma • Measure magnetization, mineralization, and geochemical compositions of basement rocks • Obtain basement rocks to ascertain the causes of sharp magnetic contrasts between different sub-basins and around magnetic Anomaly C8 • Study the paleoceanographic response to the opening of the South China Sea
Drilling program:	Hole A: • APC to refusal with nonmagnetic core barrels, core orientation (FlexIT tool), and APCT-3 • XCB to refusal • Drop FFF • RCB with nonmagnetic core barrels to 1140 mbsf
Downhole logging program:	• Triple combo • FMS-sonic
Nature of rock anticipated:	(Calcareous) mudstone, siltstone, sandstone, basalt

Site summaries (continued)

Site SCS-1C

Priority:	Alternate
Position:	21°0.15′N, 119°47.10′E
Water depth (m):	3306
Target drilling depth (mbsf):	1210
Approved maximum penetration:	Approved to basement + 100 m (Estimated total depth = 1210 mbsf)
Survey coverage (track map; seismic profile):	Bathymetric sketch and site track map (Fig. **AF40**) Deep-penetration seismic reflection: • Primary line: 973GMGS_2 (SP6396) (Fig. **AF41**) • Crossing line: ACT105 (CDP2836) (Fig. **AF42**)
Objectives:	• To determine the nature and age of the northeasternmost South China Sea basin • To determine if the northeasternmost South China Sea basin is affiliated with Mesozoic paleo-Pacific or Tethys oceanic crust, an attenuated continental block, or a continent-ocean transition zone • To test if oceanic crust as old as 37 Ma exists in the northeasternmost South China Sea basin • To examine the nature of crust subducting beneath the Luzon arc
Drilling program:	Hole A: • APC to refusal with nonmagnetic core barrels, core orientation (FlexIT tool), and APCT-3 • XCB to refusal • Drop FFF • RCB with nonmagnetic core barrels to 1210 mbsf
Downhole logging program:	• Triple combo • FMS-sonic
Nature of rock anticipated:	(Calcareous) mudstone, siltstone, sandstone, basalt

Figure AF1. Regional contoured bathymetric map showing seismic reflection profiles (yellow and pink lines) and the locations of primary Site SCS-6A, alternate Sites SCS-6B and SCS-6C, and ODP Site 1148. Contour interval = 100 m.

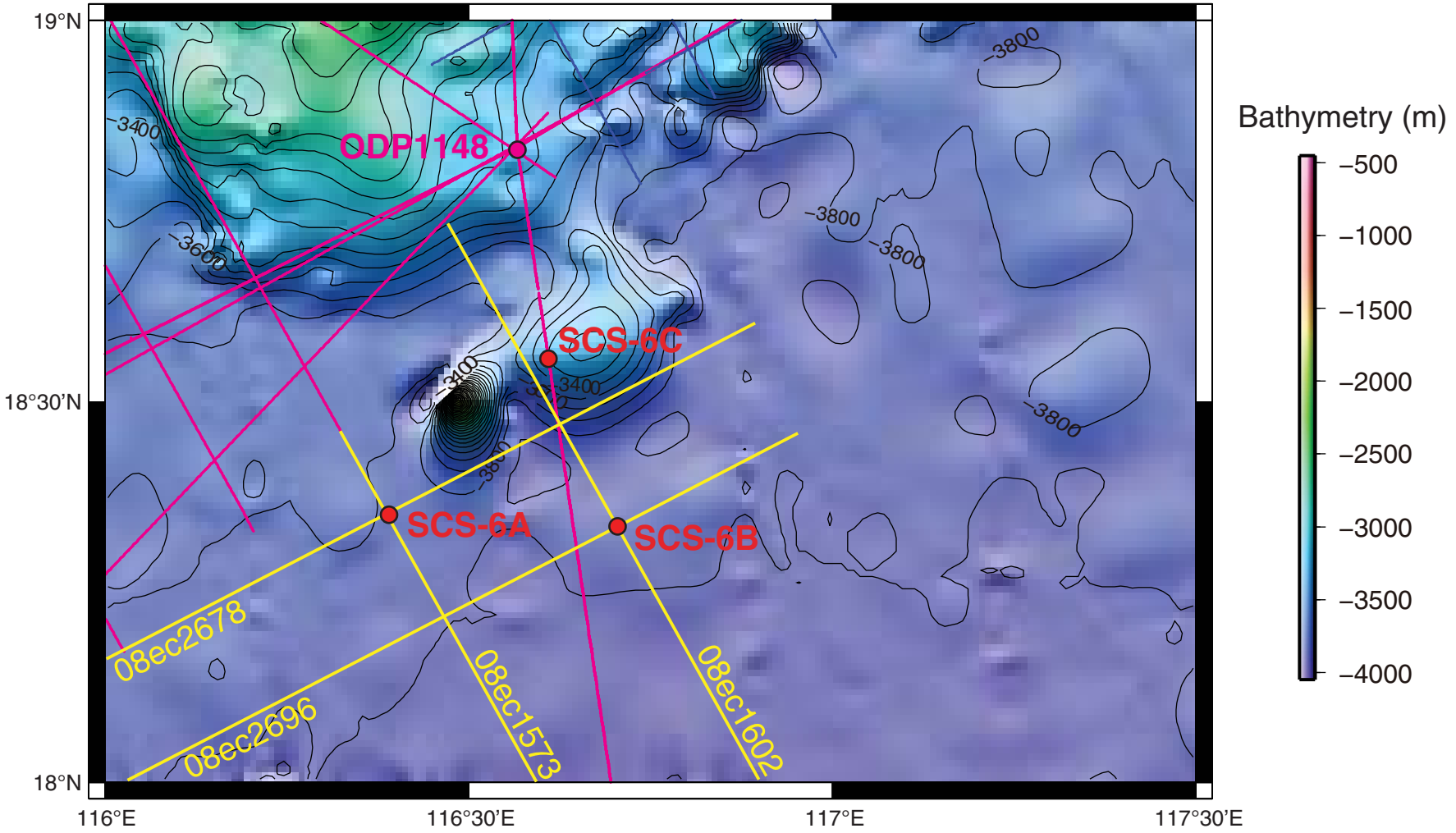

Figure AF2. Contoured bathymetric map showing seismic reflection Profiles 08ec1573 (Fig. AF3) and 08ec2678 (Fig. AF4) and the location of proposed Site SCS-6A. Contour interval = 10 m.

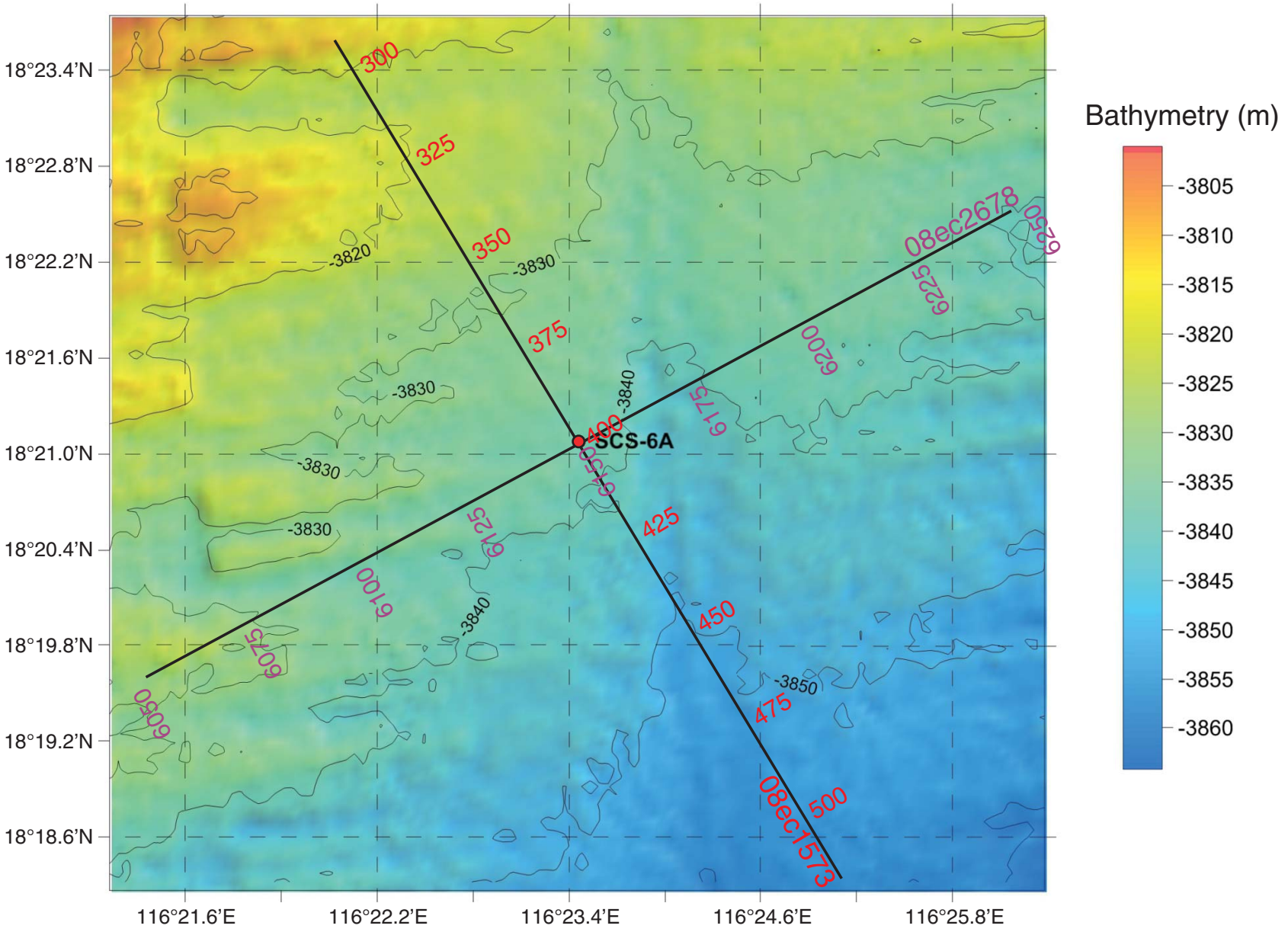

Figure AF3. Seismic profile Line 08ec1573 (northwest–southeast) with location of primary Site SCS-6A (18°21.117′N, 116°23.45′E; shotpoint [SP] 400; water depth = 3843 m; target depth = 1930 mbsf). Green line = interpreted top basement, blue line = interpreted top Oligocene.

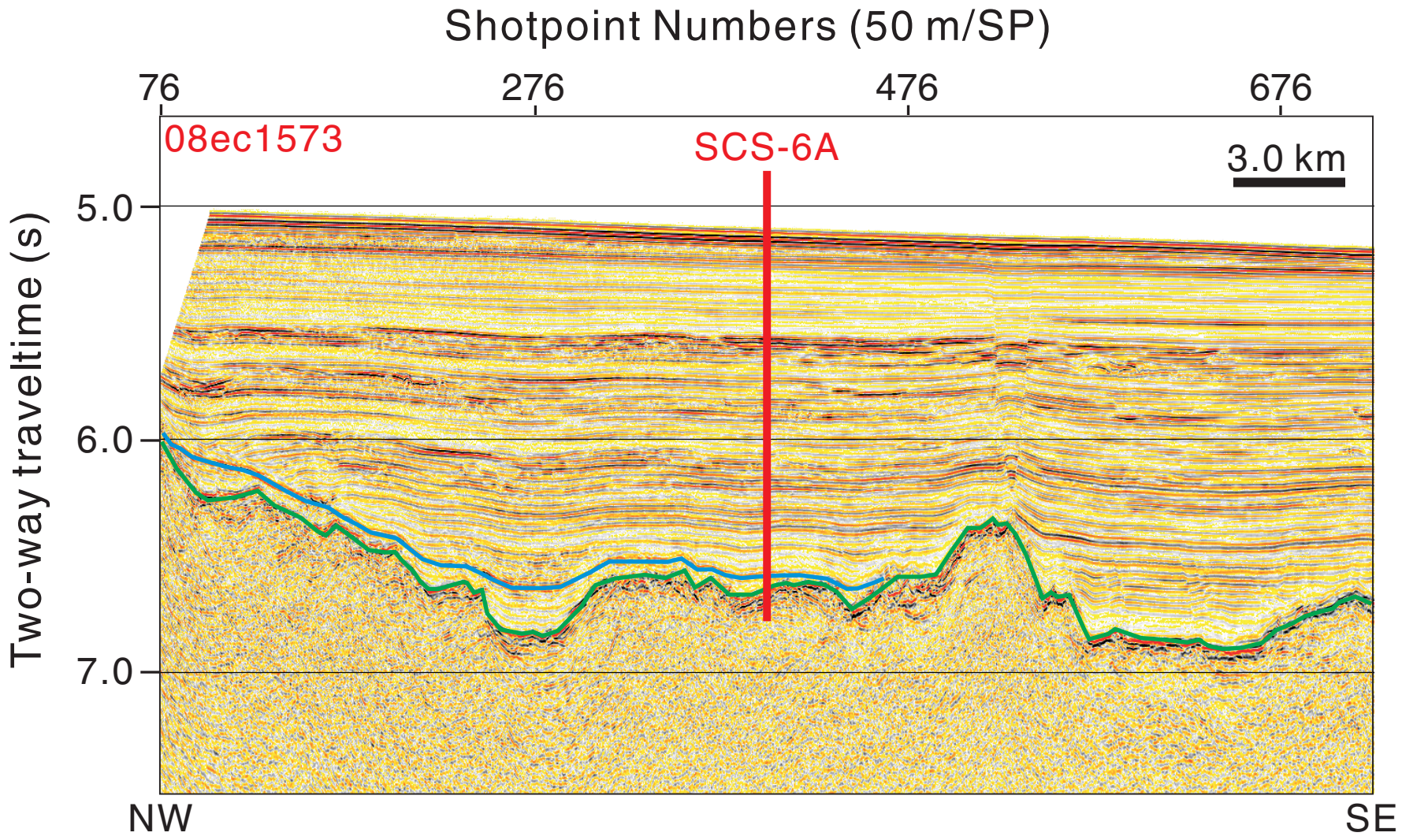

Figure AF4. Seismic profile Line 08ec2678 (southwest–northeast) with location of primary Site SCS-6A (18°21.117′N, 116°23.45′E; shotpoint [SP] 6149; water depth = 3843 m; target depth = 1930 mbsf). Green line = interpreted top basement; blue line = interpreted top Oligocene.

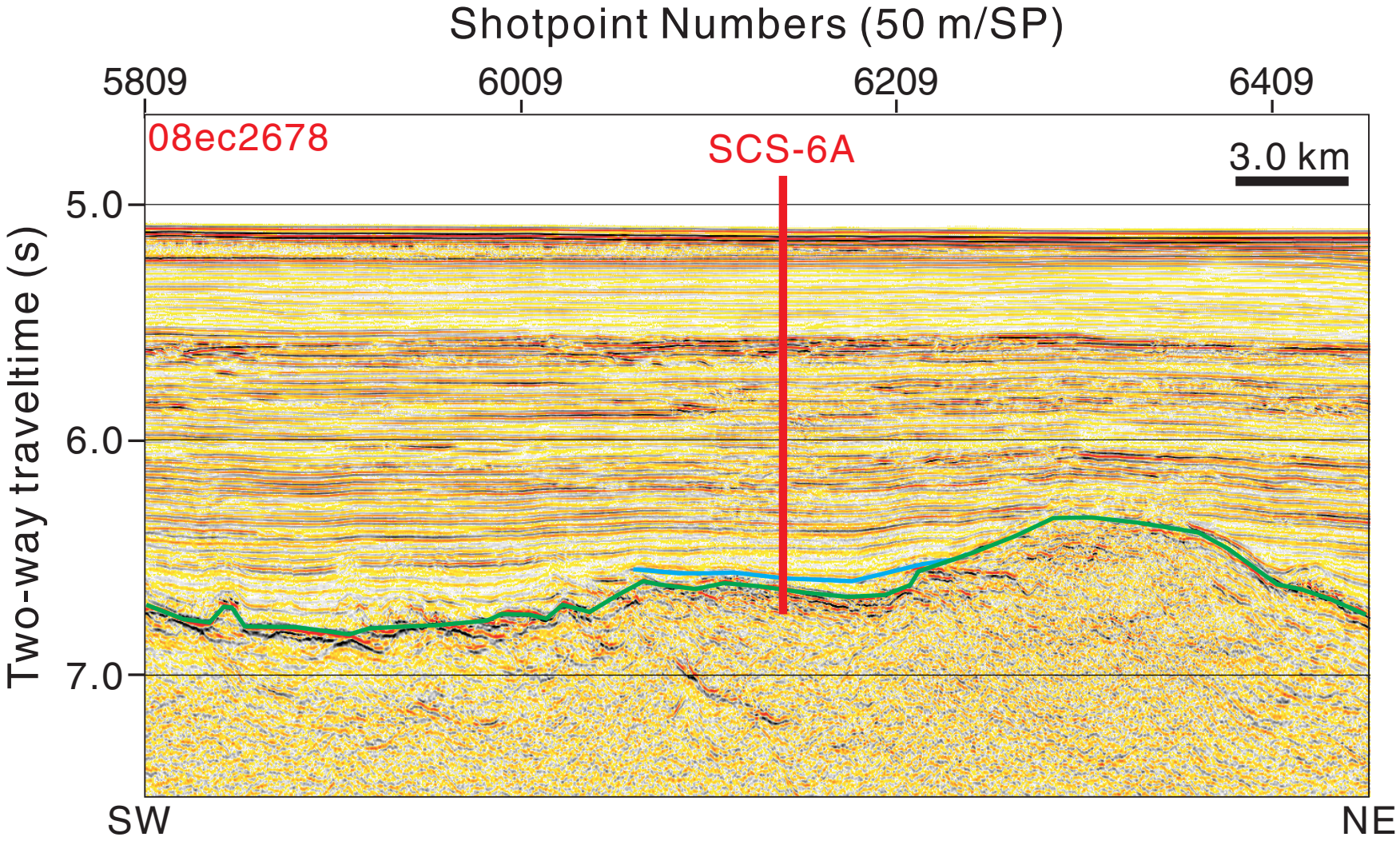

Figure AF5. Contoured bathymetric map showing seismic reflection Profiles 08ec1602 (Fig. AF6) and 08ec2696 (Fig. AF7) and the location of proposed Site SCS-6B. Contour interval = 10 m.

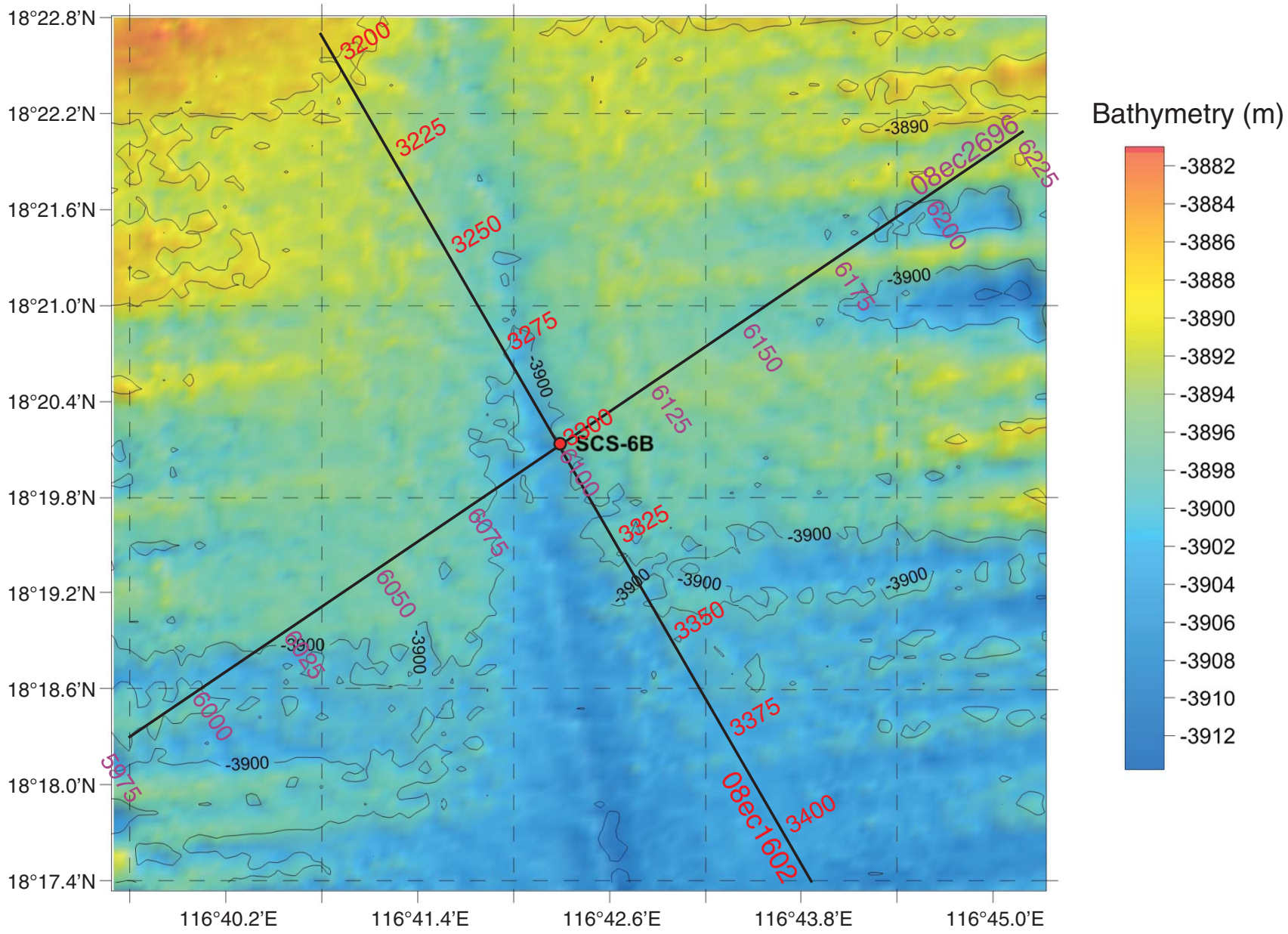

Figure AF6. Seismic profile Line 08ec1602 (northwest–southeast) with location of proposed Site SCS-6B (18°20.167′N, 116°42.28′E; shotpoint [SP] 3300; water depth = 3906 m; target depth = 1879 mbsf). Green line = interpreted top basement.

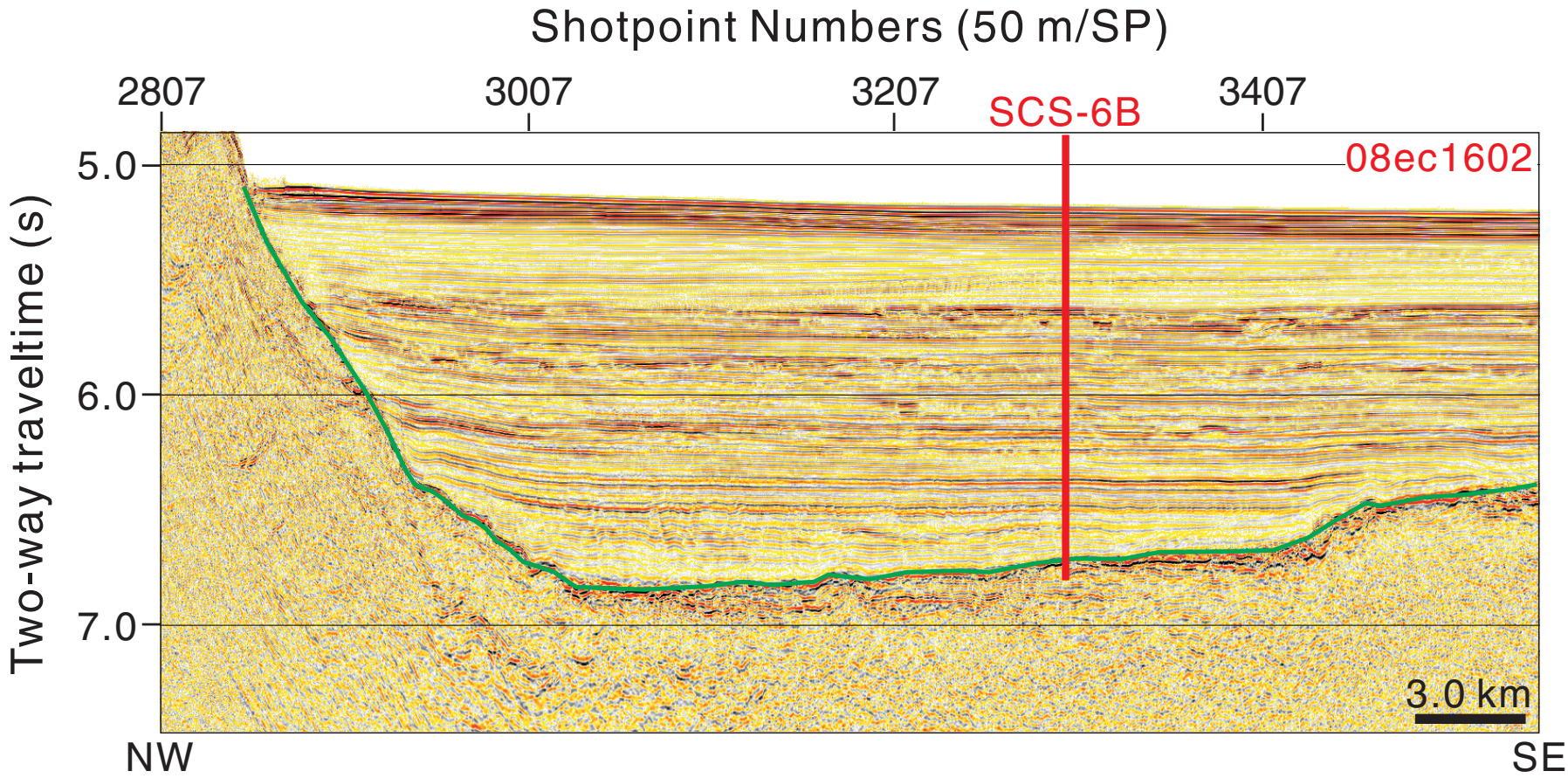

Figure AF7. Seismic profile Line 08ec2696 (southwest–northeast) with location of proposed Site SCS-6B (18°20.167′N, 116°42.28′E; shotpoint [SP] 6098; water depth = 3906 m; target depth = 1879 mbsf). Green line = interpreted top basement.

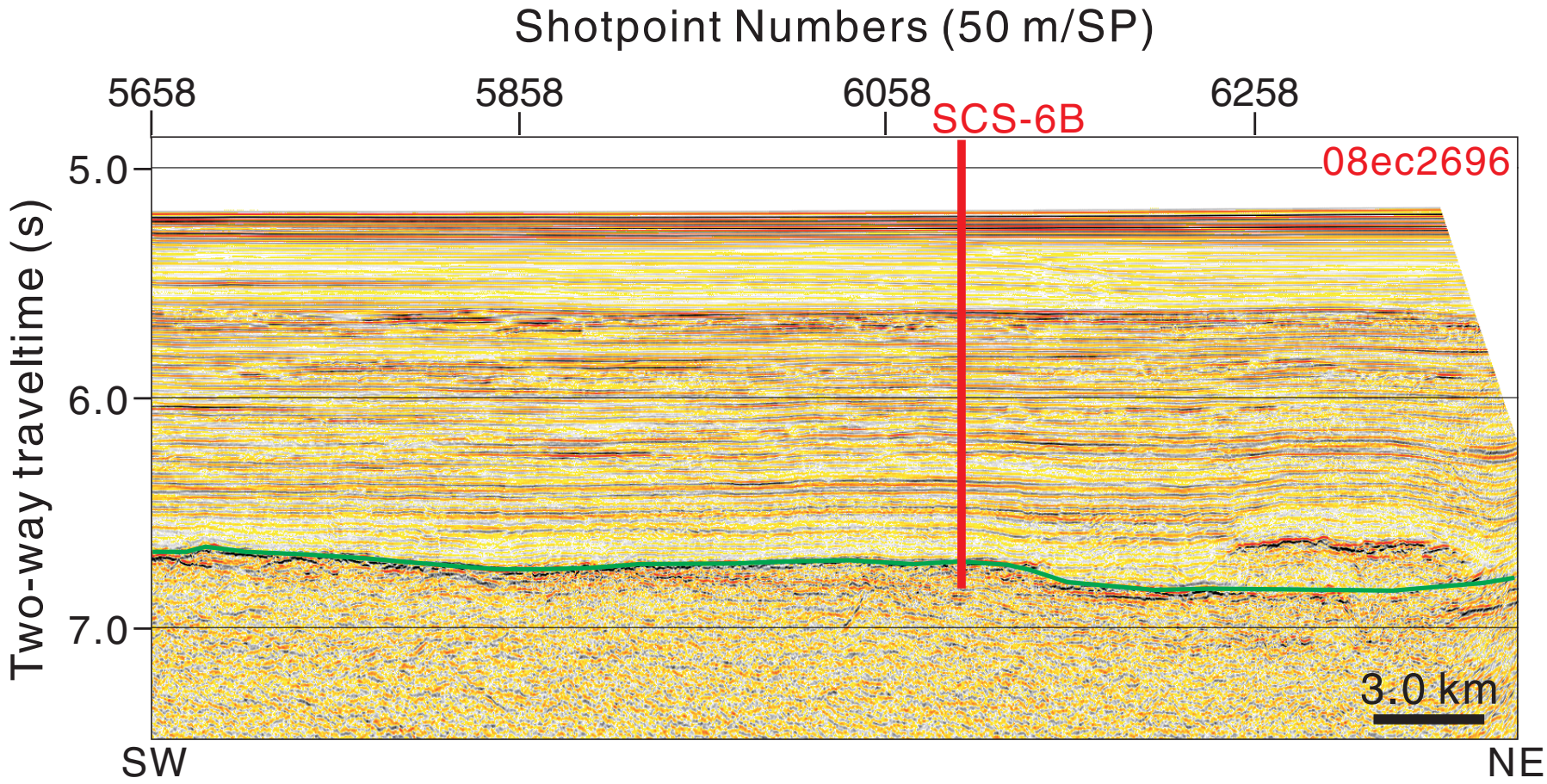

Figure AF8. Seismic profile Line 08ec1602 (northwest–southeast) with location of proposed Site SCS-6C (18°33.384′N, 116°36.576′E; common depth point [CDP] 6312; water depth = 3294 m; target depth = 110 mbsf).

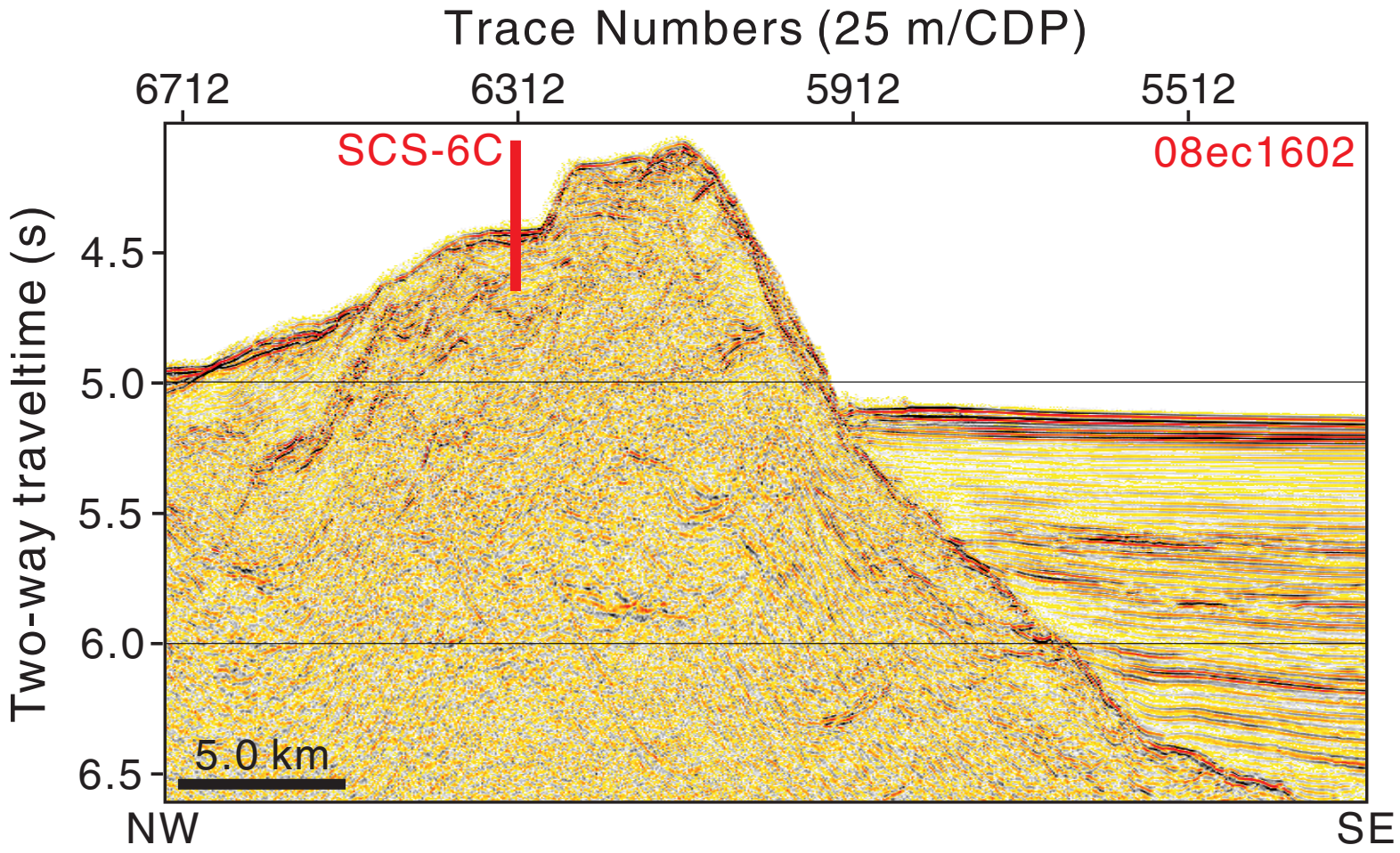

Figure AF9. Seismic profile Line 973SCSIO_01A (north–south) with location of proposed Site SCS-6C (18°33.384′N, 116°36.576′E; shotpoint [SP] 7920; water depth = 3294 m; target depth = 110 mbsf) projected ~5000 m west onto the line.

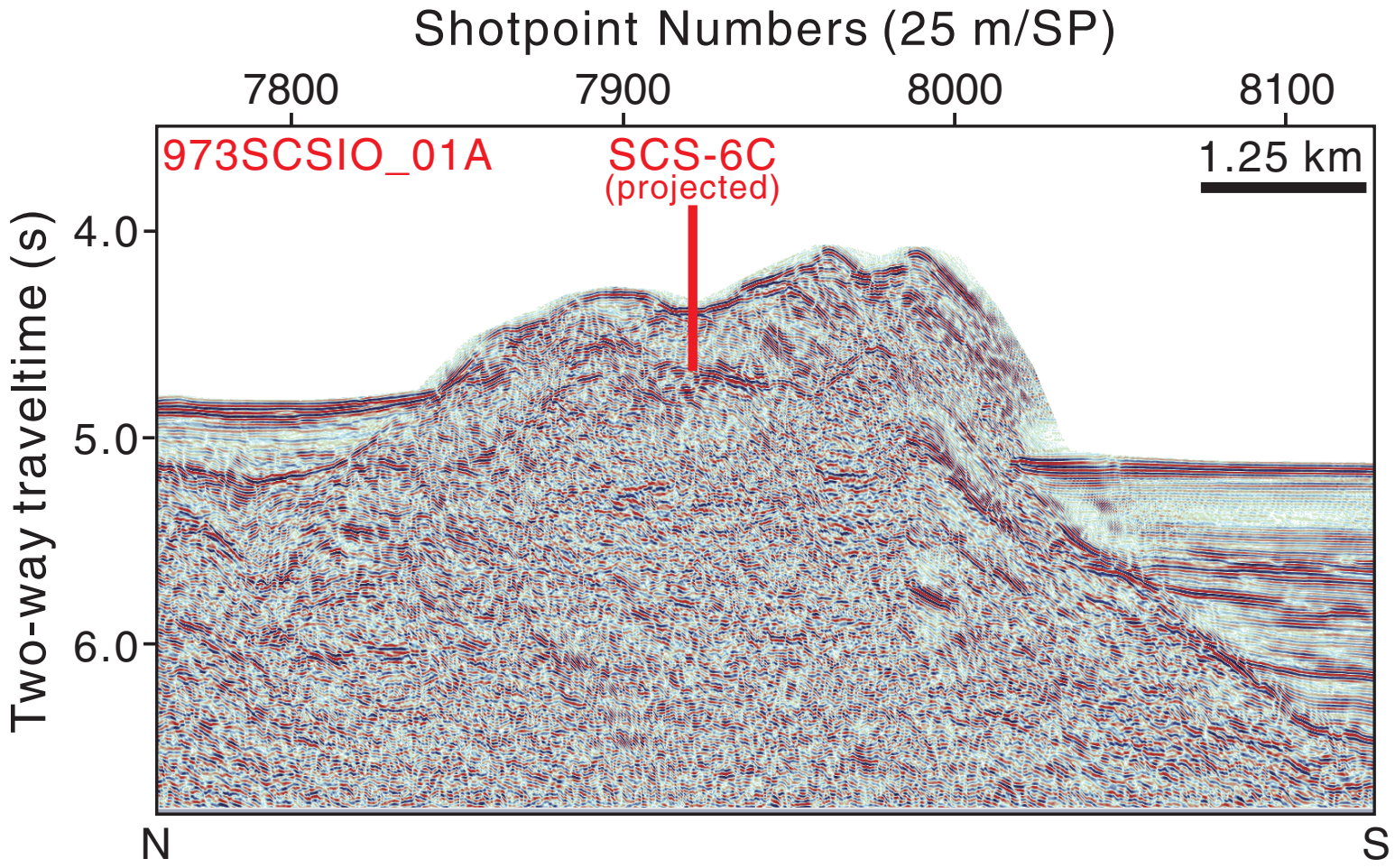

Figure AF10. Regional contoured bathymetric map showing seismic reflection profiles (orange and red lines) and the locations of primary Site SCS-3G, backup primary Site SCS-3F, and alternate Sites SCS-3E, SCS-3H, and SCS-3I. Contour interval = 1000 m.

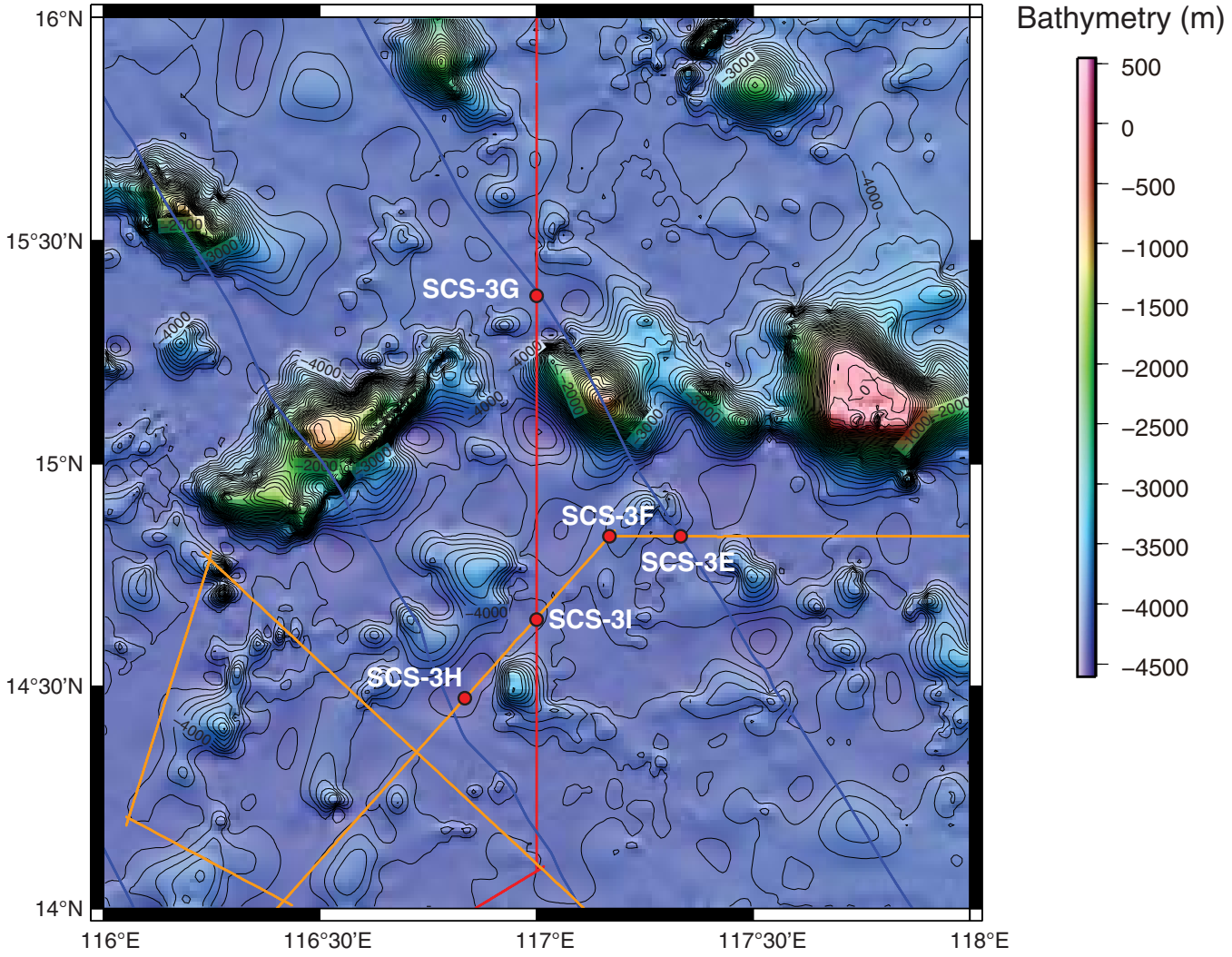

Figure AF11. Contoured bathymetric map showing seismic reflection Profiles 973SCSIO01e (Fig. AF12) and SO49-017a (Fig. AF13) and the location of proposed Site SCS-3G. Contour interval = 10 m.

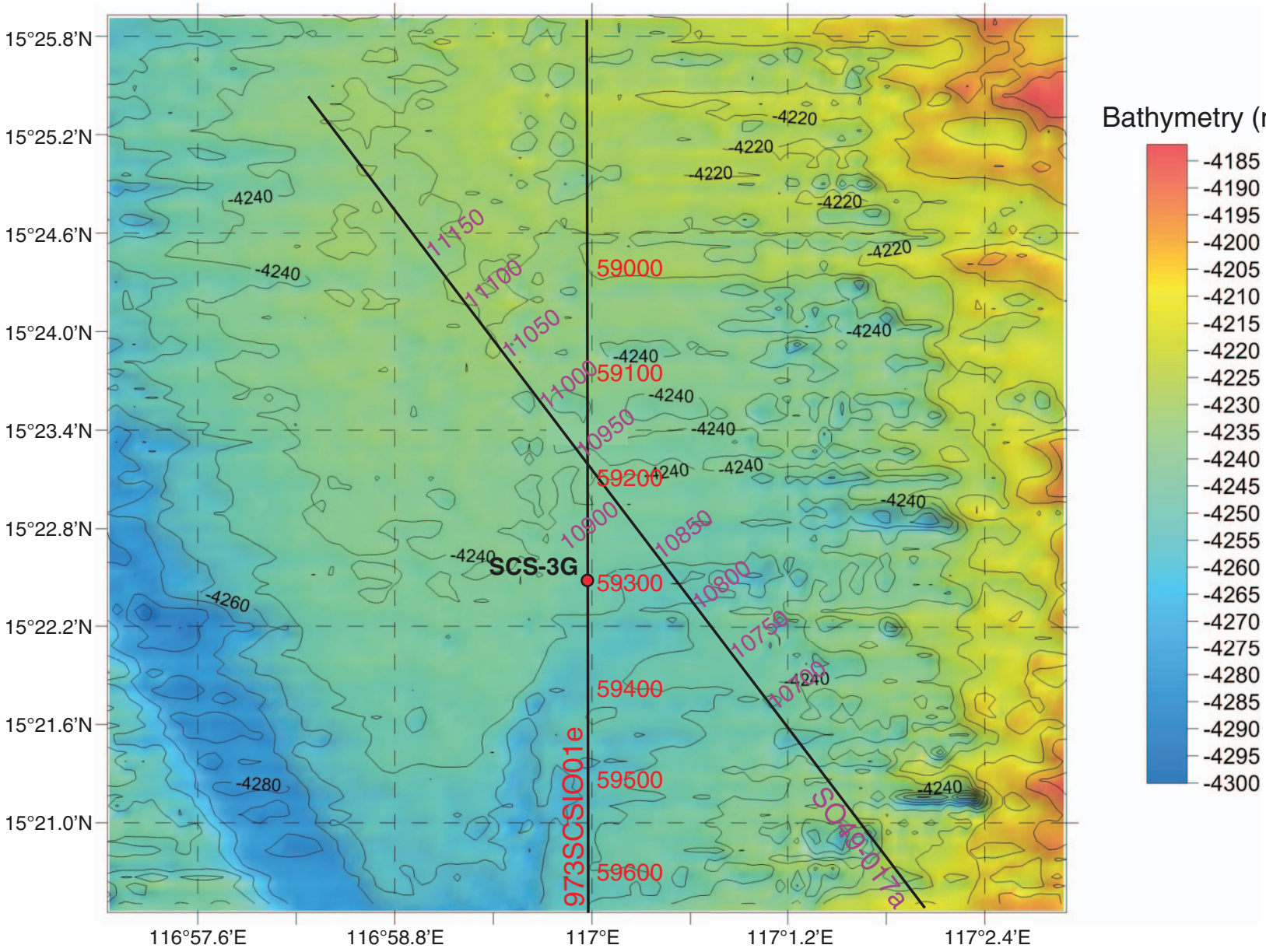

Figure AF12. Seismic profile Line 973SCSIO01e (north–south) with location of proposed Site SCS-3G (15°22.548′N, 117°E; common depth point [CDP] 59300; water depth = 4213 m; target depth = 1061 mbsf). Green line = interpreted top basement.

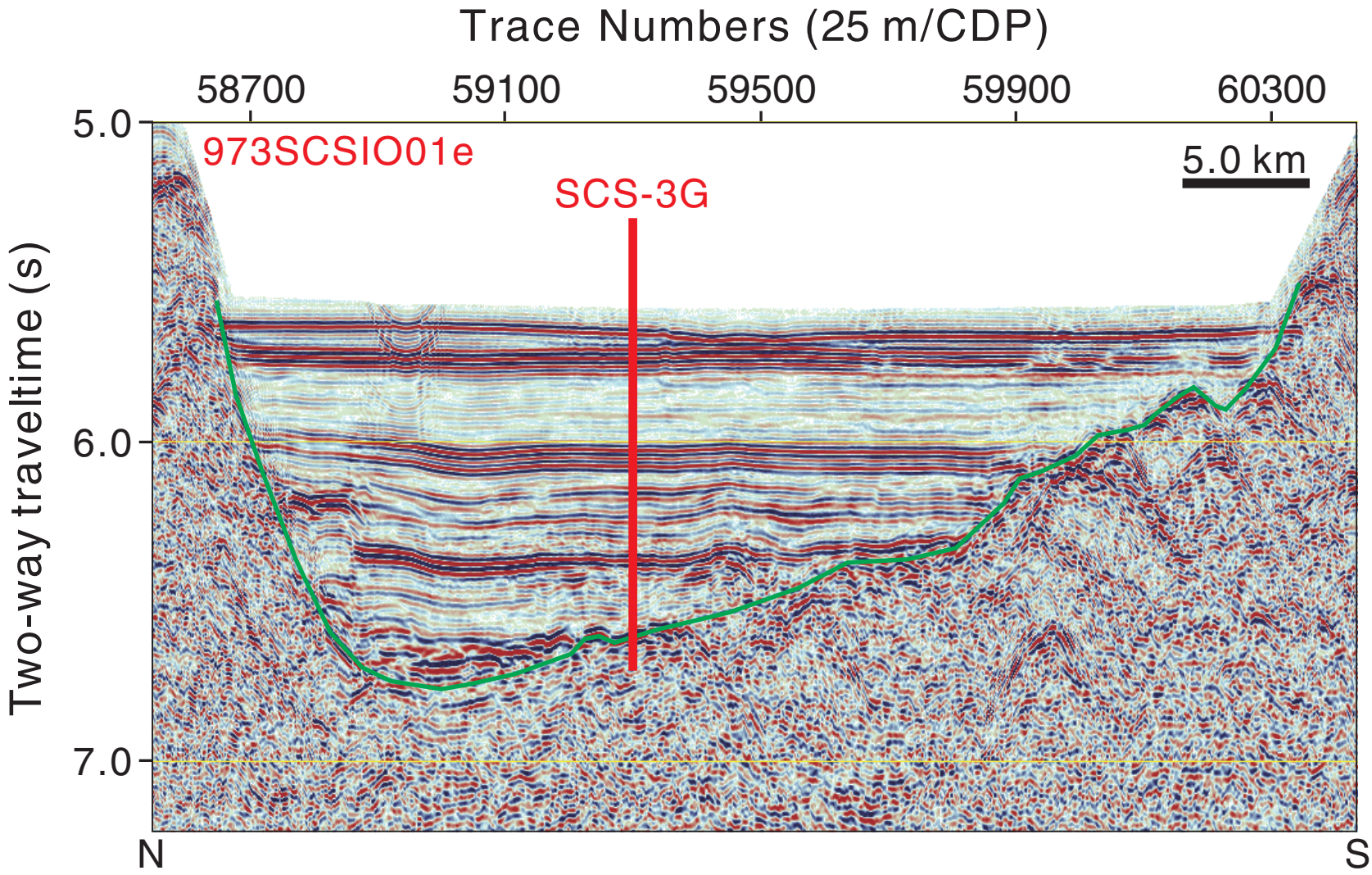

Figure AF13. Seismic profile Line SO49-017a (northwest–southeast) with location of proposed Site SCS-3G (15°22.548′N, 117°E; common depth point [CDP] 10867; water depth = 4213 m; target depth = 1061 mbsf) projected ~770 m northeast onto the line. Green line = interpreted top basement.

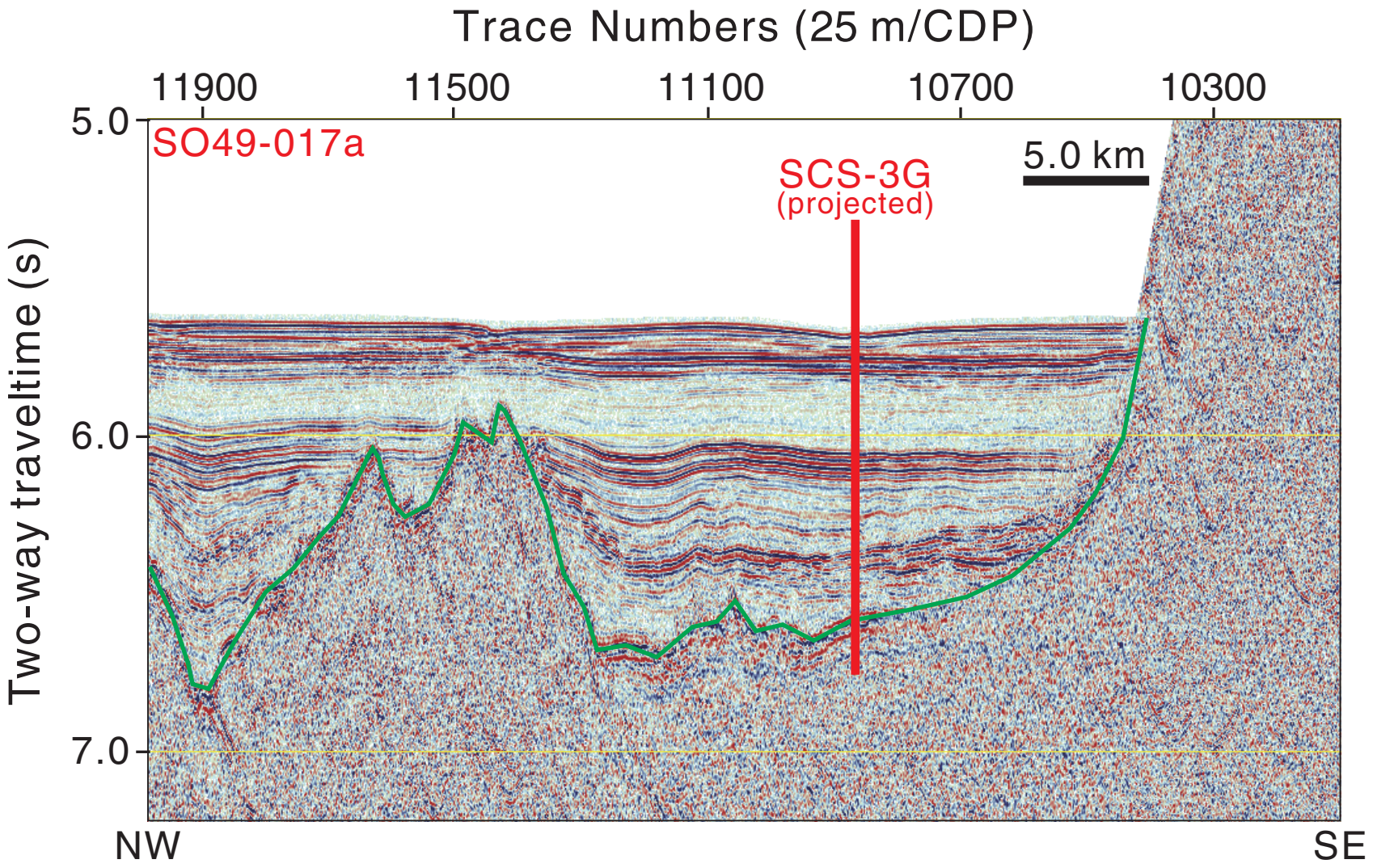

Figure AF14. Seismic profile Line BGR08-124 (west–east) with location of proposed Site SCS-3F (14°50.196′N, 117°10.08′E; common depth point [CDP] 10110; water depth = 4280 m; target depth = 297 mbsf). Green line = interpreted top basement.

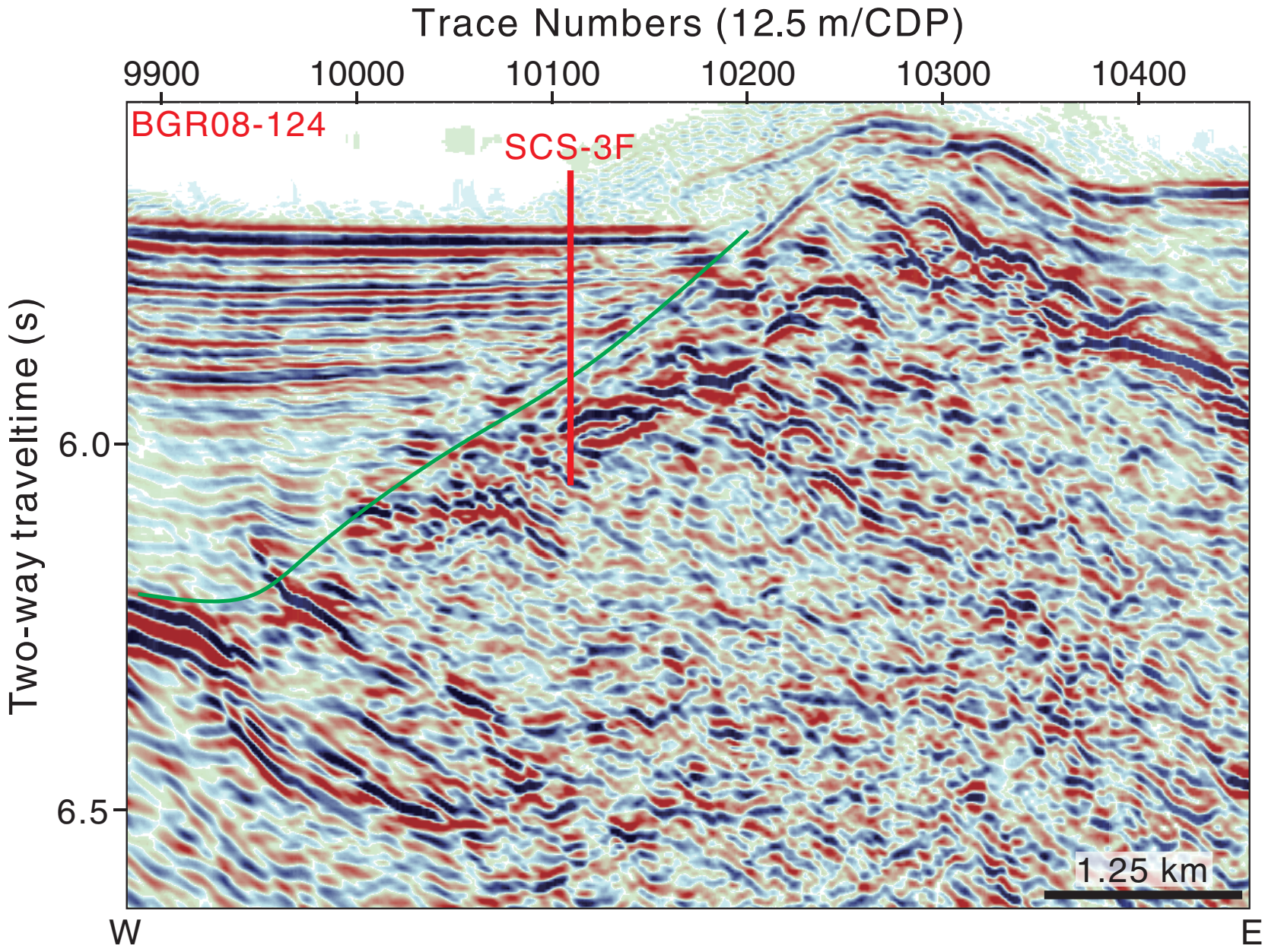

Figure AF15. Seismic profile Line BGR08-123 (southwest–northeast) with location of proposed Site SCS-3F (14°50.196′N, 117°10.08′E; common depth point [CDP] 19938; water depth = 4280 m; target depth = 297 mbsf). Green line = interpreted top basement.

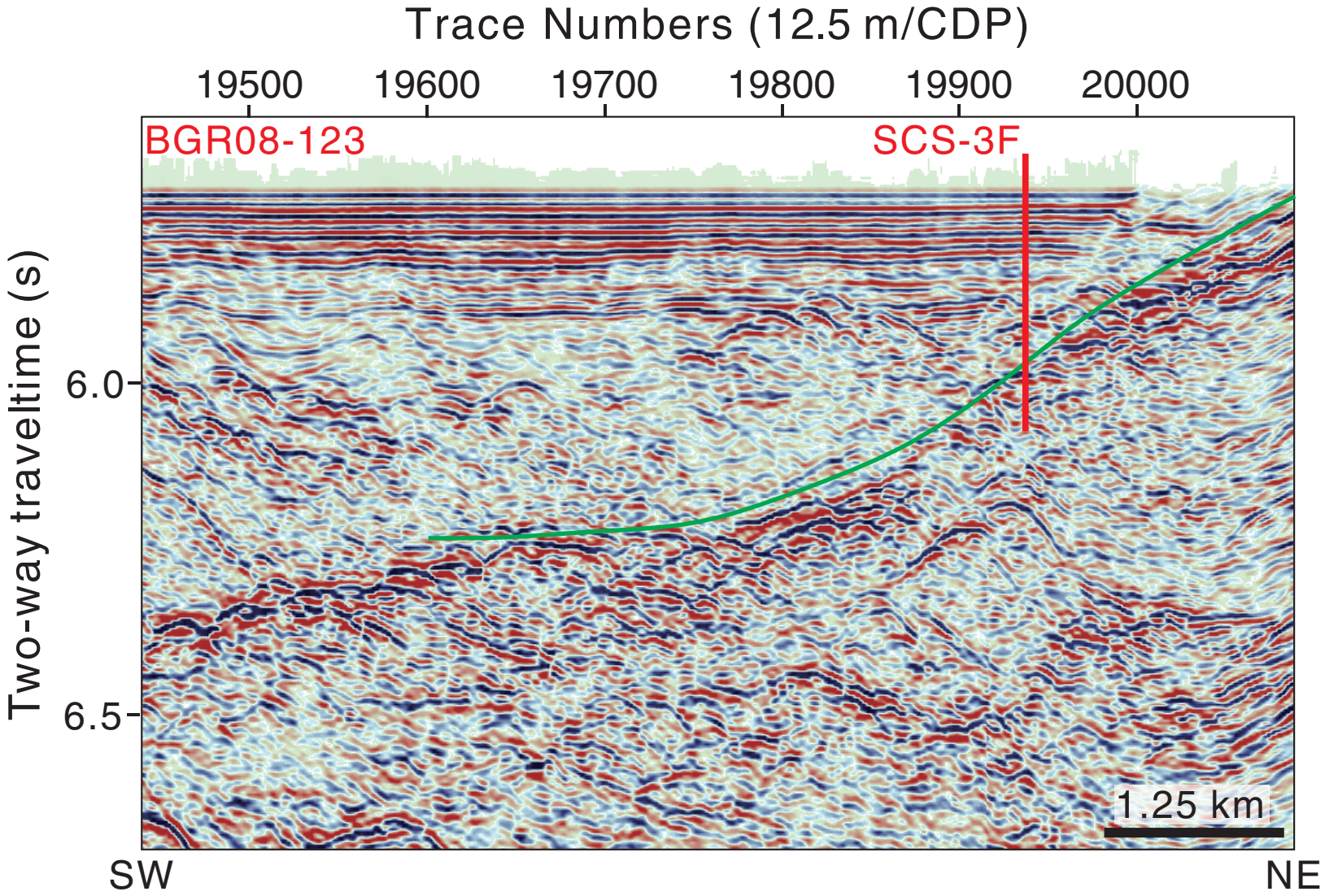

Figure AF16. Seismic profile Line BGR08-124 (west–east) with location of proposed Site SCS-3E (14°50.202′N, 117°19.956′E; common depth point [CDP] 11527; water depth = 4291 m; target depth = 605 mbsf). Green line = interpreted top basement.

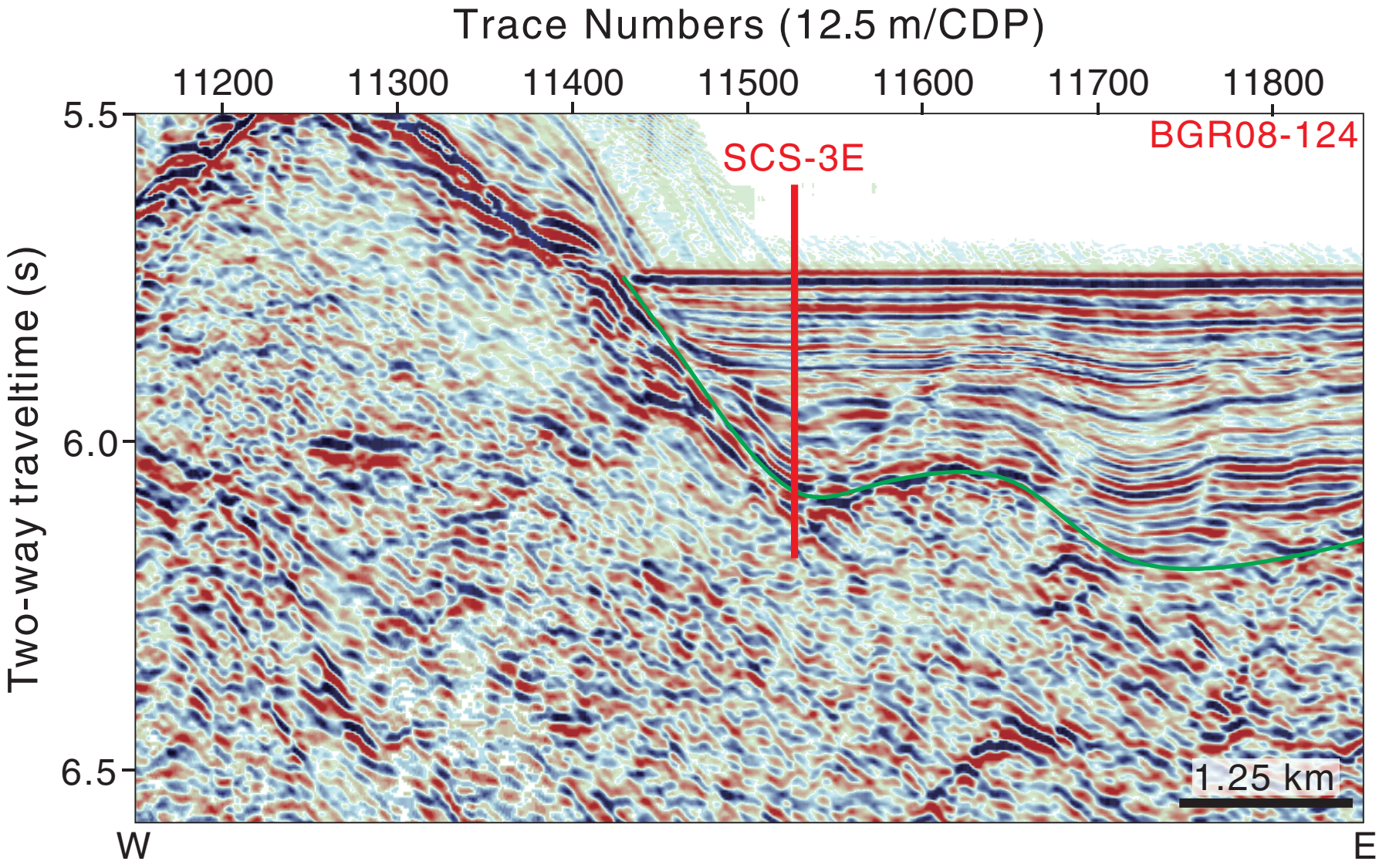

Figure AF17. Seismic profile Line SO49-017a (northwest–southeast) with location of proposed Site SCS-3E (14°50.202′N, 117°19.956′E; common depth point [CDP] 8298; water depth = 4291 m; target depth = 605 mbsf). Green line = interpreted top basement.

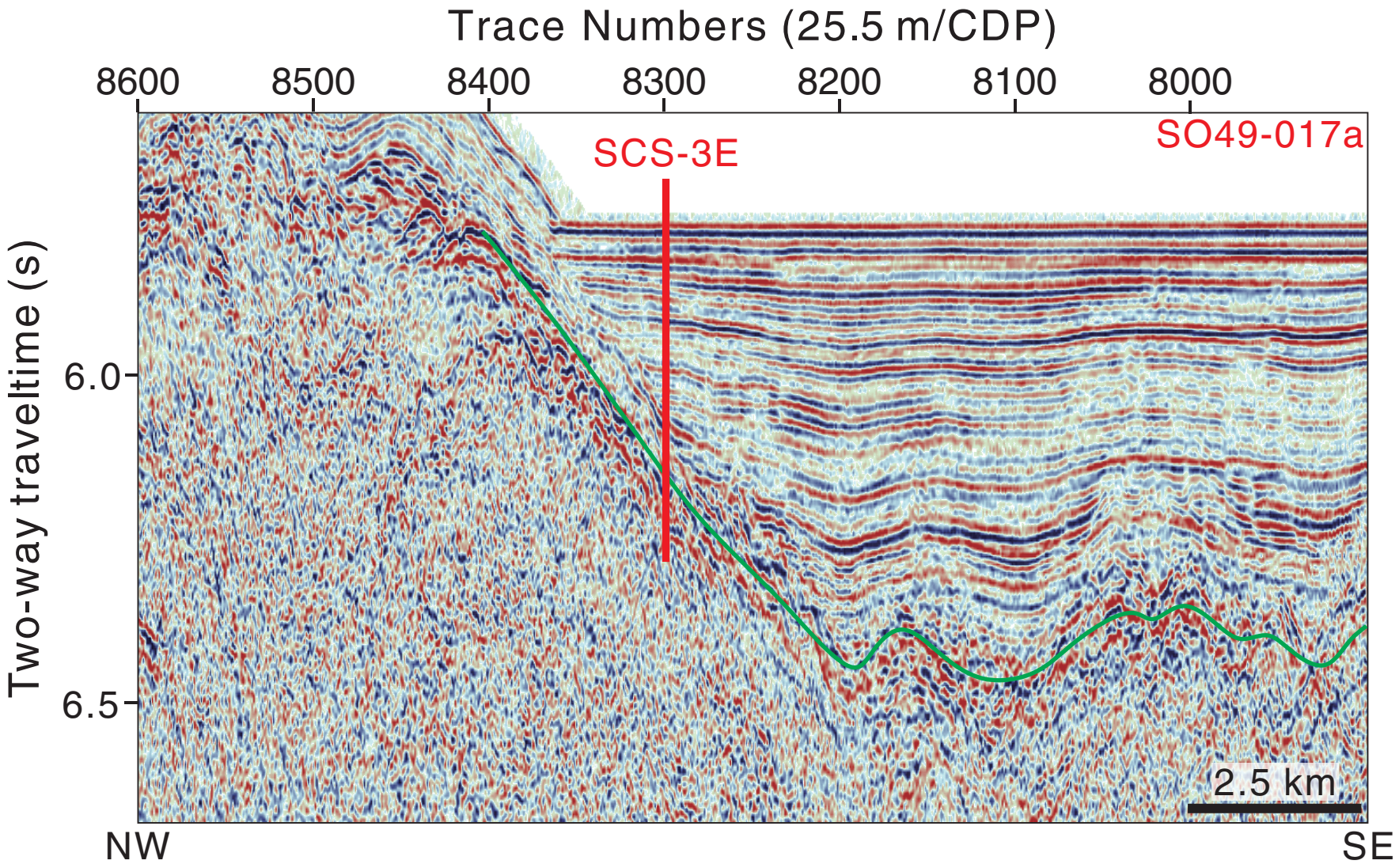

Figure AF18. Contoured bathymetric map showing seismic reflection Profiles BGR08-123 (Fig. AF19) and SO49-018_1 (Fig. AF20) and the location of proposed Site SCS-3H. Contour interval = 10 m.

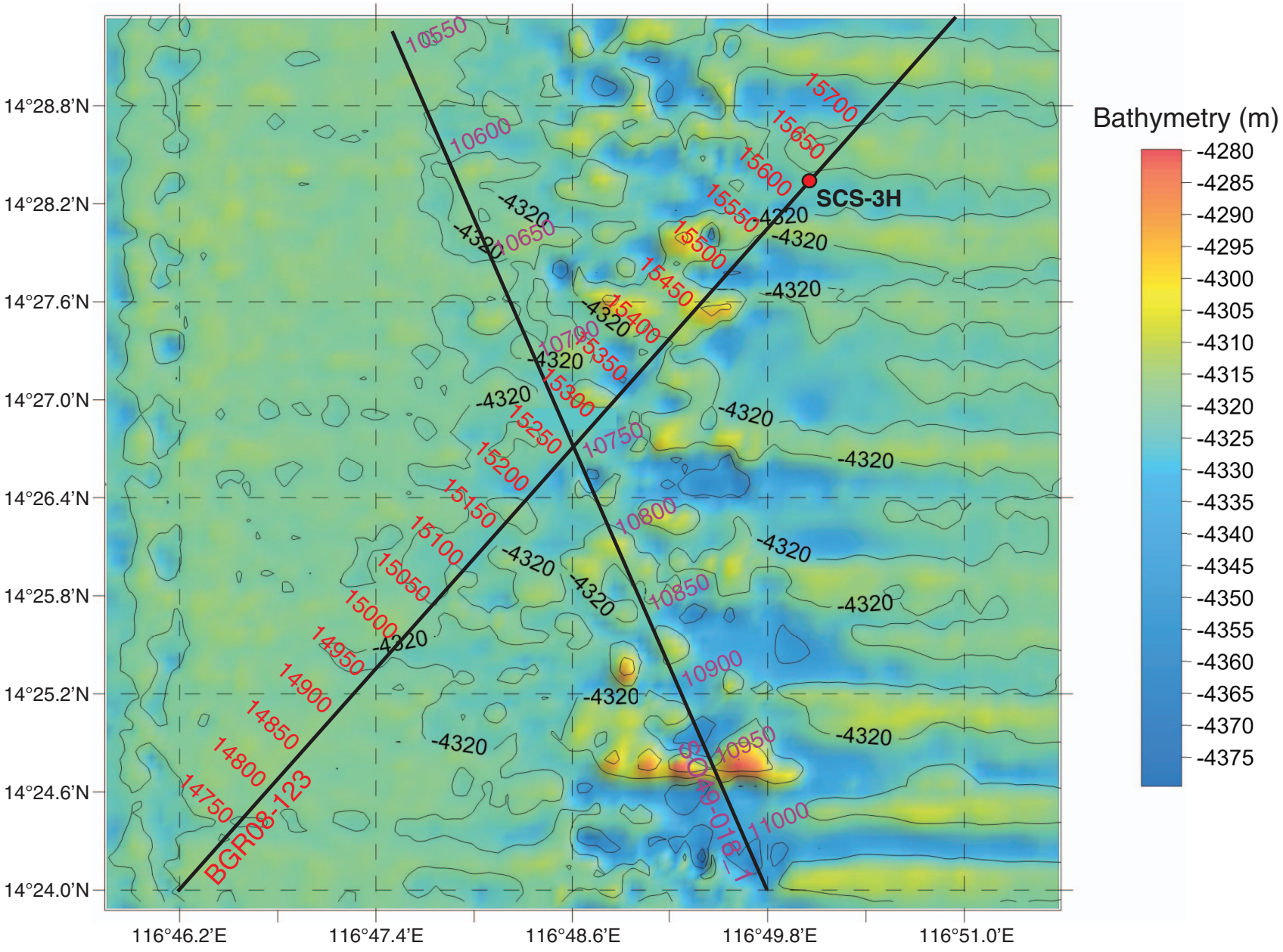

Figure AF19. Seismic profile Line BGR08-123 (southwest–northeast) with location of proposed Site SCS-3H (14°28.368′N, 116°50.082′E; common depth point [CDP] 15625; water depth = 4304 m; target depth = 866 mbsf). Green line = interpreted top basement.

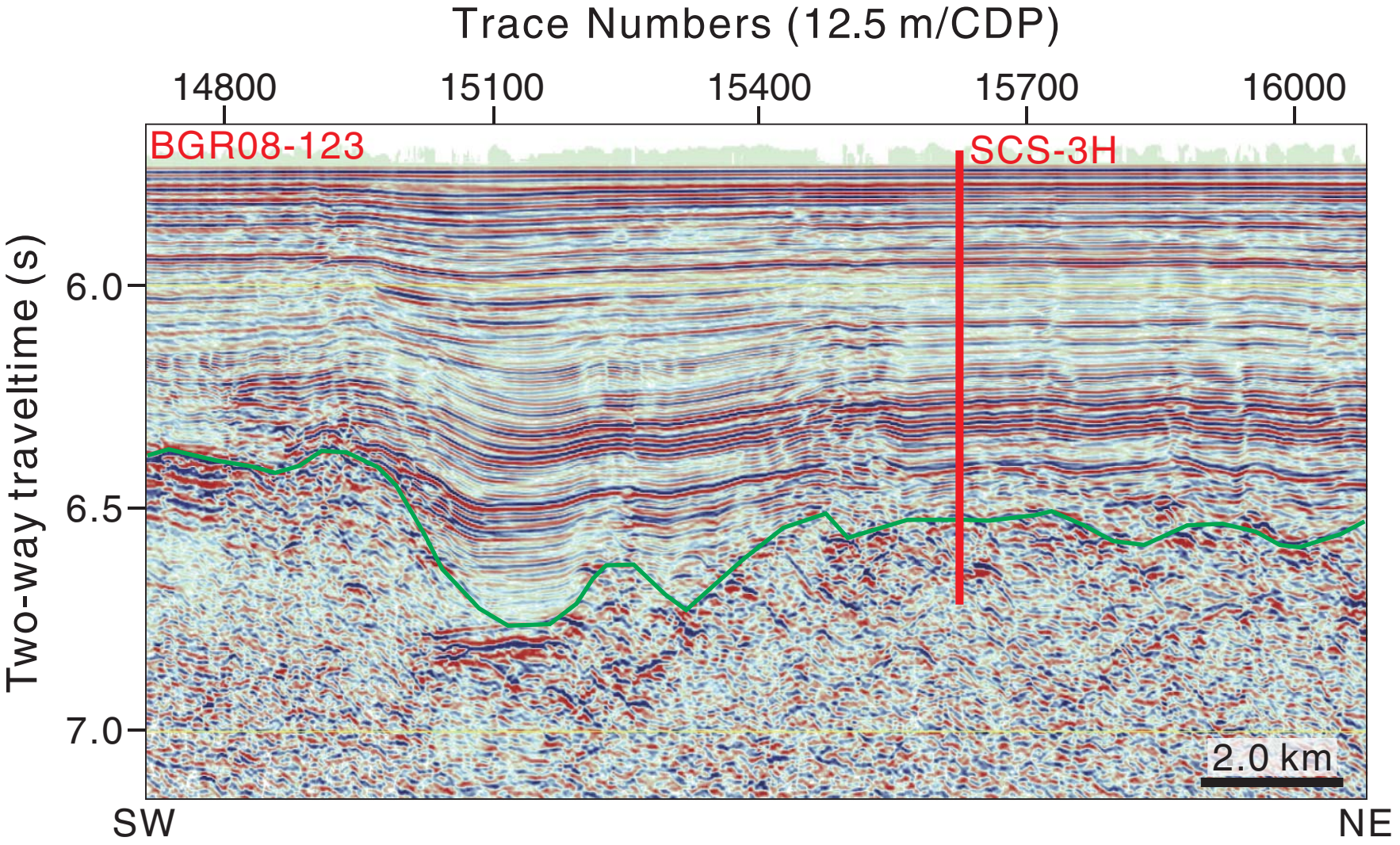

Figure AF20. Seismic profile Line SO49-018_1 (northwest–southeast) with location of proposed Site SCS-3H (14°28.368′N, 116°50.082′E; common depth point [CDP] 10680; water depth = 4304 m; target depth = 866 mbsf) projected ~3550 m southwest onto the line. Green line = interpreted top basement.

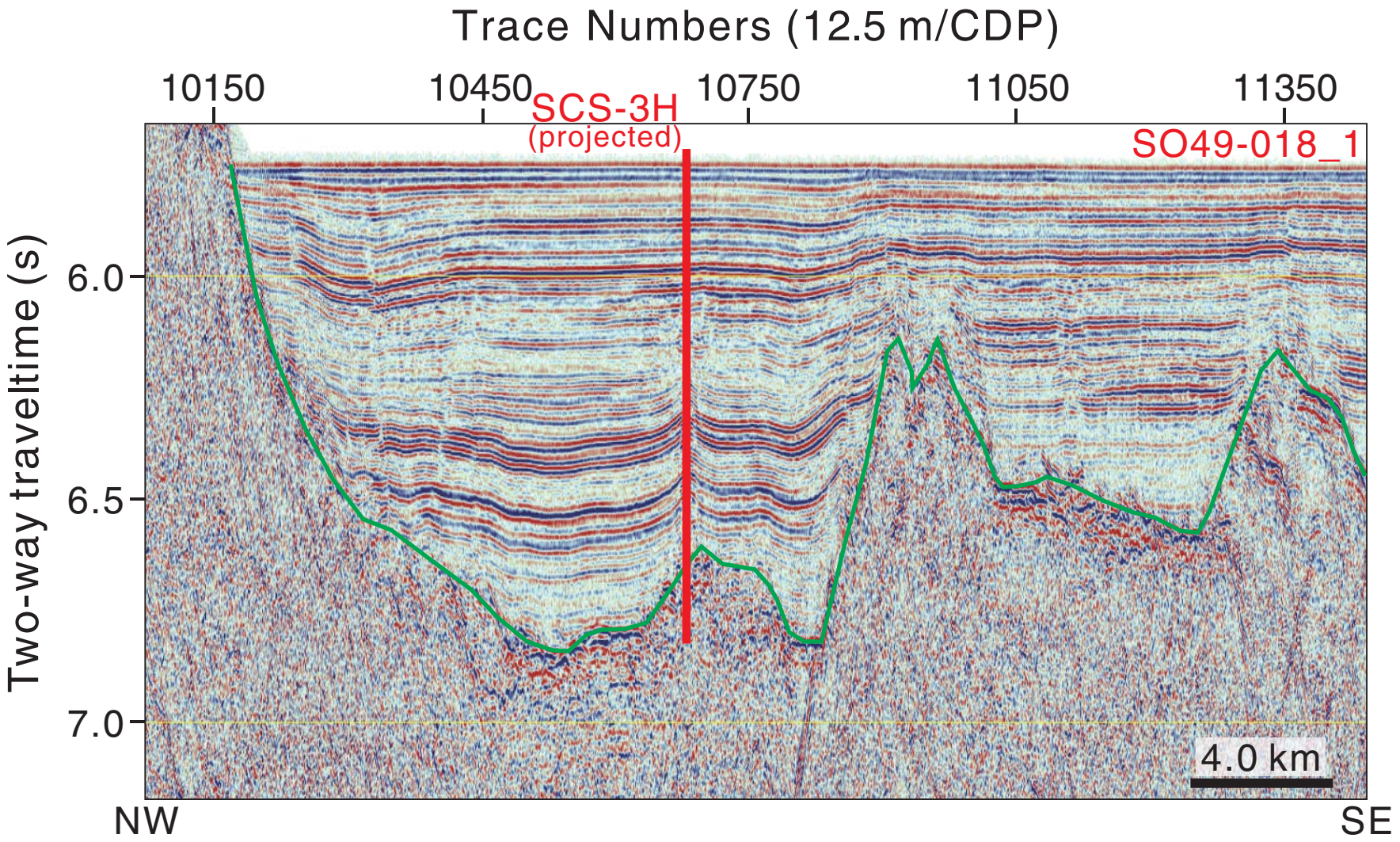

Figure AF21. Seismic profile Line 973SCSIO01e (north–south) with location of proposed Site SCS-3I (14°39.012′N, 116°59.994′E; common depth point [CDP] 65500; water depth = 4265 m; target depth = 674 mbsf). Green line = interpreted top basement.

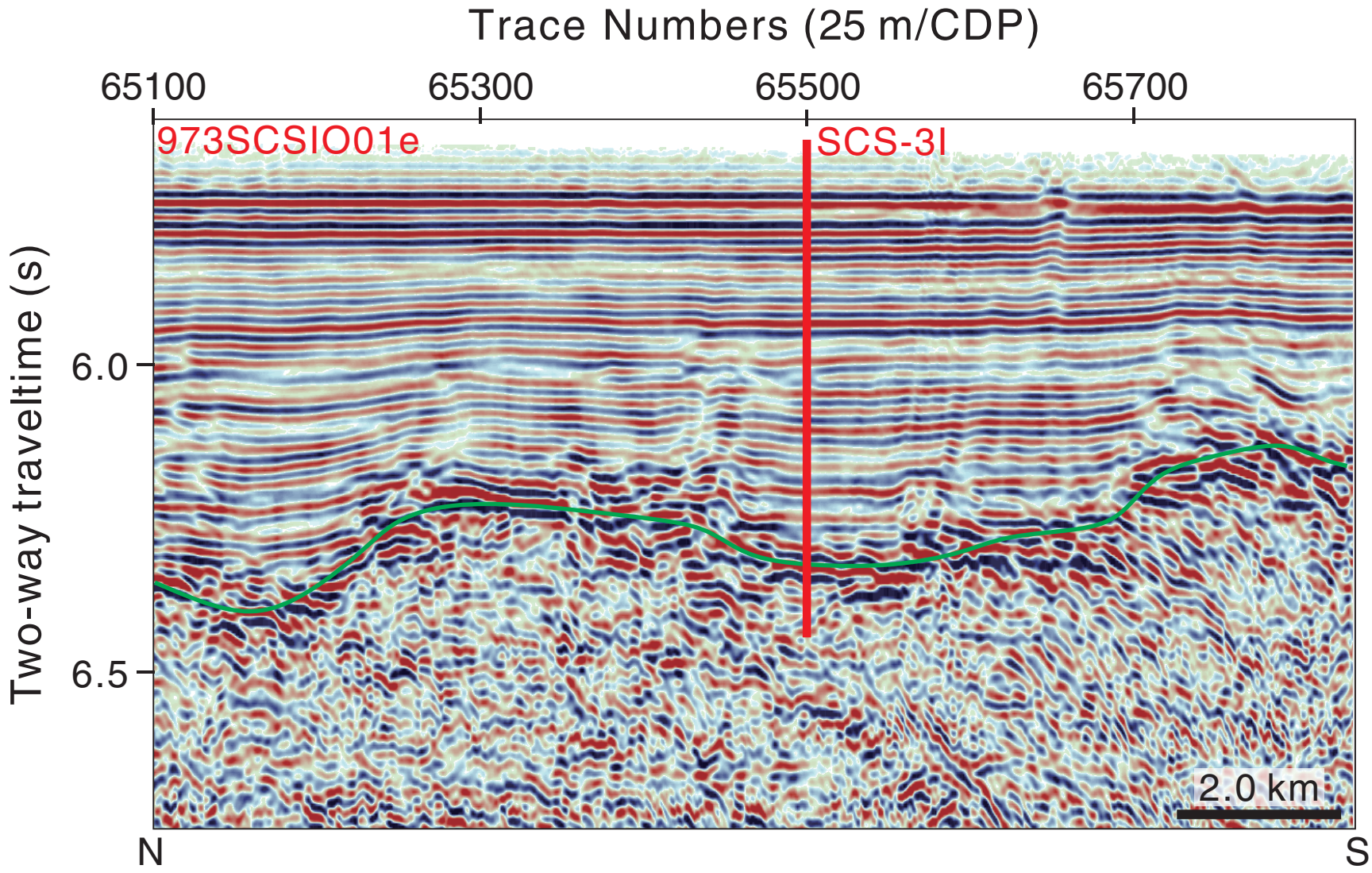

Figure AF22. Seismic profile Line BGR08-123 (southwest–northeast) with location of proposed Site SCS-3I (14°39.012′N, 116°59.994′E; common depth point [CDP] 17700; water depth = 4265 m; target depth = 674 mbsf) projected ~800 m southwest onto the line. Green line = interpreted top basement.

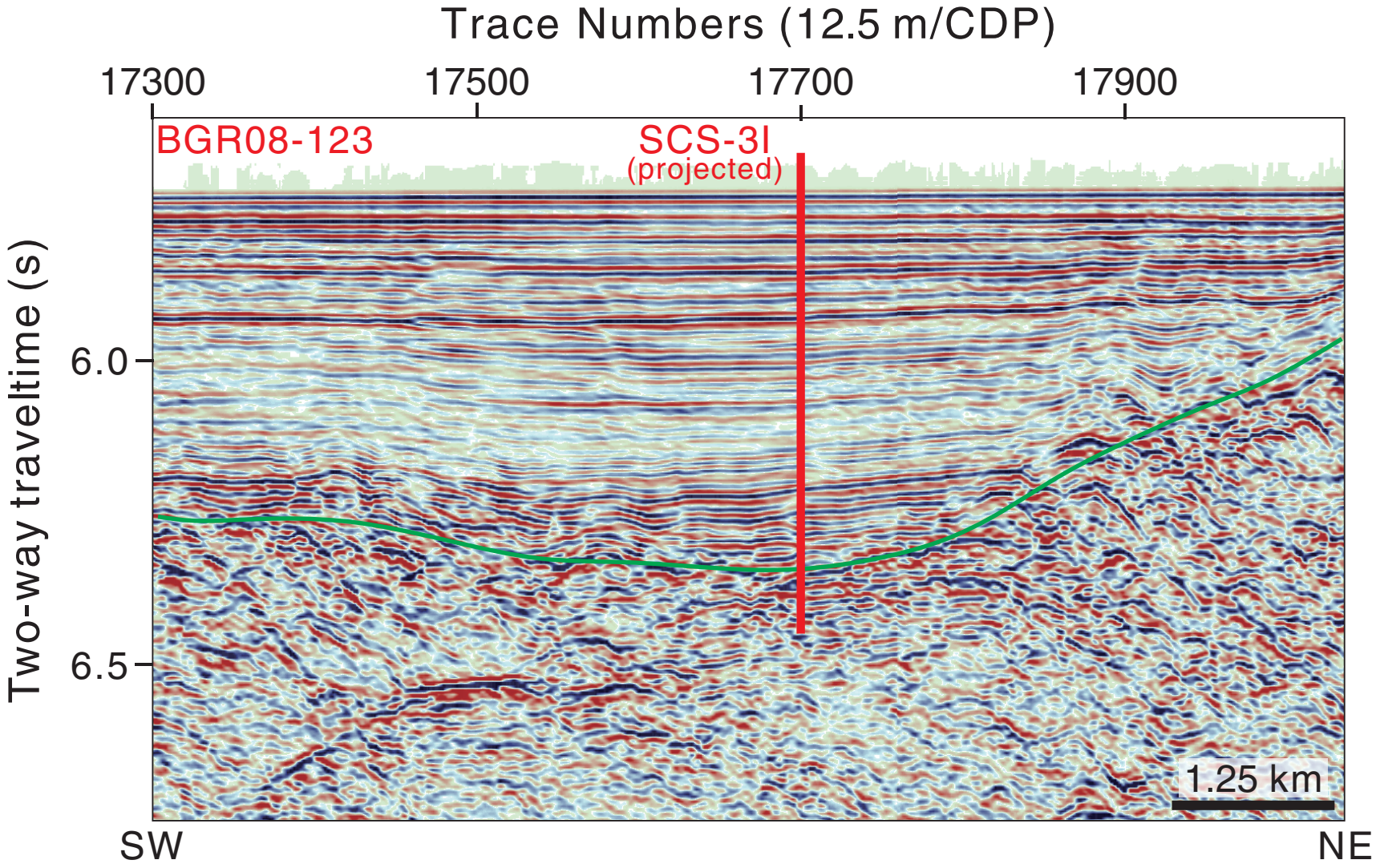

Figure AF23. Regional contoured bathymetric map showing seismic reflection profiles (red lines) and the locations of primary Site SCS-4B, backup primary Site SCS-4C, and alternate Sites SCS-4D, SCS-4E, and SCS-4F. Contour interval = 100 m.

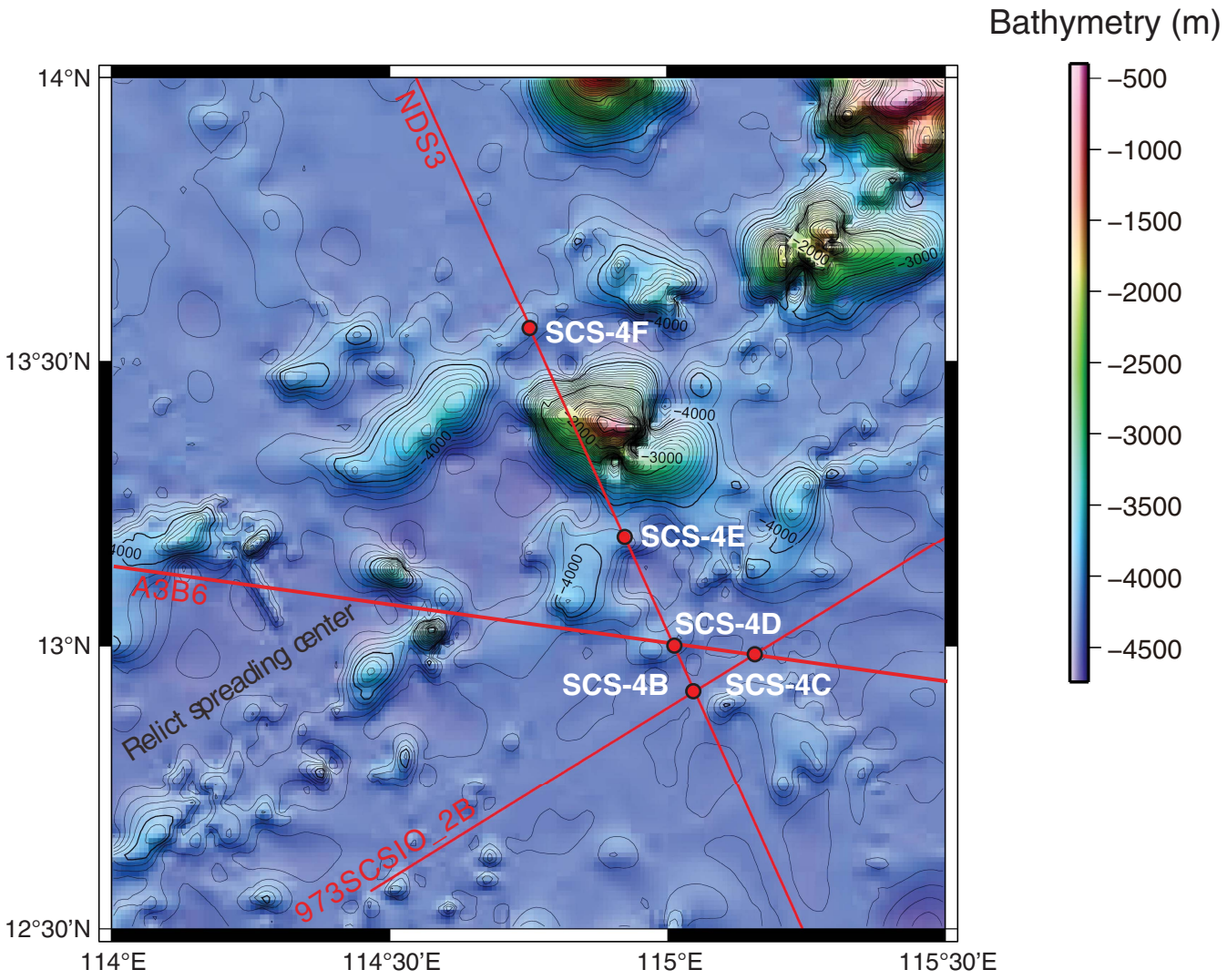

Figure AF24. Contoured bathymetric map showing seismic reflection Profiles 973SCSIO_2B (Fig. AF25) and SIOSOA_NDS3 (Fig. AF26) and the location of proposed Site SCS-4B. Contour interval = 25 m. SP = shotpoint, CMP = common midpoint.

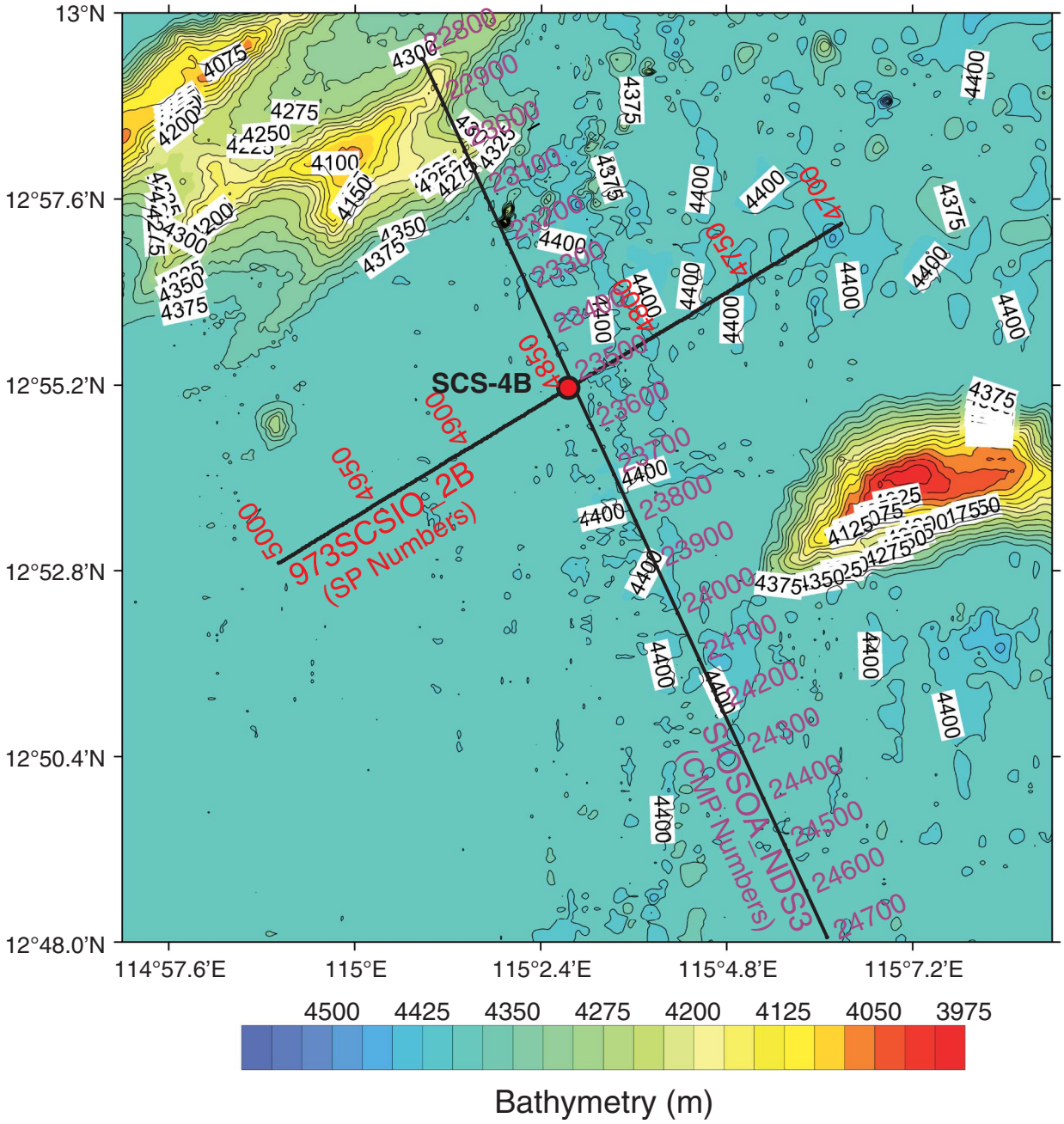

Figure AF25. Seismic profile Line 973SCSIO_2b (southwest–northeast) with location of proposed Site SCS-4B (12°55.137′N, 115°2.8326′E; shotpoint [SP] 4847; water depth = 4380 m; target depth = 965 mbsf). Green line = interpreted top basement; blue line = age uncertain.

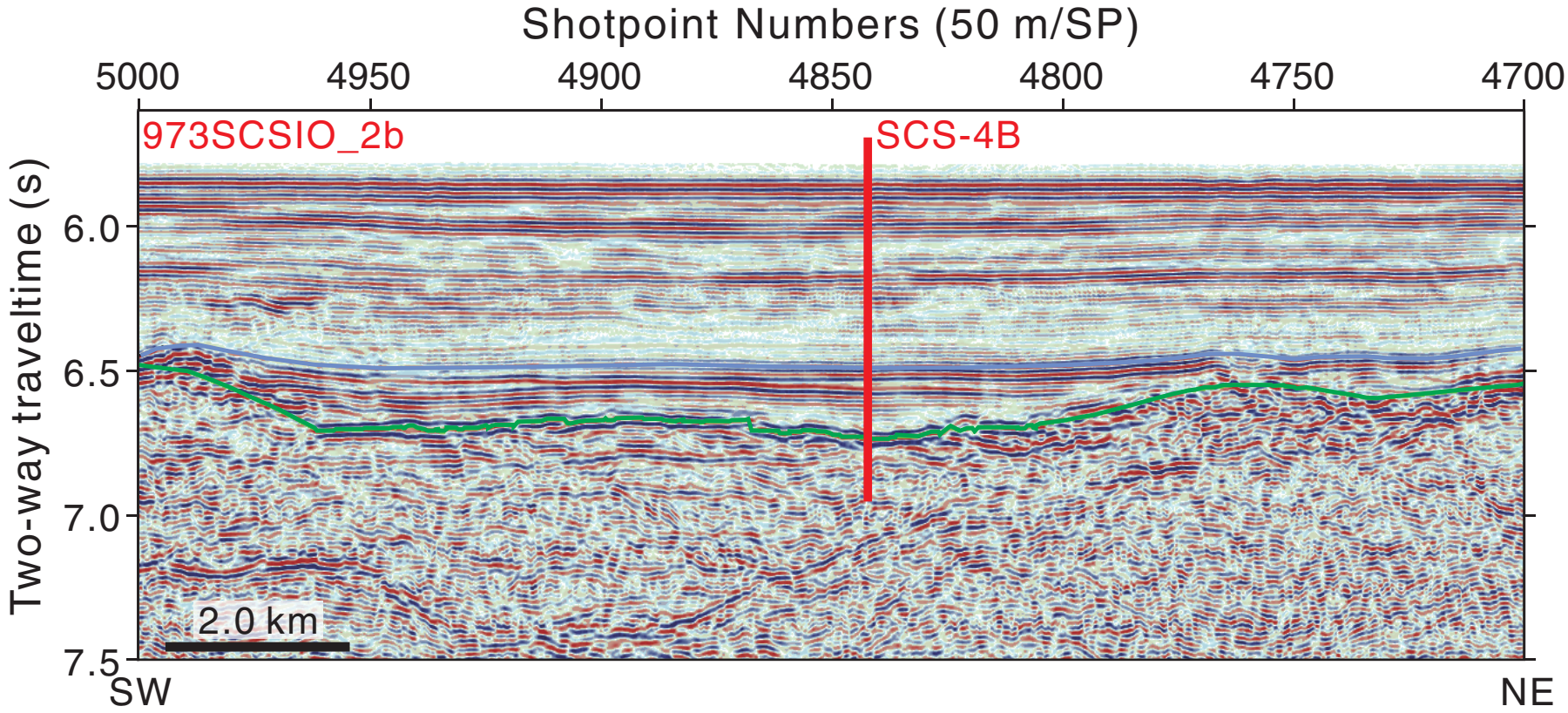

Figure AF26. Seismic profile Line SIOSOA_NDS3 (northwest–southeast) with location of proposed Site SCS-4B (12°55.137′N, 115°2.8326′E; common midpoint [CMP] 23521; water depth = 4380 m; target depth = 965 mbsf). Green line = interpreted top basement; blue line = age uncertain; pink line = interpreted top Pliocene(?); purple line = fault.

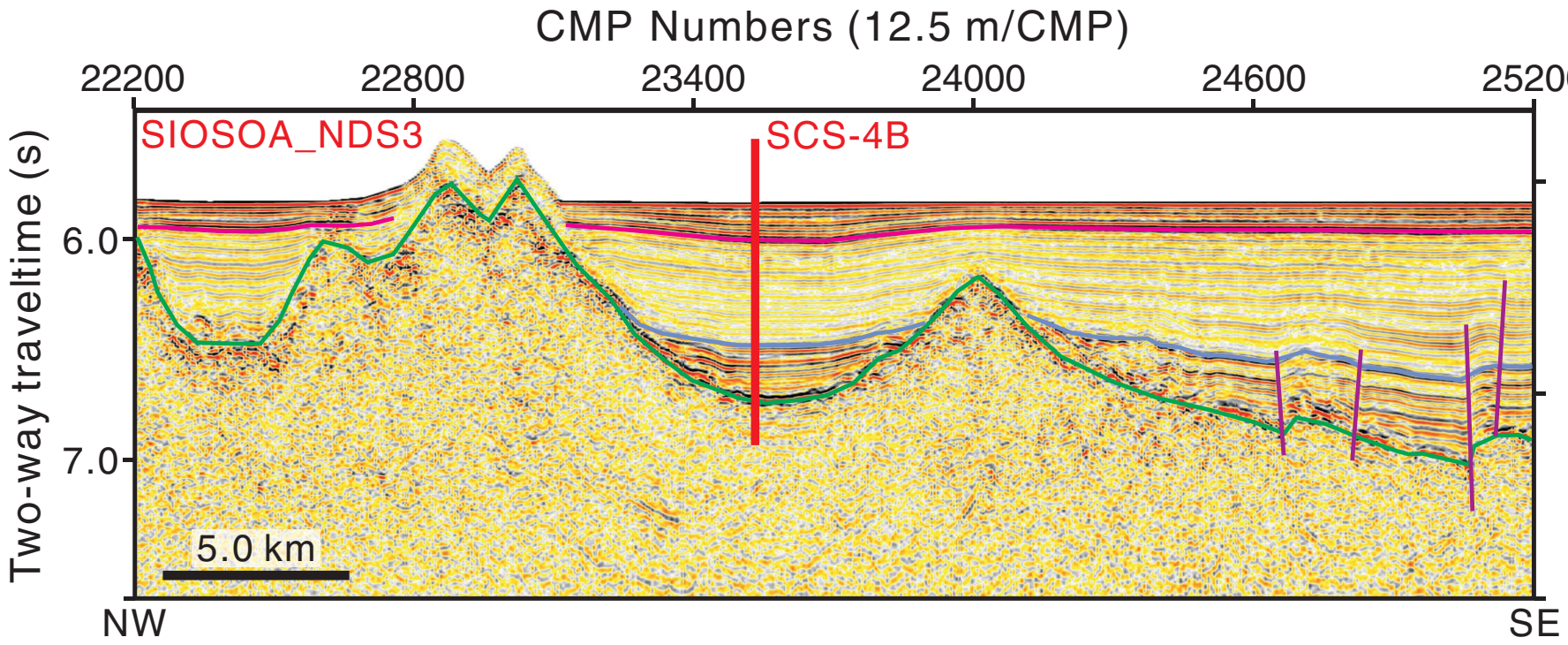

Figure AF27. Contoured bathymetric map showing seismic reflection Profiles 973SCSIO_2b (Fig. AF28) and A3B6 (Fig. AF29) and the location of proposed Site SCS-4C. Contour interval = 20 m.

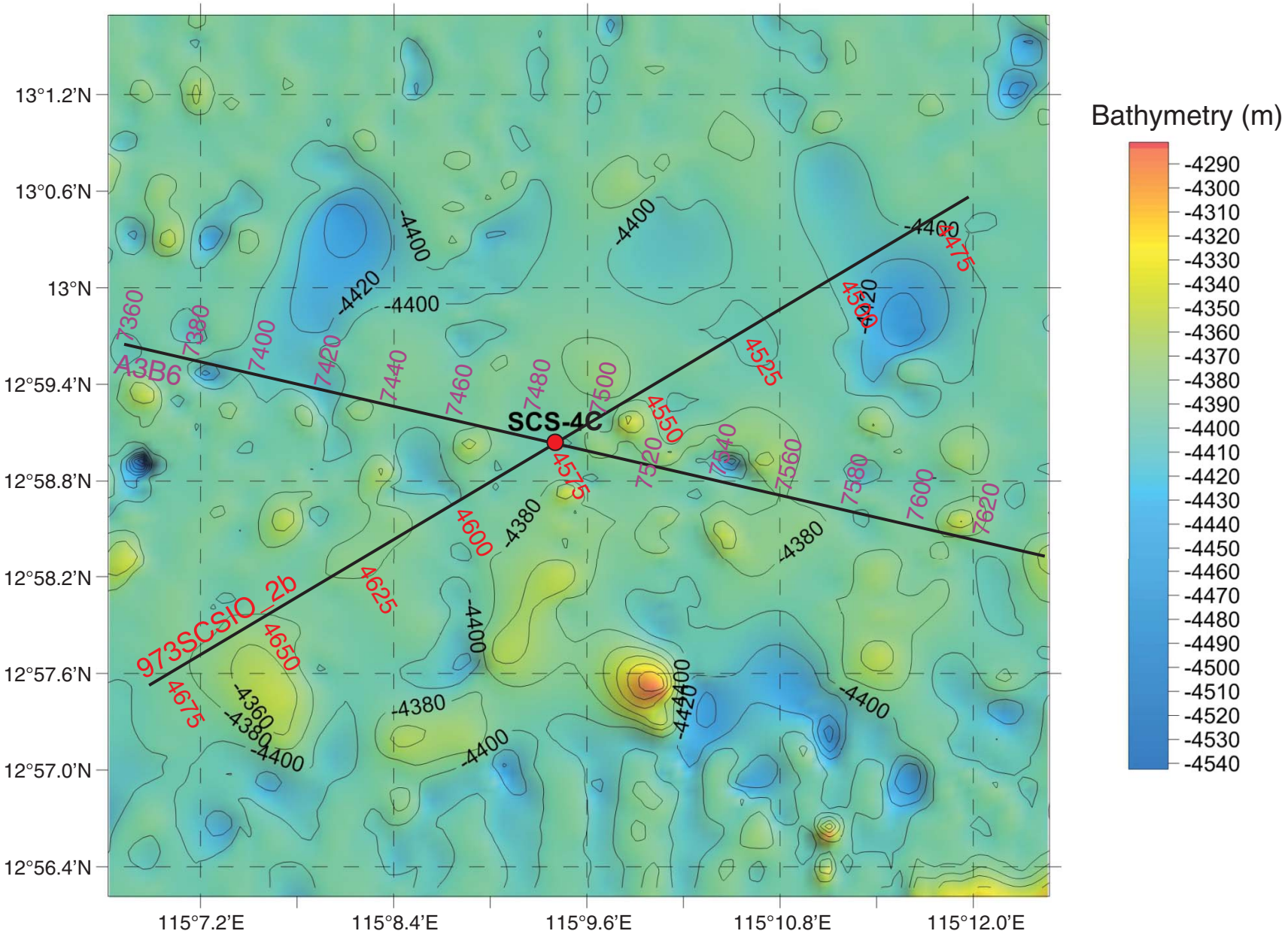

Figure AF28. Seismic profile Line 973SCSIO_2b (southwest–northeast) with location of proposed Site SCS-4C (12°59.033′N, 115°9.40′E; shotpoint [SP] 4575; water depth = 4380 m; target depth = 789 mbsf). Green line = interpreted top basement.

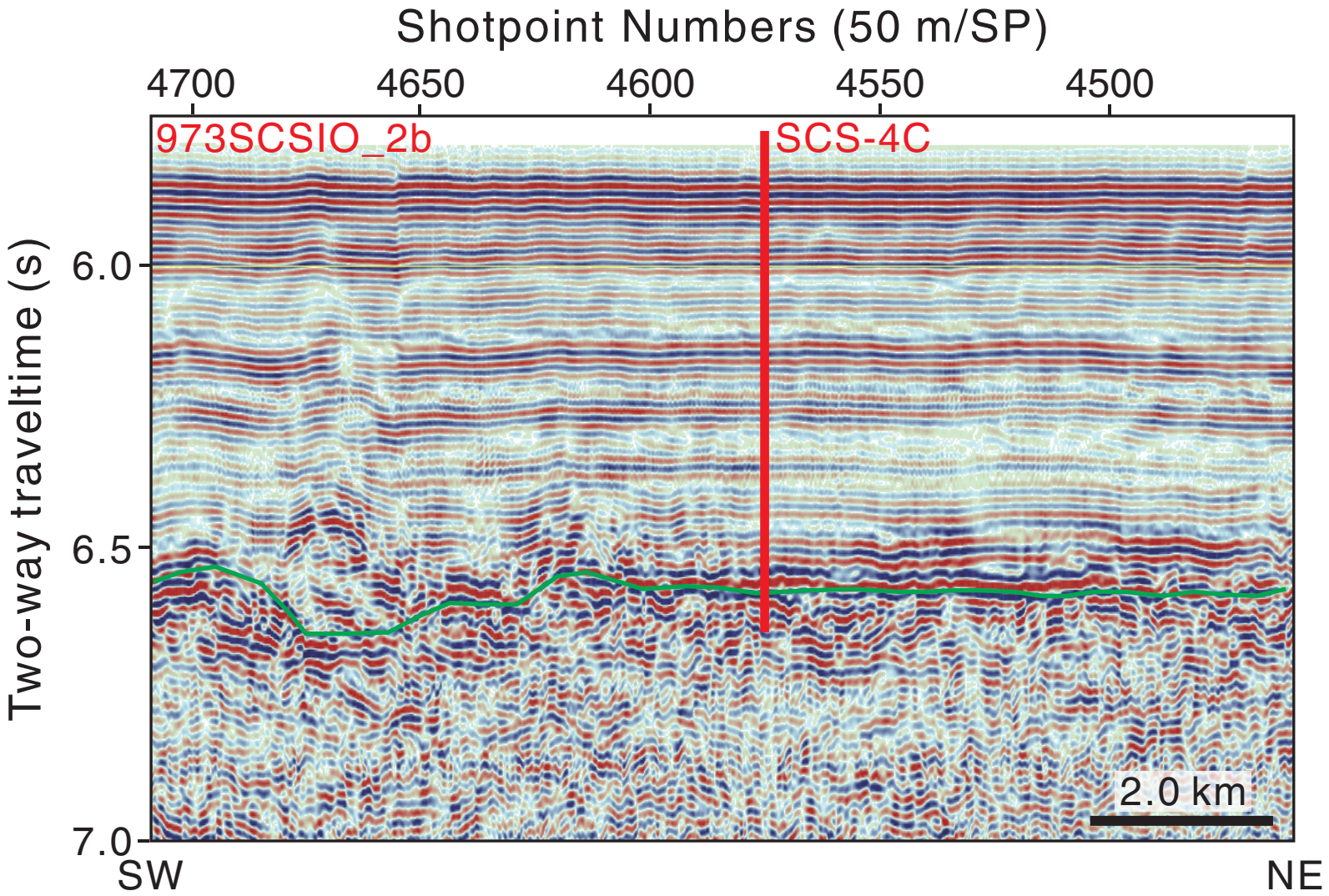

Figure AF29. Seismic profile Line A3B6 (northwest–southeast) with location of proposed Site SCS-4C (12°59.033′N, 115°9.40′E; shotpoint [SP] 7489; water depth = 4380 m; target depth = 789 mbsf). Green line = interpreted top basement.

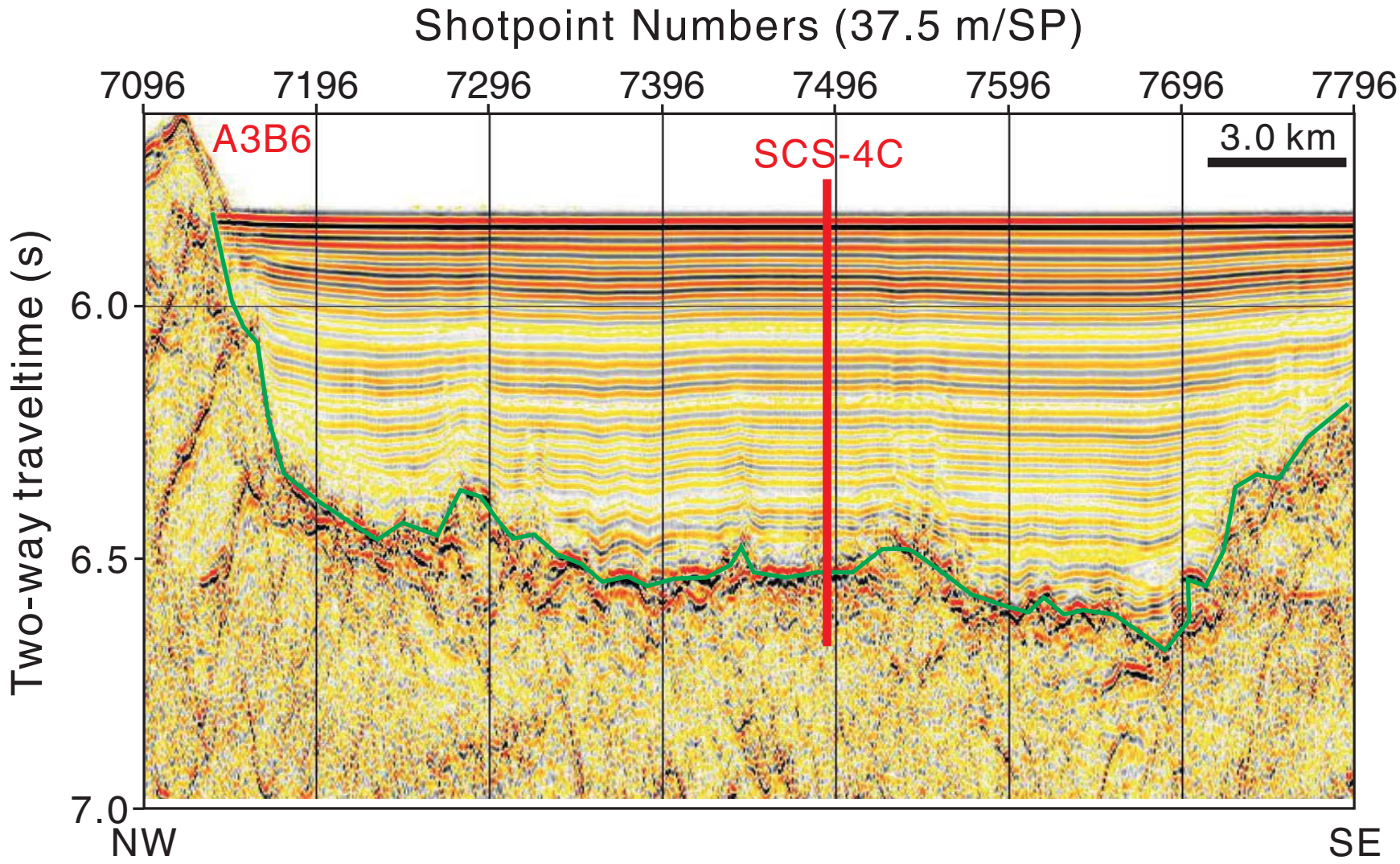

Figure AF30. Seismic profile Line NDS3-2 (NNW–SSE) with location of proposed Site SCS-4D (12°59.994′N, 115°0.744′E; common depth point [CDP] 22750; water depth = 4275 m; target depth = 304 mbsf). Green line = interpreted top basement.

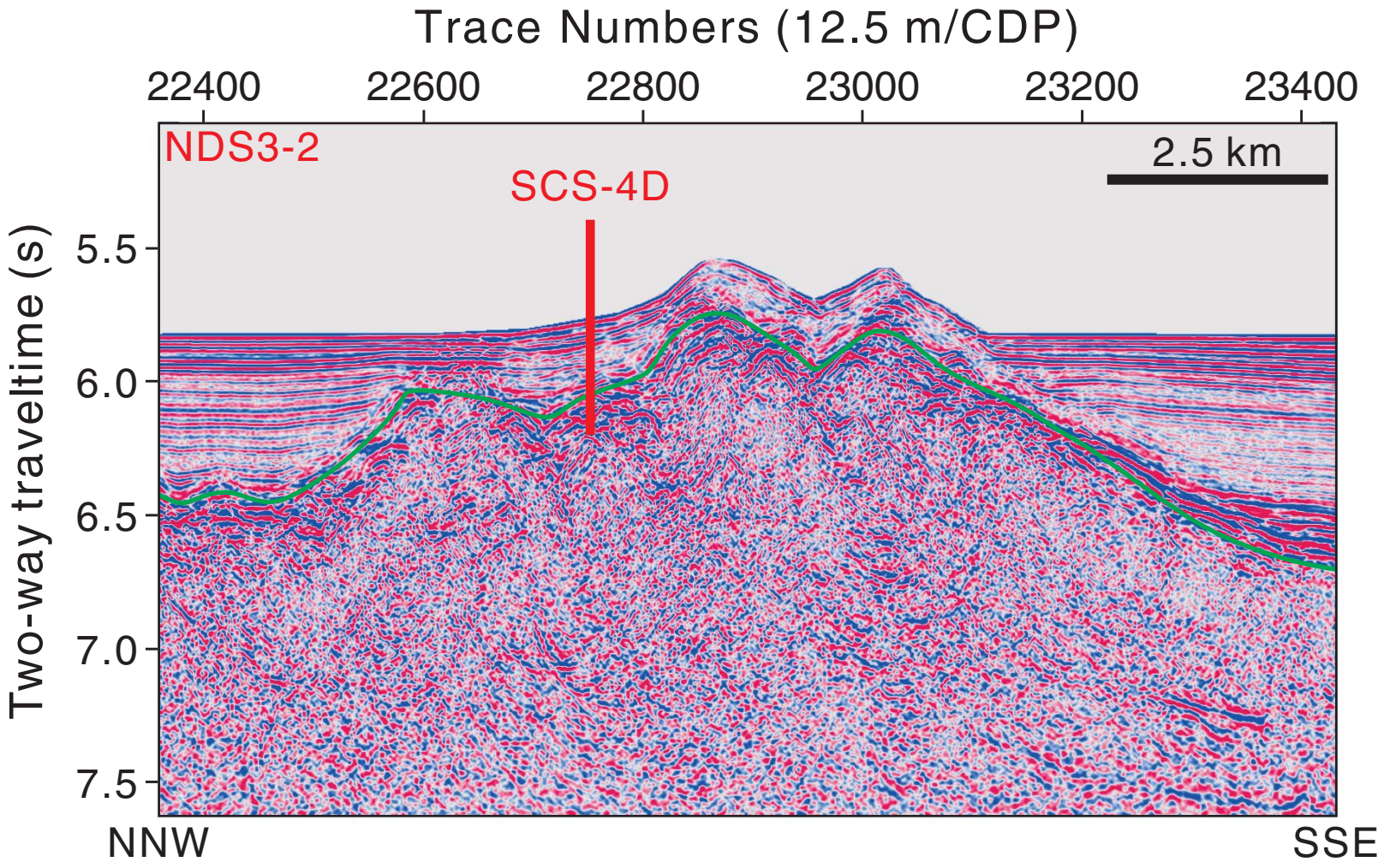

Figure AF31. Seismic profile Line A3B6 (WNW–ESE) with location of proposed Site SCS-4D (12°59.994′N, 115°0.744′E; common depth point [CDP] 740; water depth = 4275 m; target depth = 304 mbsf). Green line = interpreted top basement.

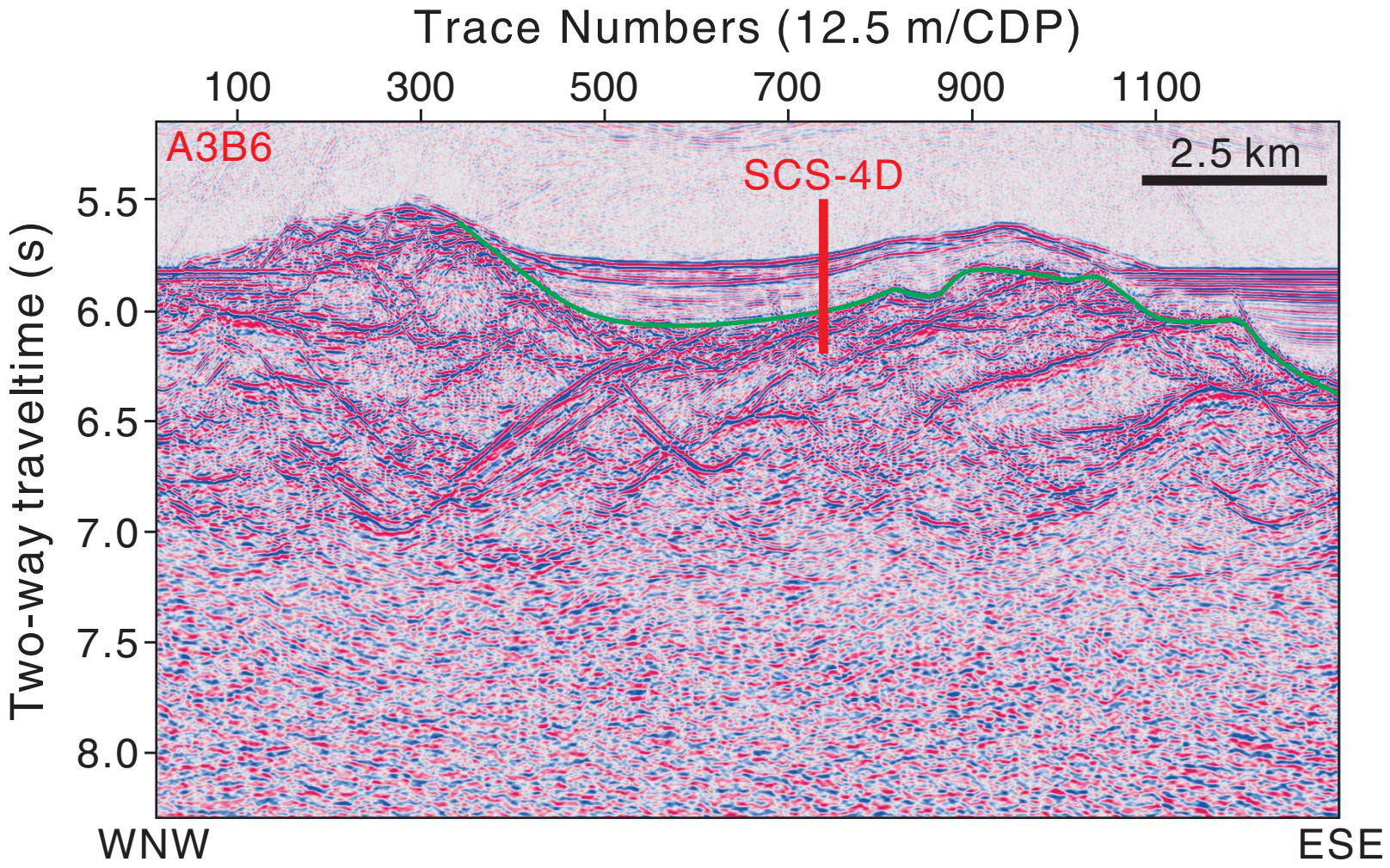

Figure AF32. Seismic profile Line NDS3-2 (NNW–SSE) with location of proposed Site SCS-4E (13°11.508′N, 114°55.398′E; common depth point [CDP] 20884; water depth = 4025 m; target depth = 404 mbsf). Green line = interpreted top basement.

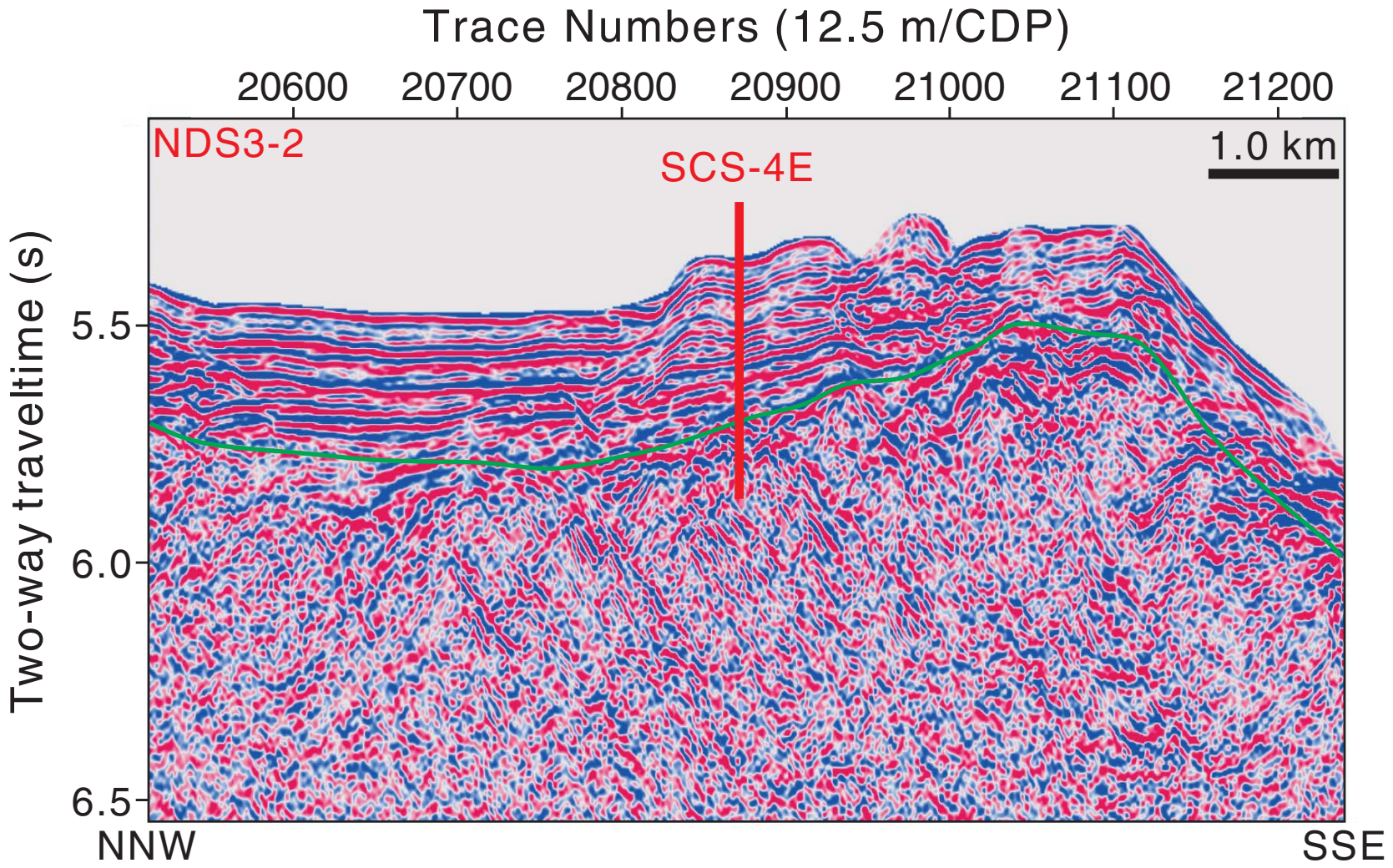

Figure AF33. Seismic profile Line NDS3-1 (NNW–SSE) with location of proposed Site SCS-4F (13°33.606′N, 114°36.414′E; common depth point [CDP] 17292; water depth = 4218 m; target depth = 290 mbsf). Green line = interpreted top basement.

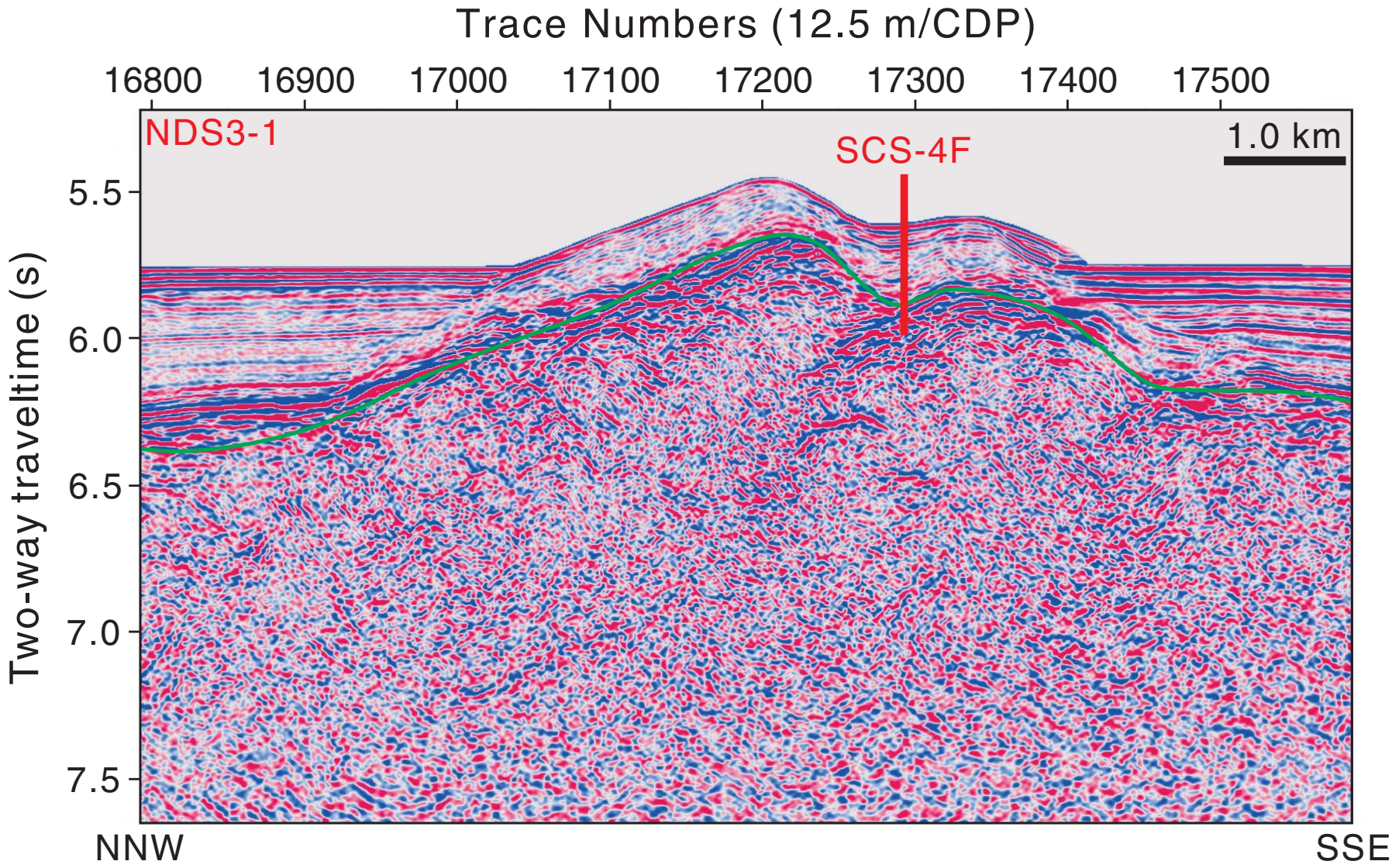

Figure AF34. Contoured bathymetric map showing seismic reflection Profiles 973SCSIO_1c (Fig. AF35) and ZSHL295 (Fig. AF36) and the location of proposed Site SCS-2C. Contour interval = 25 m.

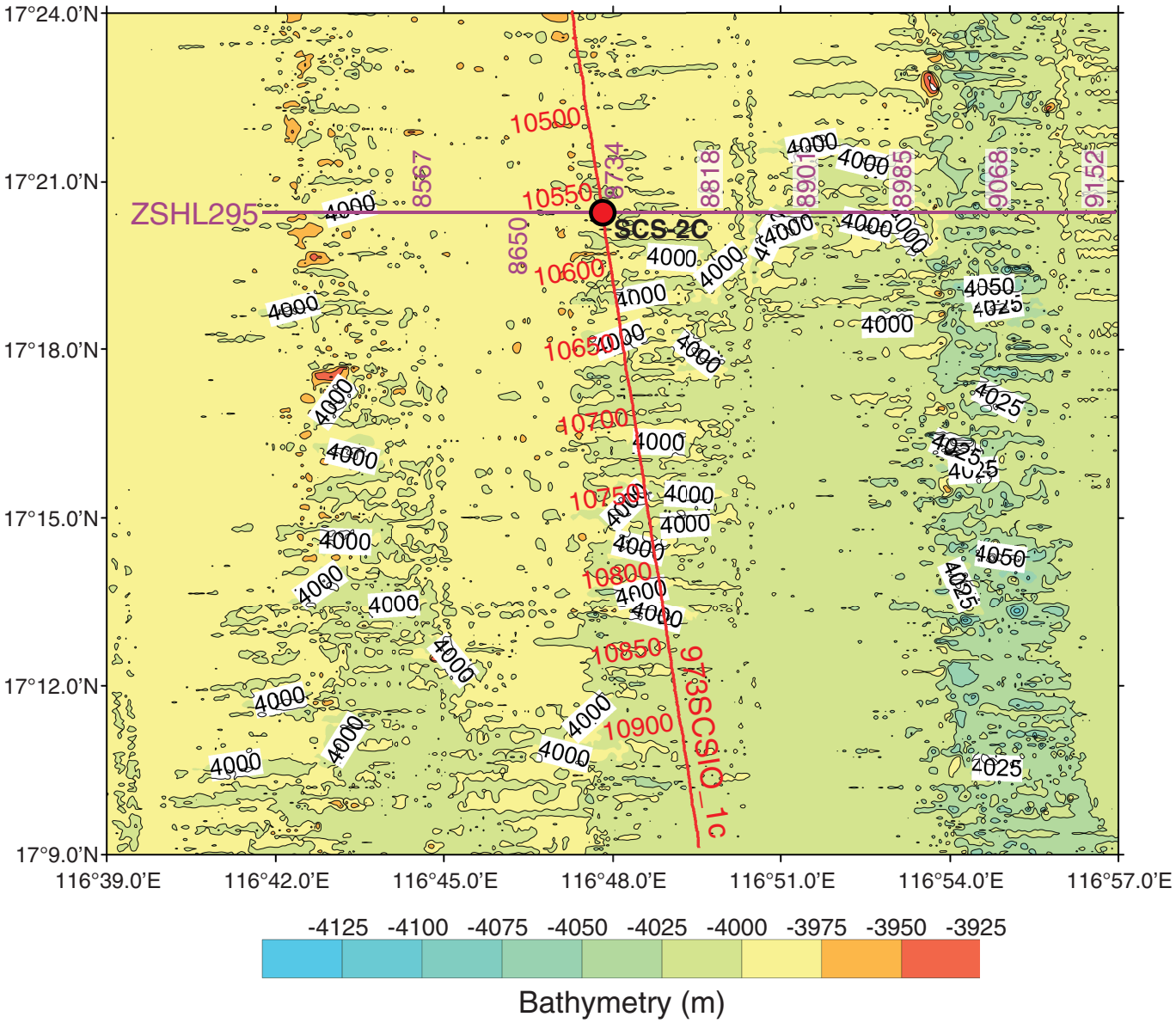

Figure AF35. Seismic profile Line 973SCSIO_1c (northwest–southeast) with location of proposed Site SCS-2C (17°20.472′N, 116°47.802′E; shotpoint [SP] 10576; water depth = 4005 m; target depth = 1215 mbsf). Green line = interpreted top basement.

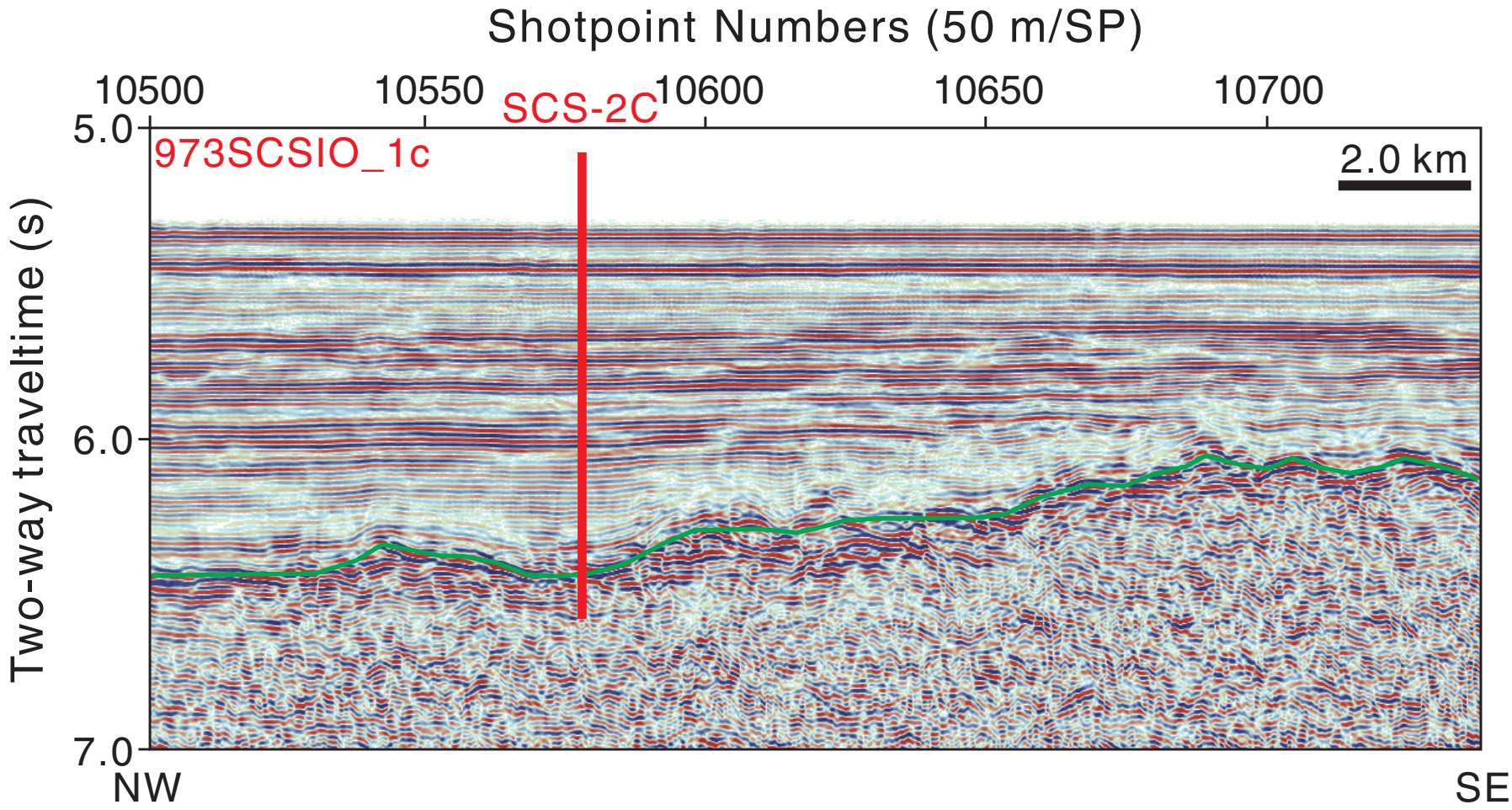

Figure AF36. Seismic profile Line ZSHL295 (west–east) with location of proposed Site SCS-2C (17°20.472′N, 116°47.802′E; shotpoint [SP] 8714; water depth = 4005 m; target depth = 1215 mbsf). Green line = interpreted top basement.

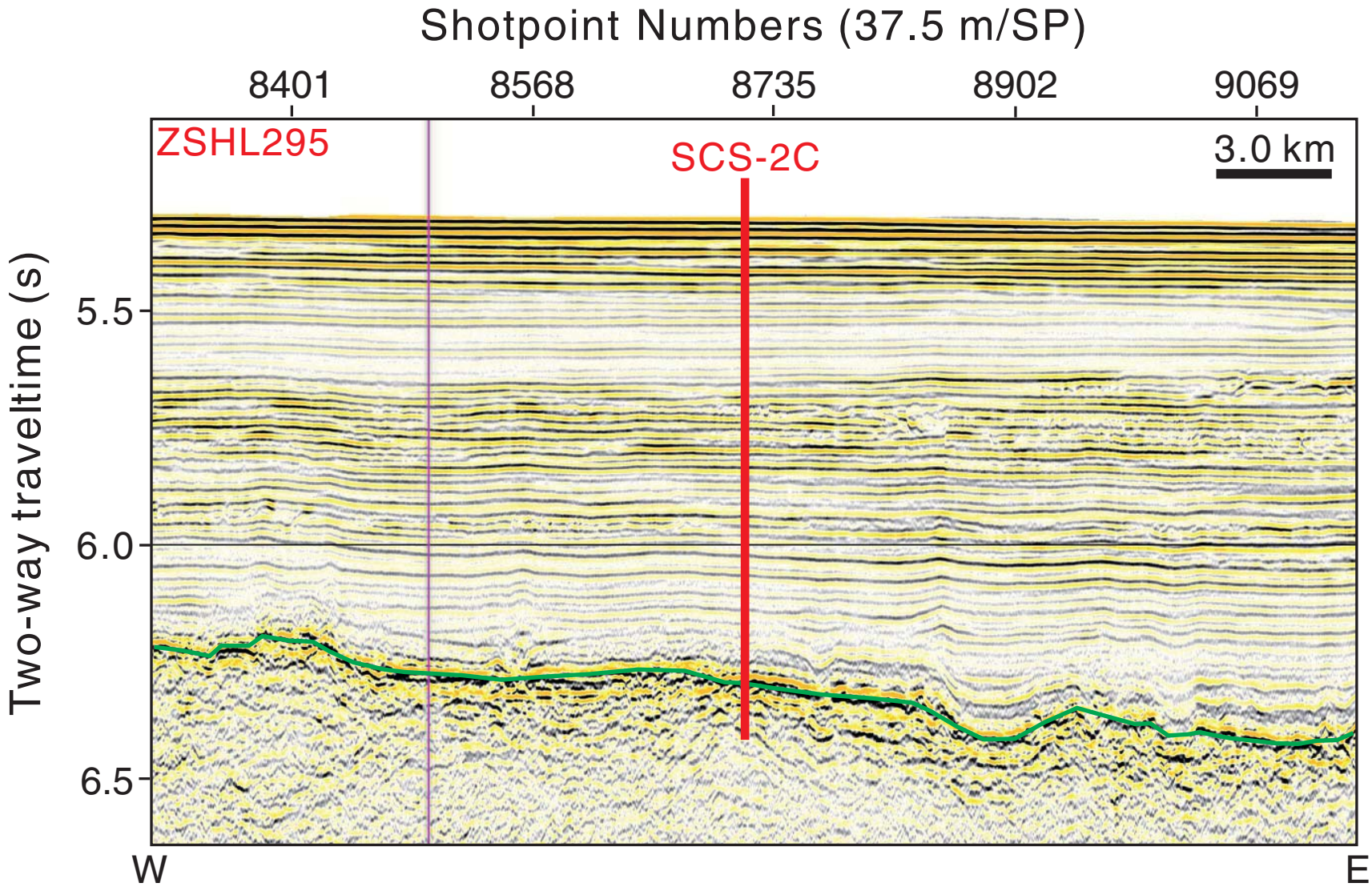

Figure AF37. Contoured bathymetric map showing seismic reflection Profiles ZSH275 (Fig. AF38) and ZSHL295 (Fig. AF39) and the location of proposed Site SCS-2D. Contour interval = 10 m.

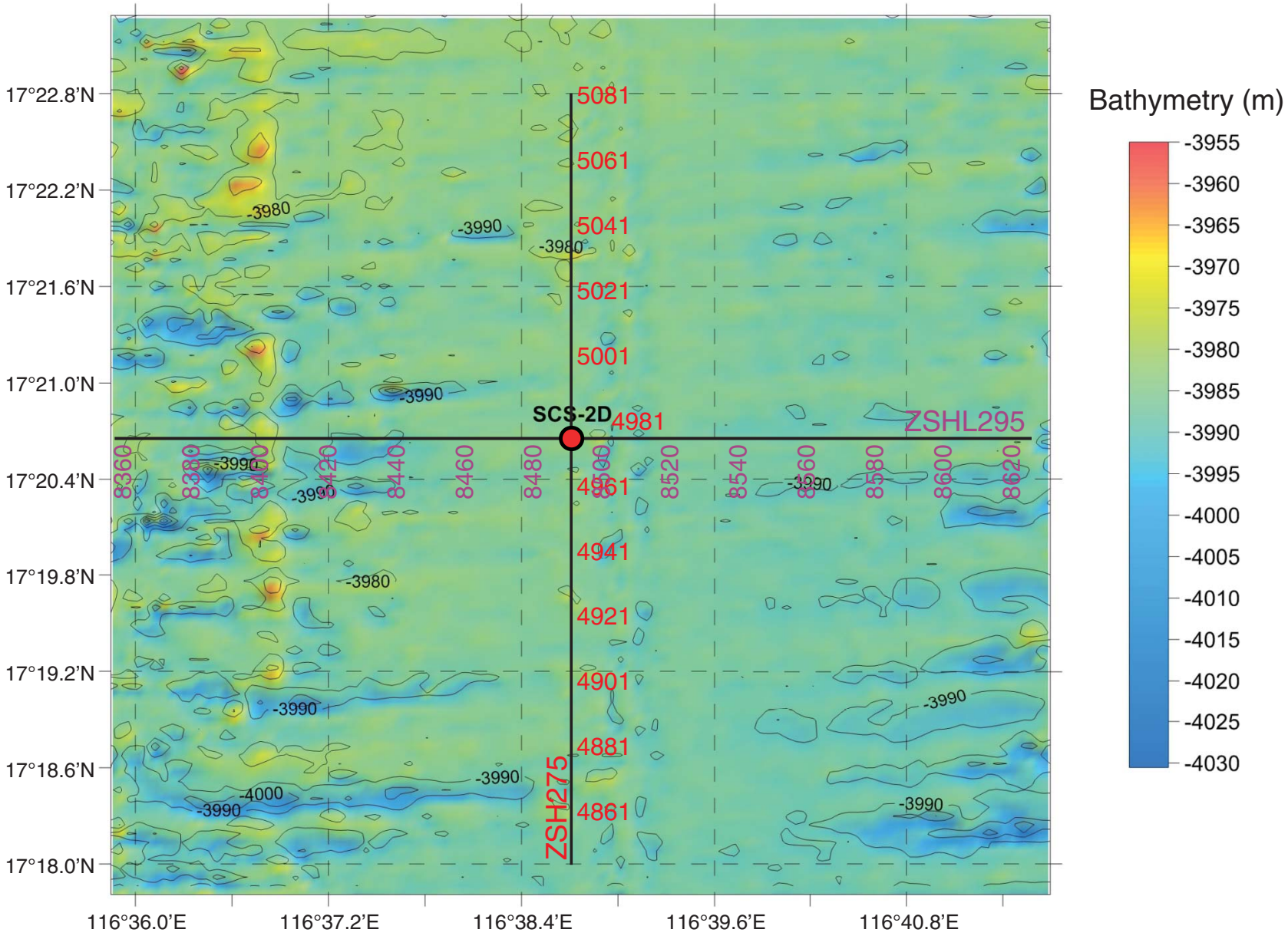

Figure AF38. Seismic profile Line ZSH275 (south–north) with location of proposed Site SCS-2D (17°20.652′N, 116°38.718′E; shotpoint [SP] 4976; water depth = 3942 m; target depth = 1140 mbsf). Green line = interpreted top basement.

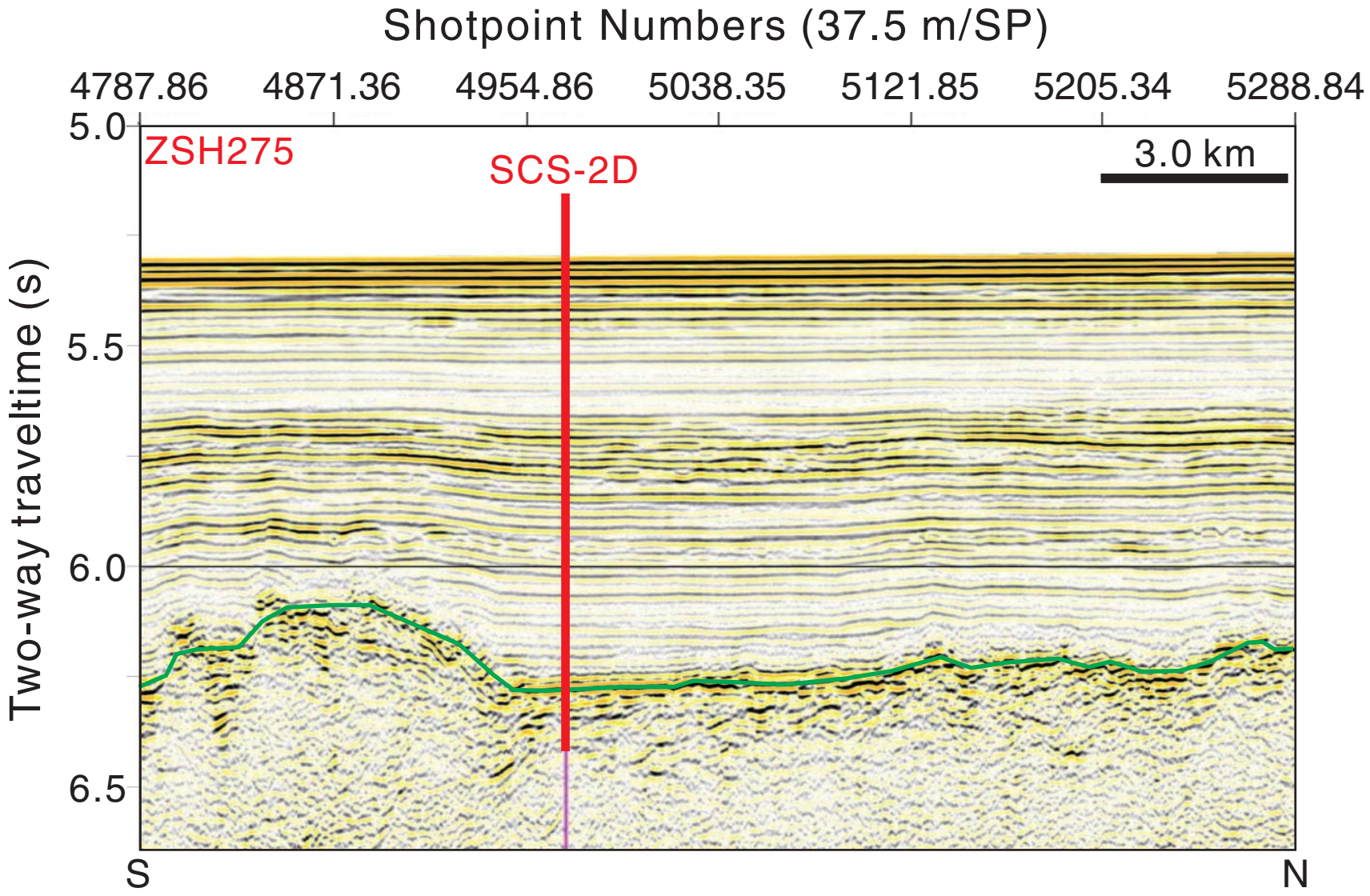

Figure AF39. Seismic profile Line ZSHL295 (west–east) with location of proposed Site SCS-2D (17°20.652′N, 116°38.718′E; shotpoint [SP] 8495; water depth = 3942 m; target depth = 1140 mbsf). Green line = interpreted top basement.

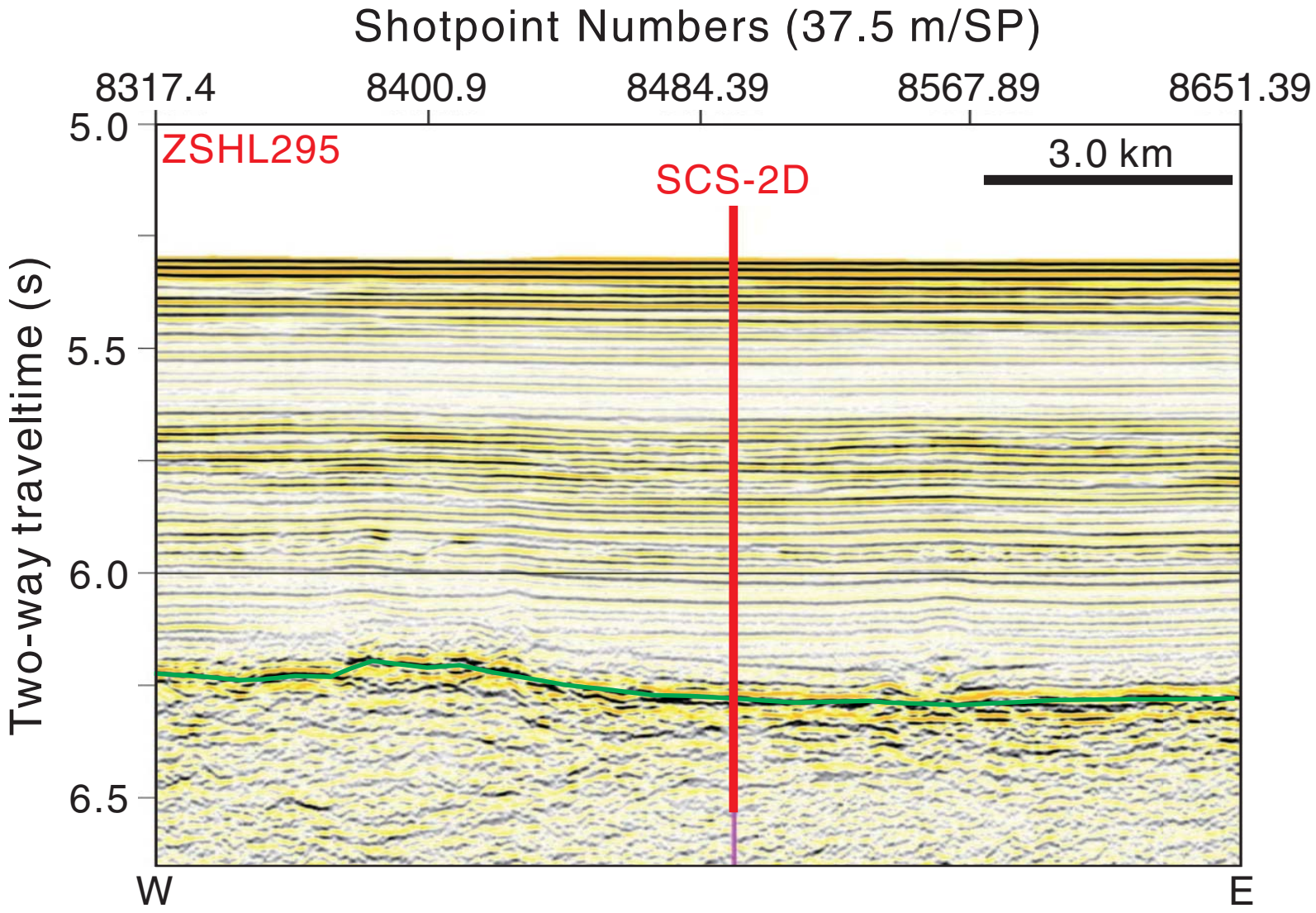

Figure AF40. Contoured bathymetric map showing seismic reflection Profiles 973GMGS_2 (Fig. AF41) and ACT105 (Fig. AF42) and the location of proposed Site SCS-1C. Contour interval = 20 m.

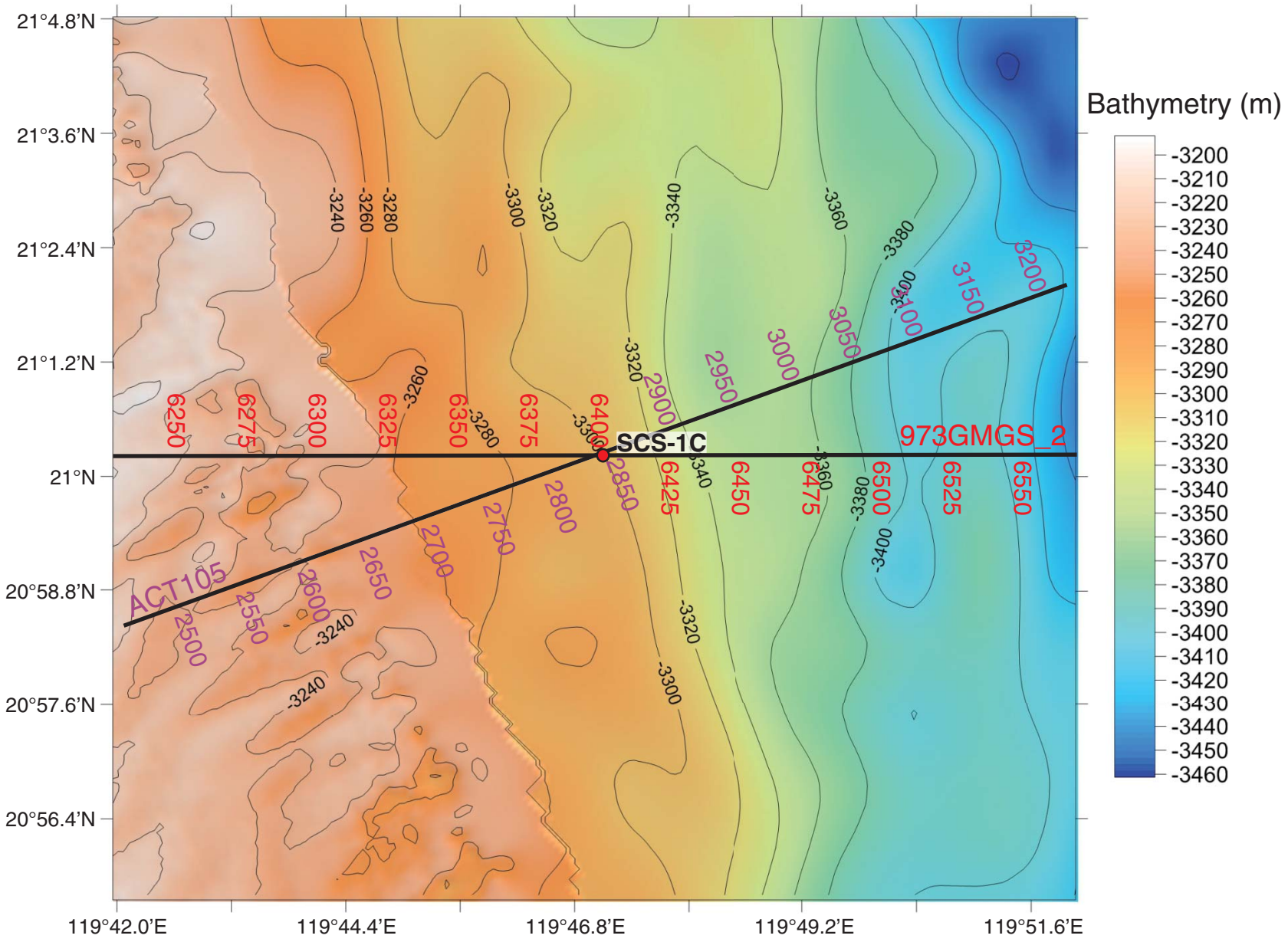

Figure AF41. Seismic profile Line 973GMGS_2 (west–east) with location of proposed Site SCS-1C (21°0.15′N, 119°47.10′E; shotpoint [SP] 6396; water depth = 3306 m; target depth = 1210 mbsf). Green line = interpreted top basement.

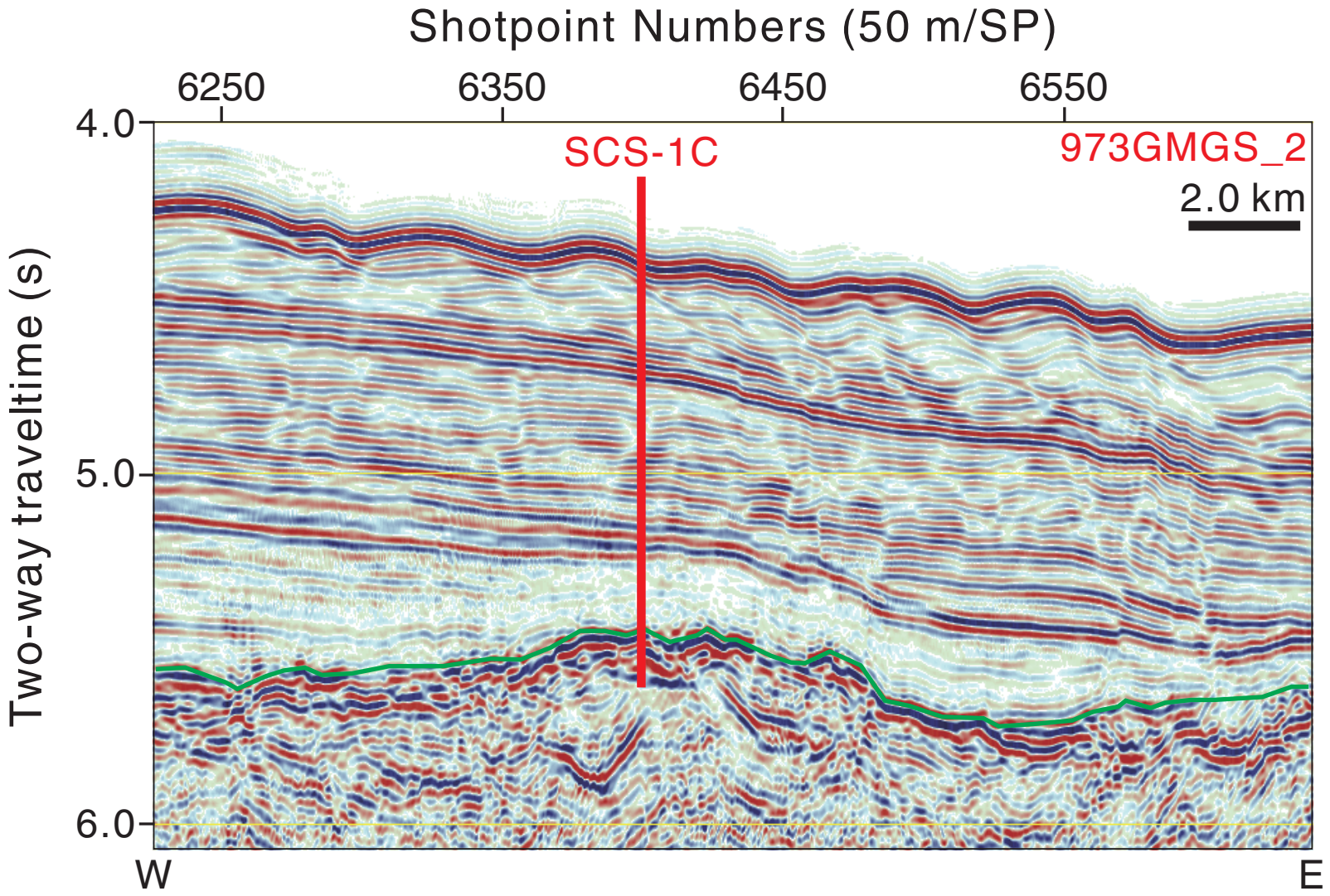

Figure AF42. Seismic profile line ACT105 (southwest–northeast) with location of proposed Site SCS-1C (21°0.15′N, 119°47.10′E; common depth point [CDP] 2836; water depth = 3306 m; target depth = 1210 mbsf). Green line = interpreted top basement.

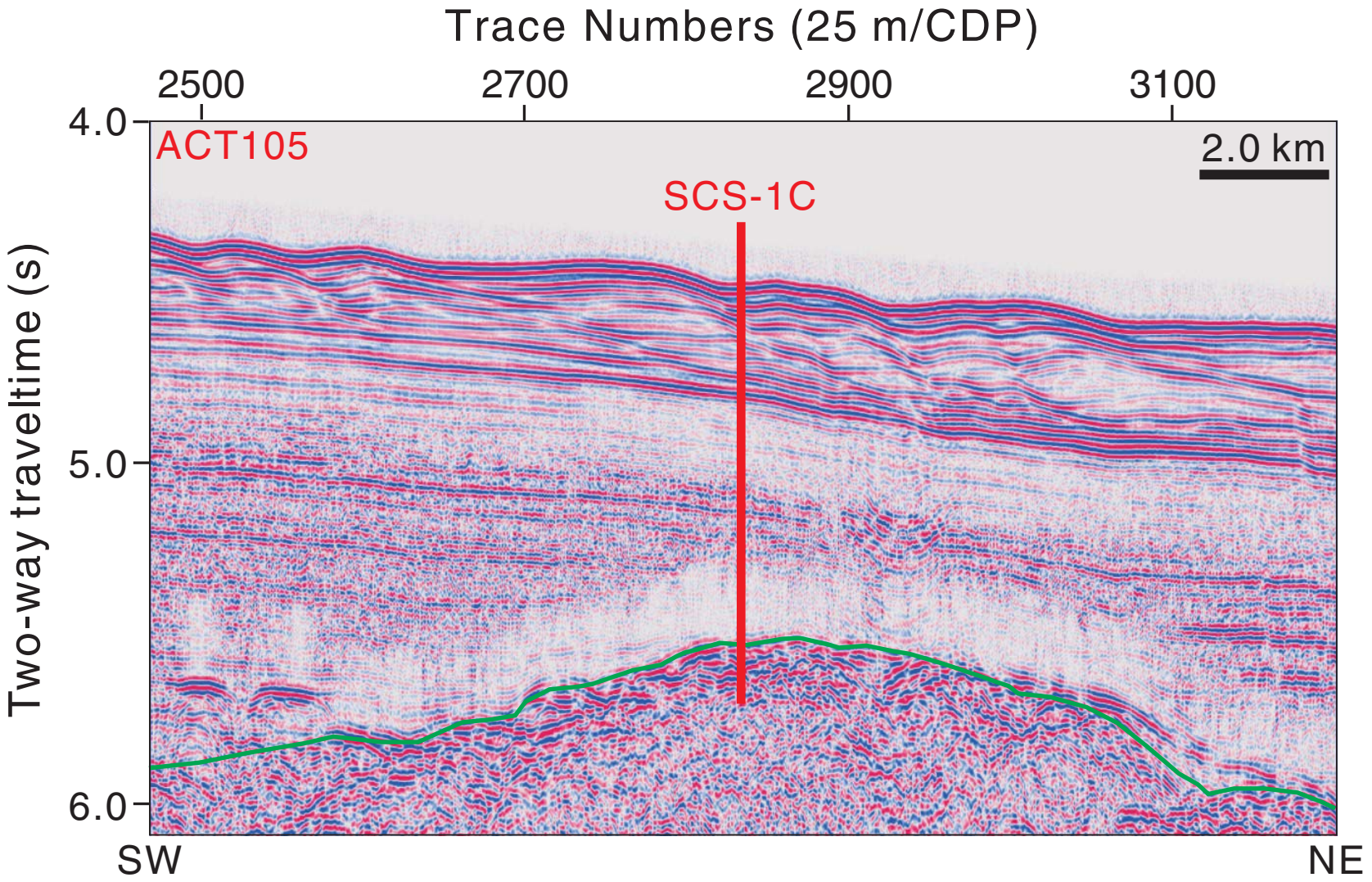

Expedition scientists and scientific participants

The current list of participants for Expedition 349 can be found at **iodp.tamu.edu/scienceops/precruise/southchinasea/participants.html.**